The Dissertation Committee for Andrew Kruse Gillette
certifies that this is the approved version of the following dissertation:

Stability of Dual Discretization Methods for Partial Differential Equations

Committee:

Chandrajit Bajaj, Supervisor

Leszek Demkowicz

Oscar Gonzalez

John Luecke

Alan Reid

James Vick

Stability of Dual Discretization Methods for Partial Differential Equations

by

Andrew Kruse Gillette, B.A.

DISSERTATION

Presented to the Faculty of the Graduate School of

The University of Texas at Austin

in Partial Fulfillment

of the Requirements

for the Degree of

DOCTOR OF PHILOSOPHY

THE UNIVERSITY OF TEXAS AT AUSTIN

May 2011

Dedicated to my grandmother,

Evaline Athena Assad Khayat Kruse,

an everlasting source of inspiration.

Acknowledgments

I would first like to thank my advisor, Dr. Chandrajit Bajaj, who has guided me through the expansive world of interdisciplinary research and encouraged me to push myself and my research at every juncture. He has been extremely generous with his time from our very first meeting and I feel honored that he has gone out of his way to make opportunities for me and introduce me to so many prominent researchers. I am deeply grateful for the breadth of knowledge he has exposed me to and I look forward to our continuing collaborations in the future.

Many additional thanks are due to the other members of my thesis committee: Dr. Leszek Demkowicz, Dr. Oscar Gonzalez, Dr. John Luecke, Dr. Alan Reid, and Dr. James Vick. My interest in finite element theory began with a course taught by Dr. Demkowicz and I thank him for his counsel

on numerous occasions since that time. Dr. Luecke served as a secondary advisor for the two years I was supported under his NSF Research Training Grant with Dr. Reid and I have appreciated his willingness to explore the subtleties of exterior calculus and its discretizations with me. Dr. Gonzalez has attended many of my talks in the math department and graciously agreed to join my committee during my last semester. Finally, I learned differential topology thanks to Dr. Vick in my first year at UT which spawned my interest in the subject.

A special round of thanks goes out to the postdoctoral members of the CVC over the years. Dr. Samrat Goswami was kind enough to bring me on to a paper while I was still new in the group and showed me the ropes of the writing and publishing process. Dr. Zhang Qin worked tirelessly on our paper from 2009 and has been an entertaining and engaging traveling companion to various conferences and workshops. Dr. Alexander Rand has been both an indispensable resource for his intuitive understanding of finite element theory and a sage mentor to me through the last phase of graduate school. All three have been very generous with their time and I am proud to list them as co-authors.

I would not be able to come close to naming all the fellow grad students at UT to whom I am indebted for help and companionship. I feel lucky to have befriended so many people from the math department, the CSEM program, the CVC research group, and many other places around campus during my time here. I would like to specially acknowledge Jose Rivera from our lab for

patiently answering so many of my technical questions and working tirelessly for the general improvement of CVC's computational capabilities. A special thanks also to my office mates Salman Baig and Brandy Guntel; I have greatly enjoyed the many lunches we have shared.

My research activities would not have been possible without the incredible administrative support I have received. Thanks to Nancy Lamm, Ben Garcia, Sandra Catlett, and Dr. Dan Knopf in the math department and Suzanne Bailey at CVC for all their work and patience over the years with my often atypical administrative requests.

To my parents, Pat and Dane Gillette, and to my brother Ryan, thank you a million times over for your love and support. You keep me grounded in times of uncertainty and help guide me through life's many choices. I could not have made it through graduate school without you.

Finally, to Epiphanie, spending time with you has been a joy from the moment we met. I am excited to embark on the next phase of our lives together.

Stability of Dual Discretization Methods for Partial Differential Equations

Publication No. _____

Andrew Kruse Gillette, Ph.D.
The University of Texas at Austin, 2011

Supervisor: Chandrajit Bajaj

This thesis studies the approximation of solutions to partial differential equations (PDEs) over domains discretized by the dual of a simplicial mesh. While 'primal' methods associate degrees of freedom (DoFs) of the solution with specific geometrical entities of a simplicial mesh (simplex vertices, edges, faces, etc.), a 'dual discretization method' associates DoFs with the geometric duals of these objects. In a tetrahedral mesh, for instance, a primal method might assign DoFs to edges of tetrahedra while a dual method for the same problem would assign DoFs to edges connecting circumcenters of adjacent tetrahedra.

Dual discretization methods have been proposed for various specific PDE problems, especially in the context of electromagnetics, but have not been analyzed using the full toolkit of modern numerical analysis as is considered here. The recent and still-developing theories of finite element exterior calculus (FEEC) and discrete exterior calculus (DEC) are shown to be essential in understanding the feasibility of dual methods. These theories treat the

solutions of continuous PDEs as differential forms which are then discretized as cochains (vectors of DoFs) over a mesh. While the language of DEC is ideal for describing dual methods in a straightforward fashion, the results of FEEC are required for proving convergence results.

Our results about dual methods are focused on two types of stability associated with PDE solvers: discretization and numerical. Discretization stability analyzes the convergence of the approximate solution from the discrete method to the continuous solution of the PDE as the maximum size of a mesh element goes to zero. Numerical stability analyzes the potential roundoff errors accrued when computing an approximate solution. We show that dual methods can attain the same approximation power with regard to discretization stability as primal methods and may, in some circumstances, offer improved numerical stability properties.

A lengthier exposition of the approach and a detailed description of our results is given in the first chapter of the thesis.

Table of Contents

List of Notation

$*$ continuous Hodge star, page 15

$||\cdot||_{\mathcal{C}^k}$ norm on primal k-cochains, page 52

$\mathcal{C}^k$ space of primal k-cochains, page 35

$\mathbb{D}_k$ kth discrete exterior derivative, page 36

$\overline{\mathrm{A}}$ dual cochain (any letter in small caps with a bar), page 35

$||\cdot||_{\overline{\mathcal{C}}^k}$ norm on dual k-cochains, page 52

$\overline{\mathcal{C}}^k$ space of dual k-cochains, page 35

$\mathfrak{D}(\Omega)$ C^{∞} functions on Ω, page 17

$\overline{\mathcal{W}}_{\star\sigma^k}$ Whitney-like function associated to $\star\sigma^k$, page 108

$||\cdot||_{[L^2]^3}$ sum of L^2 norms on components of input vector, page 23

$||\cdot||_{H(\mathrm{curl})}$ $H(\mathrm{curl})$ norm, page 23

$||\cdot||_{H(\mathrm{div})}$ $H(\mathrm{div})$ norm, page 23

$||\cdot||_{H^m}$ mth L^2 Sobolev norm, page 20

$|\cdot|_{H^m}$ mth L^2 Sobolev semi-norm, page 20

$||u||_{[H^1]^3,[H^1]^3}$ $||h||_{[H^1]^3} + ||\mathrm{curl}\, h||_{[H^1]^3}$, page 83

$||b||_{[H^1]^3,H^1}$ $||b||_{[H^1]^3} + ||\mathrm{div}\, b||_{H^1}$, page 73

$||u||_{H^1,[H^1]^3}$ $||u||_{H^1} + ||\nabla u||_{[H^1]^3}$, page 88

$||\cdot||_\mathcal{P}$ regularity norm for $\mathcal{P}$, page 48

$\mathcal{I}_k$ interpolation map from primal k-cochains, page 40

Λ^k continuous differential k-forms, page 13

λ_i barycentric function on a simplex, page 41

$||\cdot||_{H\Lambda^k}$ graph norm on $H\Lambda^k$, page 24

$\mathbb{M}_k$ diagonal discrete Hodge star, page 49

$\mathbb{M}_k^{Diag}$ diagonal discrete Hodge star, page 49

$\mathfrak{D}'(\Omega)$ space of distributions on Ω, page 18

$\left(\mathbb{M}_k^{Dual}\right)^{-1}$ dual discrete inverse Hodge star, page 117

$\mathbb{M}_k^{Whit}$ Whitney discrete Hodge star (mass matrix), page 49

$\overline{\mathcal{I}}_k$ interpolation map from dual k-cochains, page 108

$\overline{\Lambda}^k$ alternate notation for Λ^{n-k}, page 2

$\overline{\lambda}_i$ Sibson barycentric coordinate function on a polygon, page 54

$\overline{\mathcal{P}}_k$ projection map to dual k-cochains, page 39

∂^α derivative with respect to multi-index α, page 16

∂_k kth boundary operator, page 36

$\textsc{a}$ primal cochain (any letter in small caps), page 35

$^k u$ kth flat map applied to u, page 21

Chapter 1

Introduction

1.1 Problem Statement

The challenge in designing stable numerical methods comes from an interplay between the necessities of the discrete computational problem formulation and the inherent constraints of the corresponding continuous mathematical formulation. Proof of the existence and uniqueness of the solution to a partial differential equation (PDE) in a continuous setting, for instance, does not guarantee that a particular numerical method will converge to that solution. Likewise, stable numerical methods designed based on ease of implementation, backwards compatibility, or similar concerns from the discrete setting may become so popular with their users that alternative methods with equal theoretical justification and possibly greater computational value remain unconsidered.

The goal of this thesis is to exhibit how a wide class of PDE problems are amenable to solution by "dual mesh" discretization methods frequently dismissed or glossed over in the literature. The mathematical underpinnings of the continuous setting make such constructions simple to motivate from a theoretical perspective. At the same time, a variety of techniques from the dis-

crete setting, including finite element methodologies, discrete exterior calculus, and generalized barycentric interpolation, make dual methods feasible for implementation. We will show that the resulting methods are novel in definition, canonical in theoretical backing, and beneficial to practicing computational scientists.

To motivate the approach, we introduce a number of diagrams showing the various operators relating continuous and discrete function spaces, both primal and dual. Continuous PDE problems have solutions naturally over a space of continuous functions Λ^k, where the index k corresponds to the dimensionality, in a certain sense, of the solution function. The elements of these spaces can be treated as differential k-forms and the standard operators on them (grad, curl, div) can be treated as instances of the exterior derivative operator d. The rich theory of exterior calculus also gives a natural mapping called the Hodge star $*$ taking Λ^k isometrically onto Λ^{n-k} where n is the dimension of the underlying manifold domain. Using an overline to denote a dual treatment, these maps relate the spaces in the following fashion for $n = 3$.

$$
\begin{array}{ccccccc}
\text{primal forms:} & \Lambda^0 & \xrightarrow{\ d_0\ } & \Lambda^1 & \xrightarrow{\ d_1\ } & \Lambda^2 & \xrightarrow{\ d_2\ } & \Lambda^3 \\
& \updownarrow{\scriptstyle *} & & \updownarrow{\scriptstyle *} & & \updownarrow{\scriptstyle *} & & \updownarrow{\scriptstyle *} \\
\text{dual forms:} & \overline{\Lambda}^3 & \xleftarrow{\ d_2\ } & \overline{\Lambda}^2 & \xleftarrow{\ d_1\ } & \overline{\Lambda}^1 & \xleftarrow{\ d_0\ } & \overline{\Lambda}^0
\end{array}
$$

In the discrete setting, approximate solutions to a PDE are written as a linear combination of a finite number of basis functions. The coefficients of the basis functions are sufficient to describe the discrete solution and hence our discrete solution spaces consist of vectors of real coefficients. These vector spaces are

2

called *cochain spaces* and, like the continuous differential form spaces, can be associated with a dimensionality k. The emergent theory of discrete exterior calculus has shown how to recreate the essential properties of the continuous setting canonically in a discrete setting. This gives us primal and dual cochain spaces ($\mathcal{C}^k$ and $\overline{\mathcal{C}}^k$), primal and dual exterior derivative maps ($\mathbb{D}_k$ and $\mathbb{D}_{n-k}^T$) and primal and dual discrete Hodge stars ($\mathbb{M}_k$ and $\mathbb{M}_{n-k}^{-1}$) in direct analogy to their continuous counterparts.

primal cochains:
$$\mathcal{C}^0 \xrightarrow{\mathbb{D}_0} \mathcal{C}^1 \xrightarrow{\mathbb{D}_1} \mathcal{C}^2 \xrightarrow{\mathbb{D}_2} \mathcal{C}^3$$

$$(\mathbb{M}_0)^{-1} \updownarrow \mathbb{M}_0 \qquad (\mathbb{M}_1)^{-1} \updownarrow \mathbb{M}_1 \qquad (\mathbb{M}_2)^{-1} \updownarrow \mathbb{M}_2 \qquad (\mathbb{M}_3)^{-1} \updownarrow \mathbb{M}_3$$

dual cochains:
$$\overline{\mathcal{C}}^3 \xleftarrow{(\mathbb{D}_0)^T} \overline{\mathcal{C}}^2 \xleftarrow{(\mathbb{D}_1)^T} \overline{\mathcal{C}}^1 \xleftarrow{(\mathbb{D}_2)^T} \overline{\mathcal{C}}^0$$

The essential question then becomes how to define maps between the Λ^k and $\mathcal{C}^k$ spaces which allow for *a priori* estimates on the error incurred by discrete approximation of continuous functions. Maps from continuous to discrete spaces are called projection maps, denoted by $\mathcal{P}$, and maps in the opposite direction are called interpolation maps, denoted by $\mathcal{I}$. Since primal cochain spaces are associated with simplicial domain meshes (i.e. triangulations for $n = 2$ and tetrahedralizations for $n = 3$) and interpolation over simplices is well understood, the natural maps to consider are as follows.

primal forms:
$$\Lambda^0 \xrightarrow{d_0} \Lambda^1 \xrightarrow{d_1} \Lambda^2 \xrightarrow{d_2} \Lambda^3$$

$$\mathcal{I}_0 \updownarrow \mathcal{P}_0 \qquad \mathcal{I}_1 \updownarrow \mathcal{P}_1 \qquad \mathcal{I}_2 \updownarrow \mathcal{P}_2 \qquad \mathcal{I}_3 \updownarrow \mathcal{P}_3$$

primal cochains:
$$\mathcal{C}^0 \xrightarrow{\mathbb{D}_0} \mathcal{C}^1 \xrightarrow{\mathbb{D}_1} \mathcal{C}^2 \xrightarrow{\mathbb{D}_2} \mathcal{C}^3$$

An enormous amount of effort has gone into proving asymptotic optimal error estimates in this context of primal forms and primal cochains, though not

always in the language of continuous or discrete exterior calculus. With this language, however, we can immediately consider the possibility of analogous projection and interpolation maps over the dual spaces.

$$
\begin{array}{ccccccc}
\text{dual forms:} & \overline{\Lambda}^3 & \xleftarrow{\;d_2\;} & \overline{\Lambda}^2 & \xleftarrow{\;d_1\;} & \overline{\Lambda}^1 & \xleftarrow{\;d_0\;} & \overline{\Lambda}^0 \\
& \overline{\mathcal{I}}_3 \big\Updownarrow \overline{\mathcal{P}}_3 & & \overline{\mathcal{I}}_2 \big\Updownarrow \overline{\mathcal{P}}_2 & & \overline{\mathcal{I}}_1 \big\Updownarrow \overline{\mathcal{P}}_1 & & \overline{\mathcal{I}}_0 \big\Updownarrow \overline{\mathcal{P}}_0 \\
\text{dual cochains:} & \overline{\mathcal{C}}^3 & \xleftarrow{(\mathbb{D}_0)^T} & \overline{\mathcal{C}}^2 & \xleftarrow{(\mathbb{D}_1)^T} & \overline{\mathcal{C}}^1 & \xleftarrow{(\mathbb{D}_2)^T} & \overline{\mathcal{C}}^0
\end{array}
$$

Putting these four diagrams together, we see the complete set of maps relating the continuous and discrete settings. Map labels are omitted for readability, however, arrows indicate a continuous or discrete uni-directional exterior derivative operator.

A generic description of how this diagram is used to find approximate solutions to PDEs is as follows.

I. **Translate** the continuous PDE problem into the language of exterior calculus.

II. **Linearize** the problem, possibly by introducing an intermediary variable.

III. **Discretize** the k-forms into k-cochains and the operators d and $*$ into $\mathbb{D}$ and $\mathbb{M}$ matrices.

IV. **Solve** a linear system constructed from the discrete equations.

Our approach focuses on the fact that there are two canonical ways to carry out the discretization in step III. For instance, let u be a variable treated as a k-form in the linearized continuous problem. Then u can be treated as an element of Λ^k, resulting in its discretization as a primal cochain U, or as an element of $\overline{\Lambda}^k$, resulting in its discretization as a dual cochain $\overline{\mathsf{U}}$. The choice of primal or dual discretization for u fixes the discretization of the remaining variables and operators meaning there are only two fundamental methods in this framework. However, since U and $\overline{\mathsf{U}}$ are approximations of u in *different* finite dimensional vector spaces, there may be significant computational advantages to choosing one discretization over the other.

We will show in this thesis how dual discretization methods can achieve the same approximation power with the same error estimates as their primal counterparts and, in some circumstances, may be more computationally efficient or numerically stable. In the remainder of this chapter, we will put our work in the context of existing theories and summarize our results more precisely.

1.2 Context in the Literature

Exterior calculus and its relationship to the numerical analysis of partial differential equations are currently receiving increasing attention from both mathematical and computer science research communities. The recent widely

acclaimed mathematical work on Finite Element Exterior Calculus (FEEC) by Arnold, Falk and Winther [7, 6] has shown how many well known results about stable bases for finite element methods [24, 30, 72, 73, 80] can be characterized completely using the language of exterior calculus. This can be seen as a 'top-down' approach, since it starts with an abstract Hilbert complex framework and only specializes to specific interpolation operators at the last step.

Meanwhile, the theory of Discrete Exterior Calculus (DEC) [59, 32] has taken more of a 'bottom-up' approach, starting with discrete differential form spaces (i.e. cochain spaces) and building up the supporting theory as required. Many prior efforts have made strides in defining a discrete calculus in this fashion e.g. [14, 15, 56, 74, 83, 88]. DEC has gained traction in the field for its straightforward terminology, resulting in its proposed application to a variety of PDE problems [13, 45, 60, 99]. Moreover, various finite element software packages now use the terminology of discrete differential forms, including DOLFIN [67], PyDEC [12], and Lawrence Livermore National Laboratory's FEMSTER [25].

This thesis lies somewhere between these two exterior calculus camps. While the notion of a dual-based method is natural in DEC, it is less obvious from a FEEC viewpoint since FEEC does not make use of dual cochains. On the other hand, while DEC theory uses piecewise-defined functions, FEEC uses the more formal notion of piecewise-defined distributions. This allows FEEC to leverage results from applied functional analysis to ensure convergence and stability properties of numerical methods. Since DEC relies on

6

these theoretical results from FEEC to claim robustness in its methodology, the DEC-inspired dual-based methods proposed here must also be justified in a FEEC context.

1.3   Summary of Results

(1) Generalized Dual-Based Discretization Methodology

(Section 3.1) The first contribution of this thesis is a rigorous and canonical methodology for constructing dual-based discretizations. The language of DEC reveals natural numerical methods in the dual context which still respect the dimensionality of the continuous problem. While such approaches have been considered in specific contexts previously, they have not been given the general treatment afforded by the DEC approach used here. These constructions allow for rigorous error-checking and cross-confirmation of the results of large scale simulation efforts. This is particularly valuable when physical experimental confirmation of the results is impossible or expensive.

(2) Discretization Stability of Dual-Based Methods

(Sections 3.2 - 3.5) A crucial criterion for the viability of a numerical method for PDEs is a proof that the error converges to zero (in an appropriate norm) at an optimal rate as the mesh is refined. This is referred to as discretization stability or an asymptotic optimal error estimate. Starting with a proof of discretization stability for a primal-based magnetostatics sketched by Bossavit [19, 20], we show how the proof can be phrased in DEC language in a

natural fashion. We then exploit the same techniques to prove the discretization stability of dual methods in both specific and general contexts. These proofs imply that implementing a dual-based methodology would allow, in theory, equal approximation power as their primal counterparts.

(3) Discretization Stability using Generalized Barycentric Interpolation

(Section 3.6) The proofs of discretization stability of dual-based methods make use of a composed dual interpolation operator $*\mathcal{I}_{n-k}\mathbb{M}_{n-k}^{-1} : \overline{\mathcal{C}}^k \to \overline{\Lambda}^k$. This operator, in effect, translates the dual problem to a primal one in order to exploit standard stability results. While this is suitable for methods where both primal and dual variables appear, we show that it is possible to achieve the same estimate in the case $n = 2$, $k = 0$ with a node-based interpolation operator $\overline{\mathcal{I}}_0$. A form of generalized barycentric interpolation functions called Sibson or 'natural neighbor' coordinates are used to define $\overline{\mathcal{I}}_0$. The discretization stability result we prove requires only two modest assumptions on the cells of the dual mesh: an upper bound on the aspect ratio and a lower bound on the edge length when the cells are scaled to have diameter 1. The proof also gives a set of techniques that can be used toward proving similar stability results for larger values of k and n.

(4) Novel Whitney-like Interpolation Functions for Dual Meshes

(Section 4.1) The canonical construction of Whitney functions used in the definition of the primal interpolation operators $\mathcal{I}_k$ suggests a similar con-

struction should be possible for defining generalized interpolation operators $\overline{\mathcal{I}}_k$ over dual meshes. We define such operators for $n = 2$ and 3 and show they share certain similar properties with their primal counterparts, including the functional continuity properties required for use in finite element methods. These operators seem natural in the exterior calculus framework but are unexamined in the current literature.

(5) Numerical Stability from an Inverse Discrete Hodge Star

(Sections 4.2 and 4.3) The discretization stability results ensure that dual-based methods converge, but numerical stability results are required to make efficiency versus accuracy tradeoffs between primal and dual methods. Analysis of the systems considered in Chapter 3 reveals that the definition of the discrete Hodge star operator $\mathbb{M}_k$ and its inverse are crucial to the condition number of the linear system used to solve the discrete problem. In particular, we show how to construct a sparse inverse discrete Hodge star operator $\left(\mathbb{M}_k^{Dual}\right)^{-1}$ by making use of the Whitney-like interpolation functions previously defined. As a proof of concept, we show through a particular example that the condition number of $\left(\mathbb{M}_k^{Dual}\right)^{-1}$ can be an order of magnitude better than the standard diagonal and 'mass matrix' discrete Hodge stars. The example illustrates how a dual-formulated method can offer a practical alternative to the typical primal approach.

We remark that the techniques developed in this thesis are applicable to problems in any dimension n, not just $n = 3$. Since the preponderance of modern applications are concerned with problems in $\mathbb{R}^3$ however, most results

9

and definitions have been given in this context both for clarity and immediate applicability to algorithmic design.

Parts of this thesis are based on work we presented in [46, 47, 48].

Chapter 2

Background and Preliminaries

This thesis relies on a broad background of prior work from the fields of differential topology, finite element methods, and computational geometry. The material in this chapter may be read in any order, however, it has been arranged in consideration of how it is used in the results chapters. Sections 2.1-2.9 lay the groundwork for Sections 3.1-3.5 while Sections 2.10-2.12 are the prerequisites for Section 3.6. Chapter 4 relies heavily on Sections 2.6, 2.8, and 2.10.

2.1 Continuous Exterior Calculus

We begin with a formal exposition of exterior calculus in the continuous setting based on the presentations in [1, 52].

2.1.1 Exterior Algebra

Let V be a vector space and let V^p denote the Cartesian product of p copies of V. A (real) p-**tensor on** V is a function $T : V^p \longrightarrow \mathbb{R}$ that it is linear in each variable. The **tensor product** of a p-tensor T and a q-tensor

S is defined by

$$T \otimes S(v_1, \ldots, v_p, v_{p+1}, \ldots, v_{p+q}) := T(v_1, \ldots, v_p) \cdot S(v_{p+1}, \ldots, v_{p+q})$$

Note that this operation is not symmetric. A tensor T is called **alternating** or **anti-symmetric** if and only if the sign of T is reversed whenever two variables are transposed. Let S_p denote the symmetric group on p elements. An arbitrary tensor T is associated to the alternating tensor Alt T, defined by

$$\text{Alt } T := \frac{1}{p!} \sum_{\pi \in S_p} (-1)^{\pi} T^{\pi},$$

where

$$T^{\pi}(v_1, \ldots, v_p) := T(v_{\pi(1)}, \ldots, v_{\pi(p)}).$$

Alternating p-tensors are closed under scalar multiplication and addition, thereby forming a vector space:

$$\Lambda^p(V^*) := \{\text{Alt } T : T \text{ is a } p\text{-tensor on } V\}$$

Definition 2.1. If $T \in \Lambda^p(V^*)$ and $S \in \Lambda^q(V^*)$, the **wedge product** of T and S is defined by

$$T \wedge S := \text{Alt } (T \otimes S) \in \Lambda^{p+q}(V^*)$$

$$\Diamond$$

2.1.2 Exterior Calculus

Let Ω be an n-manifold embedded in some $\mathbb{R}^N$ with $n \leq N$. Minimally, we will assume Ω is a bounded subset, but we will usually consider the case

$n = N = 3$ and assume Ω has a piecewise smooth, Lipschitz boundary as this allows us to identify Ω with its primal mesh (Definition 2.29) or dual mesh (Definition 2.33).

Definition 2.2. Let Ω be a manifold of dimension n. Given a point $x \in \Omega$, we denote the **tangent space of Ω at** x by $T_x(\Omega)$. Let $0 \leq k \leq n$. A **k-form** ω is a mapping from Ω to the space of alternating k-tensors on the tangent space of Ω at the input point. We use the notation

$$\omega : \Omega \to \Lambda^k[T_x(\Omega)^*], \qquad \omega(x) : \bigoplus_{i=1}^{k} T_x(\Omega) \to \mathbb{R},$$

where $\omega(x)$ is an alternating k-tensor. A 0-form is taken to mean a real-valued function on Ω. We denote **the space of continuous differential k-forms on Ω by** $\Lambda^k(\Omega)$. $\Diamond$

Definition 2.3. A **differential** dx_i is a 1-form whose action at $x \in M$ is to assign the ith value of the input vector from $T_x(M)$. Let $I = \{i_1, \ldots, i_k\}$ be a list of indices. Define

$$dx_I := dx_{i_1} \wedge \cdots \wedge dx_{i_k}.$$

We use the notation a_I to a real-valued function in the variables of I.

Theorem 2.4. *If* $\{dx_1, \ldots, dx_n\}$ *is an orthonormal basis for* $T_x(\Omega)$ *then*

$$\{dx_I : \quad I = \{i_1, \ldots, i_k\}, \quad 1 \leq i_1 < \cdots < i_k \leq n\}$$

is a basis for $\Lambda^k(\Omega)$. *Put differently, any k-form* $\omega \in \Lambda^k(\Omega)$ *can be written in the form*

$$\omega = \sum_I a_I dx_I$$

13

where I ranges over all strictly increasing sequences of k indices.

The theorem is a standard result from differential topology.

Definition 2.5. The space of L^2**-bounded continuous differential k-forms** on Ω is given by

$$L^2\Lambda^k(\Omega) := \left\{ \sum_I a_I dx_I \in \Lambda^k(\Omega) \; : \; a_I \in L^2(\Omega) \quad \forall I \right\}$$

$\Diamond$

Definition 2.6. The **exterior derivative** operator denoted by d is a map

$$d : \Lambda^k(\Omega) \to \Lambda^{k+1}(\Omega),$$

defined as follows. Let $I := \{i_1, \ldots, i_k\}$ denote an increasing sequence of k indices $(i_j < i_{j+1})$ and let $dx_I = dx_{i_1} \wedge \cdots \wedge dx_{i_k}$. Given $\omega = \sum_I a_I dx_I$ define

$$d\omega := \sum_I da_I \wedge dx_I \quad \text{where} \quad da_I := \sum_{i \in I} \frac{\partial a_I}{\partial x_i} dx_i. \tag{2.1}$$

$\Diamond$

We note that d commutes with pullbacks (that is, $df^*\omega = f^*d\omega$) and that if ω is a k-form and θ is any form,

$$d(\omega \wedge \theta) = d\omega \wedge \theta + (-1)^k \omega \wedge d\theta.$$

The exterior derivative plays a prominent role in Stokes' Theorem, which we now state.

14

Theorem 2.7. (Stokes) *Given a compact, oriented n-dimensional manifold Ω with boundary $\partial\Omega$ and a smooth $(n-1)$ form ω on Ω, the following equality holds:*

$$\int_{\partial\Omega} \omega = \int_\Omega d\omega.$$

Stokes' Theorem provides an alternative definition for the exterior derivative.

Definition 2.8. (Alternative Definition) Let ω be a k-form on a compact oriented n-manifold Ω $(0 \leq k < n)$. The **exterior derivative** of ω is the unique $(k+1)$-form $d\omega$ such that on any $(k+1)$-dimensional submanifold $\Pi \subset \Omega$ the following equality holds:

$$\int_\Pi d\omega = \int_{\partial\Pi} \omega.$$

$\Diamond$

It can be shown that $d\omega$ is well-defined in this way by proving the existence and uniqueness of the d map via the definition (2.1). We note that this definition will motivate the discrete exterior derivative in Definition 2.42.

Definition 2.9. The continuous Hodge star $*$ maps between forms of complementary and orthogonal dimensions, i.e. $* : \Lambda^k \to \Lambda^{n-k}$. For domains in $\mathbb{R}^3$ as considered here, $*$ is defined by the equations

$$*dx_1 = dx_2 dx_3, \quad *dx_2 = -dx_1 dx_3, \quad *dx_3 = dx_1 dx_2,$$

$$*1 = dx_1 dx_2 dx_3, \quad ** = 1,$$

where $\{dx_1, dx_2, dx_3\}$ is an orthonormal basis for $\Lambda^1(\Omega)$. $\Diamond$

A more general treatment of $*$ is given in Appendix A.

2.2 Functional Analysis

2.2.1 Distributions

The classical notion of a derivative relies strongly on the notion of well-defined point values of functions; one cannot compute $f(x + h) - f(x)$, for instance, without a definition of the values of f near x. When solving for solutions of a PDEs, it becomes useful to relax the notion of point values and, instead, to seek solutions over a space of generalized functions called distributions. This is especially relevant in solving PDEs over meshes as one can efficiently seek a solution which is smooth on each element of the mesh satisfying only minimal continuity requirements at element interfaces.

To make all this precise, we must fix a number of definitions; a complete treatment can be found in [68]. We use the usual notation for partial derivatives in arbitrary dimensions. An m-tuple $\alpha = (\alpha_1, \ldots, \alpha_m)$ of non-negative integers is called a **multi-index**. Define

$$|\alpha| := \sum_{j=1}^{m} \alpha_j \quad \text{and} \quad \alpha! := \prod_{j=1}^{m} (\alpha_j!)$$

The **derivative with respect to** α is

$$\partial^\alpha := \prod_{j=1}^{m} \left(\frac{\partial}{\partial x_j} \right)^{\alpha_j} = \frac{\partial^{|\alpha|}}{\partial x_1^{\alpha_1} \cdots \partial x_m^{\alpha_m}}.$$

Hence ∂^α is an $|\alpha|^{\text{th}}$ partial derivative where α_i derivatives are taken with respect to the ith variable.

16

The space of continuous functions on Ω with continuous mth (mixed) partial derivatives is denoted

$$C^m(\Omega) := \left\{ \psi \in C^0(\Omega) : \partial^\alpha \psi \in C^0(\Omega) \quad \text{for all } |\alpha| \leq m \right\}.$$

The L^∞ norm on $C^m(\Omega)$ is given by

$$||\psi||_{m,\infty,\Omega} := \sum_{|\alpha| \leq m} ||\partial^\alpha \psi||_{L^\infty(\Omega)}$$

The space of continuous, infinitely differentiable functions on Ω with compact support is denoted

$$\mathfrak{D}(\Omega) := C_0^\infty(\Omega) = \{\psi \in C^\infty(\Omega) : \text{supp}(\psi) \text{ is compact.}\}$$

A sequence of functions can converge in $||\cdot||_{m,\infty,\Omega}$ norm to a function without compact support meaning a stronger norm is required to get a complete metric space on $\mathfrak{D}(\Omega)$.

Definition 2.10. A sequence $\{\psi_j\}_{j=1}^\infty \subset \mathfrak{D}(\Omega)$ **converges to ψ in $\mathfrak{D}(\Omega)$** if and only if there exists a *fixed* compact set $K \subset \Omega$ such that $\text{supp}(\psi_j) \subset K$ for all j and $\lim_{j \to \infty} ||\psi_j - \psi||_{n,\infty,\Omega} = 0$ for all n. $\diamond$

In words, a sequence $\{\psi_j\}$ converges in $\mathfrak{D}(\Omega)$ if and only if the ψ_j have support in the same compact set K and their derivatives converge uniformly. From this definition, the usual notion of Cauchy sequences can be used to show that $\mathfrak{D}(\Omega)$ is complete. We can now define distributions as functionals on $\mathfrak{D}(\Omega)$.

Definition 2.11. A **distribution** on an open domain $\Omega \subset \mathbb{R}^n$ is a (sequentially)[1] continuous linear functional on $\mathfrak{D}(\Omega)$. The space of all distributions on Ω is denoted $\mathfrak{D}'(\Omega)$. The action of a distribution u on an element $\psi \in \mathfrak{D}(\Omega)$ is denoted $< u, \psi >$ ◇

Definition 2.12. A function $f : \Omega \longrightarrow \mathbb{R}$ is said to be in L^1_{loc} if it is **locally integrable**, i.e. if

$$\int_K |f| < \infty$$

for all bounded, measurable subsets $K \subset \Omega$. Any such function can be associated with the distribution u defined by

$$< u, \psi >:= \int_\Omega f\psi$$

for any $\psi \in \mathfrak{D}(\Omega)$. Hence we have a canonical inclusion mapping

$$\iota : L^1_{\text{loc}} \hookrightarrow \mathfrak{D}'(\Omega).$$

A distribution $u \in \mathfrak{D}'(\Omega)$ is said to be **regular** if there exists $f \in L^1_{\text{loc}}$ such that $\iota f = u$.   ◇

Note that if $x_0 \in \Omega$ and α is a multi-index, the distribution $< u, \psi >:= \partial^\alpha \psi(x_0)$ is an example of a non-regular or 'singular' distribution. In this thesis, however, we will only be concerned with regular distributions.

The action of an operator on a distribution is expressed via a pullback operation. Suppose $T : \mathfrak{D}(\Omega) \longrightarrow \mathfrak{D}(\Omega)$ is sequentially continuous and linear.

---

[1] It can be shown that a linear functional on $\mathfrak{D}(\Omega)$ is continuous if and only if it is sequentially continuous, hence we put sequentially in parentheses.

Given a distribution $u \in \mathfrak{D}'(\Omega)$, the **pullback** $T^* : \mathfrak{D}'(\Omega) \longrightarrow \mathfrak{D}'(\Omega)$ is defined by the relationship

$$< u, T\psi > = < T^*u, \psi > \quad \forall \psi \in \mathfrak{D}(\Omega),$$

where T^*u denotes the pullback of u by T, that is, $T^*u := u \circ T \in \mathfrak{D}'(\Omega)$. This allows us to define a generalization of the derivative.

Definition 2.13. Given a regular distribution $u \in \mathfrak{D}'(\Omega)$ and a multi-index α, the derivative of u with respect to α is denoted D^α. It is defined as the pullback of ∂^α on f, i.e.

$$< D^\alpha u, \psi > := (-1)^{|\alpha|} < u, \partial^\alpha \psi > \quad \forall \psi \in \mathfrak{D}(\Omega).$$

With this tool, we can now think about the ∇ operator in $\mathbb{R}^3$ as a differential operator on distributions given by

$$\nabla := (D^{(1,0,0)}, D^{(0,1,0)}, D^{(0,0,1)}).$$

The curl and div operators in $\mathbb{R}^3$ act on vectors of distributions and will be denoted as usual by $\nabla \times$ and $\nabla \cdot$, respectively. $\Diamond$

In the remainder of the thesis, functions should be understood in a distributional sense, but we will only need to resort to the terminology defined here when it is required for proofs and arguments.

We will make use, in particular of the following Sobolev norms and semi-norms on distributions.

Definition 2.14. Let $m \geq 0$ be an integer. The m**th** L^2 **Sobolev semi-norm** over a set $\Omega \in \mathbb{R}^n$ is defined by

$$|u|^2_{H^m} := \sum_{|\alpha|=m} \left(\int_\Omega |D^\alpha u|^2 \right)^{\frac{1}{2}}$$

The m**th** L^2 **Sobolev norm** is given by

$$||u||^2_{H^m} := \sum_{0 \leq k \leq m} |u|^2_{H^k}$$

The H^0 norm is the L^2 norm and will be denoted by $||\cdot||_{L^2}$. ◇

2.2.2 Hilbert Complexes

Definition 2.15. A real **Hilbert space** W is a vector space with a real-valued inner product $(\cdot, \cdot)$ such that W is complete with respect to the norm given by

$$||w||_W := (w, w)^{1/2}.$$

A **Hilbert complex** (W, d) is a sequence of Hilbert spaces W^k and a sequence of closed, densely defined linear operators $d_k : W^k \to W^{k+1}$ such that the range of d_k is contained in the kernel of d_{k+1}, i.e.

$$d_{k+1} \circ d_k = 0.$$

The **domain complex** (V, d) associated to (W, d) is the sequence of spaces $V^k := \text{domain}(d_k) \subset W^k$ along with the **graph norm** defined via the inner product

$$(u, v)_{V^k} := (u, v)_{W^k} + (d_k u, d_k v)_{W^{k+1}}.$$

◇

2.2.3 The deRham Complex

Definition 2.16. The space of L^2-bounded differential forms (Definition 2.5) along with the exterior derivative map define a Hilbert complex $(L^2\Lambda, d)$. The associated domain complex, denoted $(H\Lambda, d)$ is called the L^2 **deRham complex**:

$$0 \longrightarrow H\Lambda^0 \xrightarrow{d_0} H\Lambda^1 \xrightarrow{d_1} \cdots \xrightarrow{d_{n-1}} H\Lambda^n \longrightarrow 0$$

$\diamondsuit$

In the case $n = 3$, the norms on the spaces $H\Lambda^k$ reduce to standard scalar and vector norms from finite element theory. To understand this reduction, however, we must define maps between the spaces of differential forms Λ^k and spaces of scalar and vector fields over Ω. The maps from forms to fields are called the **sharp** ($\#$) maps while the maps from fields to forms are called the **flat** ($\flat$) maps.

Since the maps are primarily a technical tool for proving convergence results, we will only define the flat maps in the case $n = 3$. A general treatment of these maps can be found in, for instance, [1, 59].

Definition 2.17. Let $n = 3$ and let $k = 0$, 1, 2, or 3. The **flat map** converts a scalar field $\phi : \Omega \to \mathbb{R}$ (for $k = 0$ or 3) or vector field $\vec{u} : \Omega \to \mathbb{R}^3$ (for $k = 1$ or 2) to a k-form as indicated in Table 2.1. The pre-superscript indicates the value of k. The field is called the scalar or vector **proxy** for the associated form.

21

k	field	associated k-form on Ω given by flat operator
0	ϕ	$^0\phi(x)$ $:$ $\emptyset \longrightarrow \mathbb{R}$ s.t. $\emptyset \mapsto \phi(x)$
1	$\vec{u}$	$^1\vec{u}(x)$ $:$ $T_x(\Omega) \longrightarrow \mathbb{R}$ s.t. $v_1 \mapsto \vec{u}(x) \cdot v_1$
2	$\vec{u}$	$^2\vec{u}(x)$ $:$ $(T_x(\Omega))^2 \longrightarrow \mathbb{R}$ s.t. $(v_1, v_2) \mapsto \vec{u}(x) \cdot (v_1 \times v_2)$
3	ϕ	$^3\phi(x)$ $:$ $(T_x(\Omega))^3 \longrightarrow \mathbb{R}$ s.t. $(v_1, v_2, v_3) \mapsto \phi(x)(v_1 \cdot (v_2 \times v_3))$

Table 2.1: Definition of flat maps for $n = 3$.

The flat operators allow us to understand the continuous exterior calculus operators d and $*$ in terms of their actions on the associated scalar and vector fields.

Lemma 2.18. *For $n = 3$, and ϕ, $\vec{u}$ as in Definition 2.17, the following relationships between flat operators hold:*

$$d(^0\phi) = {}^1(\text{grad } \phi) \qquad d(^1\vec{u}) = {}^2(\text{curl } \vec{u}) \qquad d(^2\vec{u}) = {}^3(\text{div } \vec{u}).$$

$$* \, ^0\phi = {}^3\phi \qquad * \, ^1\vec{u} = {}^2\vec{u} \qquad * \, ^2\vec{u} = {}^1\vec{u} \qquad * \, ^3\phi = {}^0\phi$$

$$^0\phi \wedge {}^3\phi = {}^3(|\phi|^2) \qquad ^1\vec{u} \wedge {}^2\vec{u} = {}^3(|\vec{u}|^2)$$

Proof. Fix ϕ and $\vec{u}$ as in Definition 2.17. Fix $x \in \Omega$. Write $\vec{u}$ in terms of its component functions $u_i : \Omega \to \mathbb{R}$, i.e. $\vec{u} = (u_1, u_2, u_3)$. For ease of notation, we have omitted notation indicating that all partial derivatives are meant to

22

be evaluated at x. By Definition 2.17,

$$^0\phi = \phi$$

$$^1\vec{u} = u_1 dx_1 + u_2 dx_2 + u_3 dx_3$$

$$^2\vec{u} = u_1 dx_2 dx_3 + u_2 dx_3 dx_1 + u_3 dx_1 dx_2$$

$$^3\phi = \phi dx_1 dx_2 dx_3$$

Using the fact that $dx_i \wedge dx_i = 0$, we compute

$$d(^0\phi) = \left(\frac{\partial\phi}{\partial x_1}\right) dx_1 + \left(\frac{\partial\phi}{\partial x_2}\right) dx_2 + \left(\frac{\partial\phi}{\partial x_3}\right) dx_3$$

$$d(^1\vec{u}) = \left(\frac{\partial u_2}{\partial x_1} - \frac{\partial u_1}{\partial x_2}\right) dx_1 dx_2 + \left(\frac{\partial u_1}{\partial x_3} - \frac{\partial u_3}{\partial x_1}\right) dx_3 dx_1$$

$$+ \left(\frac{\partial u_3}{\partial x_2} - \frac{\partial u_2}{\partial x_3}\right) dx_2 dx_3$$

$$d(^2\vec{u}) = \left(\frac{\partial u_1}{\partial x_1} + \frac{\partial u_2}{\partial x_2} + \frac{\partial u_3}{\partial x_3}\right) dx_1 dx_2 dx_3$$

$$d(^3\phi) = 0$$

The results are immediate from the definitions of grad, curl, div, d, and $*$. $\square$

Definition 2.19. Let $n = 3$. The $H(\mathrm{curl})$ **and** $H(\mathrm{div})$ **norms** on a vector function $\vec{u} : \Omega \to \mathbb{R}^3$ are defined by

$$||\vec{u}||_{H(\mathrm{curl})} := ||\vec{u}||^2_{[L^2]^3} + ||\mathrm{curl}\ \vec{u}||^2_{[L^2]^3}$$

$$||\vec{u}||_{H(\mathrm{div})} := ||\vec{u}||^2_{[L^2]^3} + ||\mathrm{div}\ \vec{u}||^2_{L^2}$$

where $||\cdot||_{[L^2]^3}$ denotes the sum of the L^2 norms of the component functions of the vector-valued input. $\Diamond$

23

Remark 2.20. For $n = 3$, there is a natural equivalence between norms on scalar and vector functions and the graph norms of their images under an appropriate flat mapping. More precisely,

$$
\begin{aligned}
\left\|{}^0\phi\right\|_{H\Lambda^0} &= \|\phi\|_{H^1} \\
\left\|{}^1\vec{u}\right\|_{H\Lambda^1} &= \|\vec{u}\|_{H(\mathrm{curl})} \\
\left\|{}^2\vec{u}\right\|_{H\Lambda^2} &= \|\vec{u}\|_{H(\mathrm{div})} \\
\left\|{}^3\phi\right\|_{H\Lambda^3} &= \|\phi\|_{L^2}
\end{aligned}
$$

Accordingly, the L^2 deRham complex can be written equivalently as

$$
H^1 \xrightarrow{\mathrm{grad}} H(\mathrm{curl}) \xrightarrow{\mathrm{curl}} H(\mathrm{div}) \xrightarrow{\mathrm{div}} L^2. \tag{2.2}
$$

2.3 Primal and Dual Domain Meshes

2.3.1 Manifold-like Simplicial Complexes

In algebraic topology, manifolds are discretized using simplicial complexes, a notion which guides the entire theory of discrete exterior calculus. We state the definition of simplicial complex here, along with supporting definitions to be used throughout. These definitions can be found in algebraic topology texts such as Armstrong [4], Hatcher [53] and Hirani [59].

Definition 2.21. A k-**simplex** σ^k is the convex hull of $k + 1$ geometrically independent points $v_0, \ldots, v_k \in \mathbb{R}^N$. Any simplex spanned by a (proper) subset of $\{v_0, \ldots, v_k\}$ is called a **(proper) face** of σ^k. The union of the proper faces of σ^k is called its **boundary** and denoted $\mathrm{Bd}(\sigma^k)$. The **interior** of σ^k is

$\text{Int}(\sigma^k) = \sigma^k \backslash \text{Bd}(\sigma^k)$. Note that $\text{Int}(\sigma^0) = \sigma^0$. The **volume** of σ^k is denoted $|\sigma^k|$. Define $|\sigma^0| = 1$. $\diamondsuit$

We will indicate that a simplex has dimension k with a superscript, e.g. σ^k, and will index simplices of any dimension with subscripts, e.g. σ_i.

Definition 2.22. A **simplicial complex** K in $\mathbb{R}^N$ is a collection of simplices in $\mathbb{R}^N$ such that

I. Every face of a simplex of K is in K.

II. The intersection of any two simplices of K is either a face of each of them or it is empty.

The union of all simplices of K treated as a subset of $\mathbb{R}^N$ is called the underlying space of K and is denoted by $|K|$. $\diamondsuit$

Definition 2.23. A simplicial complex of dimension n is called a **manifold-like simplicial complex** if and only if $|K|$ is a C^0-manifold, with or without boundary. More precisely,

I. All simplices of dimension k with $0 \le k \le n-1$ must be a face of some simplex of dimension n in K.

II. Each point on $|K|$ has a neighborhood homeomorphic to $\mathbb{R}^n$ or n-dimensional half-space. $\diamondsuit$

Remark 2.24. Since DEC is meant to treat discretizations of manifolds, we will assume all simplicial complexes are manifold-like from here forward. We note that $|K|$ is thought of as a piecewise linear approximation of a smooth manifold Ω. Formally, this is taken to mean that there exists a homeomorphism h between $|K|$ and Ω such that h is isotopic to the identity. In applications, however, knowing h or Ω explicitly may be irrelevant or impossible as K often encodes everything known about Ω. This emphasizes the usefulness of DEC as a theory built for discrete settings. $\Diamond$

2.3.2 Orientation of Simplicial Complexes

We now review how to orient a simplicial complex K. The definitions and conventions adopted here are taken from Hirani [59].

Definition 2.25. Define two orderings of the vertices of a simplex σ^k ($k \geq 1$) to be equivalent if they differ by an even permutation. Thus, there are two equivalence classes of orderings, each of which is called an **orientation** of σ^k. If σ^k is written as $[v_0, \ldots, v_k]$, the orientation of σ^k is understood to be the equivalence class of this ordering. $\Diamond$

Definition 2.26. Let $\sigma^k = [v_0, \ldots, v_k]$ be an oriented simplex with $k \geq 2$. This gives an **induced orientation** on each of the $(k-1)$-dimensional faces of σ^k as follows. Each face of σ^k can be written uniquely as $[v_0, \ldots, \hat{v}_i, \ldots, v_k]$, where $\hat{v}_i$ means v_i is omitted. If i is even, the induced orientation on the face is the same as the oriented simplex $[v_0, \ldots, \hat{v}_i, \ldots, v_k]$. If i is odd, it is the opposite. $\Diamond$

We note that this formal definition of induced orientation agrees with the notion of orientation induced by the boundary operator (Definition 2.41). In that setting, a 0-simplex can also receive an induced orientation.

Remark 2.27. We will need to be able to compare the orientation of two oriented k-simplices σ^k and τ^k. This is possible only if at least one of the following conditions holds:

I. There exists a k-dimensional affine subspace $P \subset \mathbb{R}^N$ containing both σ^k and τ^k.

II. σ^k and τ^k share a face of dimension $k - 1$.

In the first case, write $\sigma^k = [v_0, \ldots, v_k]$ and $\tau^k = [w_0, \ldots, w_k]$. Note that $\{v_1 - v_0, v_2 - v_0, \ldots, v_k - v_0\}$ and $\{w_1 - w_0, w_2 - w_0, \ldots, w_k - w_0\}$ are two ordered bases of P. We say σ^k and τ^k have the same orientation if these bases orient P the same way. Otherwise, we say they have opposite orientations. In the second case, σ^k and τ^k are said to have the same orientation if the induced orientation on the shared $k - 1$ face induced by σ^k is *opposite* to that induced by τ^k. $\diamond$

Definition 2.28. Let σ^k and τ^k with $1 \leq k \leq n$ be two simplices whose orientations can be compared, as explained in Remark 2.27. If they have the same orientation, we say the simplices have a **relative orientation** of $+1$, otherwise -1. This is denoted as $\mathrm{sgn}(\sigma^k, \tau^k) = +1$ or -1, respectively. $\diamond$

Definition 2.29. A manifold-like simplicial complex K of dimension n is called an **oriented manifold-like simplicial complex** if adjacent n-simplices agree on the orientation of their shared face. Such a complex will be called a **primal mesh** from here forward. $\diamond$

2.3.3 Dual Complexes

Dual complexes are defined relative to a primal mesh. While they represent the same subset of $\mathbb{R}^N$ as their associated primal mesh, they create a different data structure for the geometrical information and become essential in defining the various operators needed for DEC.

Definition 2.30. The **circumcenter** of a k-simplex σ^k is given by the center of the unique k-sphere that has all $k+1$ vertices of σ^k on its surface. It is denoted $c(\sigma^k)$. A simplex σ^k is said to be **well-centered** if $c(\sigma^k) \in \mathrm{Int}(\sigma^k)$. A **well-centered simplicial complex** is one in which all simplices (of all dimensions) in the complex are well-centered. $\diamond$

Definition 2.31. Let K be a well-centered primal mesh of dimension n and let σ^k be a simplex in K. The **circumcentric dual cell** of σ^k, denoted $D(\sigma^k)$, is given by

$$D(\sigma^k) := \bigcup_{r=0}^{n-k} \bigcup_{\sigma^k \prec \sigma_1 \prec \cdots \prec \sigma_r} \mathrm{Int}(c(\sigma^k)c(\sigma_1)\ldots c(\sigma_r)).$$

To clarify, the inner union is taken over all sequences of r simplices such that σ^k is the first element in the sequence and each sequence element is a proper face of its successor. Hence, σ_1 is a $(k+1)$ simplex and σ_r is an n simplex.

For $r = 0$, this is to be interpreted as the sequence σ^k only. The closure of the dual cell of σ^k is denoted $\bar{D}(\sigma^k)$ and called the **closed dual cell**. We will use the notation $\star$ to indicate dual cells, i.e.

$$\star \sigma := \bar{D}(\sigma).$$

Each $(n-k)$-simplex on the points $c(\sigma^k), c(\sigma_1), \ldots, c(\sigma_r)$ is called an **elementary dual simplex** of σ^k. The collection of dual cells is called the **dual cell decomposition** of K and denoted $D(K)$ or $\star K$. $\qquad \Diamond$

Some examples of dual cells are shown in Figure 2.1 and discussed in its caption. Note that the dual cell decomposition forms a CW complex (see Munkres [71] for more on this).

2.3.4 Orientation of Dual Complexes

Orientation of the dual complex must be done in a such a way that it "agrees" with the orientation of the primal mesh. This can be done canonically since a primal simplex and any of its elementary dual simplices have complementary dimension and live in orthogonal affine subspaces of $\mathbb{R}^N$. We make this more precise and fix the necessary conventions with the following definitions.

Definition 2.32. Let K be a primal mesh containing a sequence of simplices $\sigma^0 \prec \sigma^1 \prec \cdots \prec \sigma^n$ and let σ^k be one of these simplices with $1 \leq k \leq n-1$. The **orientation** of the elementary dual simplex with vertices $c(\sigma^k), \ldots, c(\sigma^n)$

29
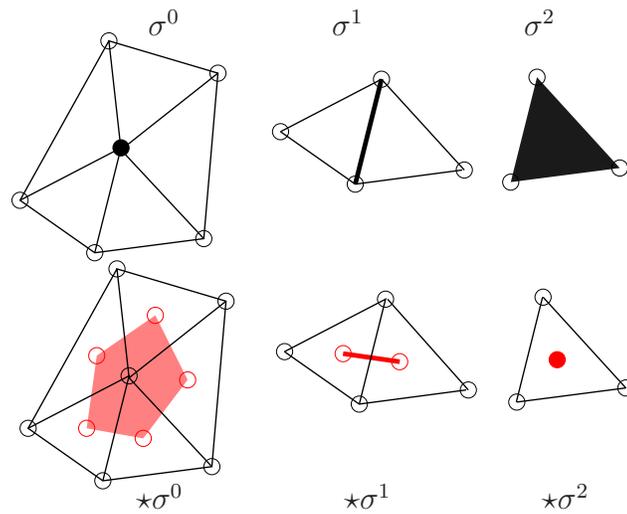
Figure 2.1: Primal simplices are shown in black in the top row: σ^0 is a vertex, σ^1 is an edge, and σ^2 is a face. Their corresponding dual cells for $n = 2$ are shown in red (or grey, if no color) on the bottom row: $\star\sigma^2$ is the barycenter of σ^2, $\star\sigma^1$ is an edge between barycenters, and $\star\sigma^0$ is a planar polygon with barycenters as vertices. In three dimensions ($n = 3$), primal vertices have dual polytopes, primal edges have dual polygonal facets, primal faces have dual edges, and primal volumes have dual vertices.

is $s[c(\sigma^k), \ldots, c(\sigma^n)]$ where $s \in \{-1, +1\}$ is given by the formula

$$s := \mathrm{sgn}\left([c(\sigma^0), \ldots, c(\sigma^k)], \sigma^k\right) \times \mathrm{sgn}\left([c(\sigma^0), \ldots, c(\sigma^n)], \sigma^n\right).$$

The sgn function was defined in Definition 2.28.

For $k = n$, the dual element is a vertex which has no orientation. For $k = 0$, define $s := \mathrm{sgn}\left([c(\sigma^0), \ldots, c(\sigma^n)], \sigma^n\right).$ ◊

The above definition serves to orient all the elementary dual simplices associated to σ^k and hence all simplices in a dual cell decomposition. Further, the orientations on the elementary dual simplices induce orientations on the boundaries of dual cells in the same manner as given in Definition 2.26. The induced orientations on adjacent $(n-1)$ cells will agree since the dual cell decomposition comes from a primal mesh (see Definition 2.29).

Definition 2.33. The oriented dual cell decomposition of a primal mesh is called the **dual mesh**. ◊

2.4 Functional Conformity over Meshes

Having described domain decomposition via primal and dual meshes and their refinements, we can now seek solutions to PDEs defined piecewise over each mesh element. To ensure that the global solution lies in the appropriate space of the L^2 deRham complex (see (2.2)), certain compatibility conditions must be satisfied at the interface of two adjacent mesh elements. A useful reference for this material is Ern and Guermond [38].

31

Theorem 2.34. *Let K denote a primal or dual mesh with $n = 3$. Let u be a distribution over K such that for each element $T \in K$, $u \in C^1(\operatorname{Int} T)$ and u has a continuous extension from $\operatorname{Int} T$ to ∂T. Let F denote a codimension 1 internal facet in T, shared by mesh elements denoted T_1 and T_2. Let $\hat{n}_i$ denote the outward normal vector to T_i with respect to facet F, and let u_i denote the continuous extension of u from T_i to F. Then*

$$u \in H^1(K) \iff u_1 \hat{n}_1 + u_2 \hat{n}_2 = 0, \quad \forall F \in K. \tag{2.3}$$

Proof. The proof is adapted from Ern and Guermond [38]. Let $w_j \in L^2(K)$ be defined by $w_j|_{\operatorname{Int} T} := \partial_j(u|_{\operatorname{Int} T})$. Let $\psi \in \mathfrak{D}(K)$. By the definitions in Section 2.2.1 and by Stokes' theorem,

$$
\begin{aligned}
< w_j, \psi > \ &= \ \int_K w_j \psi = \sum_{T \in K} \int_T w_j \psi \\
&= \ -\sum_{T \in K} \int_T u|_{\operatorname{Int} T} \partial_j \psi + \sum_{T \in K} \int_{\partial T} \psi(u|_{\operatorname{Int} T} n_{T,j}) \\
&= \ - < D^j u, \psi > + \sum_{T \in K} \int_{\partial T} \psi(u|_{\operatorname{Int} T} n_{T,j})
\end{aligned}
$$

where $n_{T,j}$ is the jth component of $\hat{n}_T$. Hence showing that the last sum is identically zero is both necessary and sufficient to say that u has a jth partial derivative in $L^2(K)$ in a distributional sense. Regroup this sum to arrive at

$$\sum_{T \in K} \int_{\partial T} \psi(u|_{\operatorname{Int} T} n_{T,j}) = \sum_{F \in K} \psi e_j \cdot (u_1 \hat{n}_1 + u_2 \hat{n}_2)$$

where $\{e_1, e_2, e_3\}$ is the standard basis for $\mathbb{R}^3$. Thus $e_j \cdot (u_1 \hat{n}_1 + u_2 \hat{n}_2)$ must be identically zero for $j = 1, 2, 3$, yielding the result. $\square$

Corollary 2.35. *If $u_1 \equiv u_2$ on each face $F \in K$ then $u \in H^1(K)$.*

Proof. Since $\hat{n}_2 = -\hat{n}_1$, condition (2.3) can be re-written as

$$(u_1 - u_2)\hat{n}_1 = 0, \quad \forall F \in K,$$

from which the result follows. $\qquad\square$

Theorem 2.36. *Let K denote a primal or dual mesh with $n = 3$. Let $\vec{z} :=\; < u_1, u_2, u_3 >$ be a vector of distributions over K where each u_i satisfies the hypotheses of Theorem 2.34. Let $\vec{z}_i$ denote the continuous extension of $\vec{z}$ from T_i to F. The following characterizations hold.*

$$\vec{z} \in H(\mathrm{curl}) \iff \vec{z}_1 \times \hat{n}_1 + \vec{z}_2 \times \hat{n}_2 = 0, \quad \forall F \in K,$$

$$\vec{z} \in H(\mathrm{div}) \iff \vec{z}_1 \cdot \hat{n}_1 + \vec{z}_2 \cdot \hat{n}_2 = 0, \quad \forall F \in K.$$

The proof of Theorem 2.36 works in the same way as the proof of Theorem 2.34.

Corollary 2.37. *For each $F \in K$, write $\vec{z}_i = T_F(\vec{z}_i) + N_F(\vec{z}_i)$ where $T_F(\vec{z}_i)$ and $N_F(\vec{z}_i)$ are the tangential and normal components of $\vec{z}_i$ on F, respectively.*

    i. If $T_F(\vec{z}_1) = T_F(\vec{z}_2)$ for all $F \in K$ then $\vec{z} \in H(\mathrm{curl})$.

   ii. If $N_F(\vec{z}_1) = N_F(\vec{z}_2)$ for all $F \in K$ then $\vec{z} \in H(\mathrm{div})$.

Proof. The result follows from the observations that $N_F(\vec{z}_i) \times \hat{n}_i = 0$ and $T_F(\vec{z}_i) \cdot \hat{n}_i = 0$. $\qquad\square$

The functional conformity theorems provide sufficient conditions to ensure the various types of continuity required for piecewise approximation of solutions to PDEs. It will be shown how associating degrees of freedom of the solutions with mesh vertices, edges, or faces can yield solutions guaranteed to be in H^1, $H(\mathrm{curl})$, or $H(\mathrm{div})$, respectively. Hence, the take-away message from the functional conformity theorems is that functions with $H\Lambda^k$ conformity require agreement along k-dimensional mesh elements.

In the finite element world, this dimensionality observation was made famous by the elements of Nédélec [72, 73] and Raviart and Thomas [80]. It was popularized in the field of electromagnetics [33, 9] and expanded to nearly-rectangular grids by Hyman and Shashkov [64, 63, 65]. Bossavit [20] and Hiptmair [55] championed a more general theory along these lines, leading the way toward the theories of finite element exterior calculus and discrete exterior calculus of today.

2.5 Discrete Exterior Calculus

2.5.1 Discrete Differential Forms

Definition 2.38. Let K be a primal mesh of a compact n-manifold Ω. Let K_k denote the k-simplices of K. A **primal k-chain** c is a linear combination of the elements of K_k:

$$c = \sum_{\sigma \in K_k} c_\sigma \sigma,$$

where $c_\sigma \in \mathbb{R}$. The set of all such chains form the **vector space of primal k-chains**, denoted $\mathcal{C}_k$. It has dimension $|\mathcal{C}_k|$, equal to the number of elements

of K_k. A k-chain c is represented as a column vector of length $|\mathcal{C}_k|$.

Similarly, a **dual k-chain** is a linear combination of k-cells of the dual complex $\star K$. The vector space of dual k-chains is denoted $\overline{\mathcal{C}}_k$. ◇

Definition 2.39. A **primal k-cochain** w is a linear functional on primal k-chains, i.e.

$$\mathrm{w} : \mathcal{C}_k \to \mathbb{R} \quad \text{via} \quad c \mapsto \mathrm{w}(c),$$

where w is a linear mapping. It is represented as a column vector of length $|\mathcal{C}_k|$ so that the action of w on a k-chain c is the matrix multiplication $\mathrm{w}^T c$, yielding the scalar $\mathrm{w}(c)$. The space of primal cochains is denoted $\mathcal{C}^k$.

A **dual k-cochain** $\overline{\mathrm{w}}$ is a linear functional on dual k-chains, i.e.

$$\overline{\mathrm{w}} : \overline{\mathcal{C}}_k \to \mathbb{R} \quad \text{via} \quad c \mapsto \overline{\mathrm{w}}(c),$$

where $\overline{\mathrm{w}}$ is a linear mapping. The space of dual cochains is denoted $\overline{\mathcal{C}}^k$. ◇

Cochains are the discrete analogues of differential forms as they can be evaluated over k-dimensional subspaces. To make this precise, we define the integration of a cochain over a chain to be the evaluation of the cochain as a function.

Definition 2.40. The **integral** of a primal k-cochain w over a primal k-chain c is defined to be

$$\int_c \mathrm{w} := \mathrm{w}^T c = \mathrm{w}(c).$$

Hence, the integration of w over c is exactly the same as the evaluation of w on c. ◇

35

2.5.2 Discrete Exterior Derivative

The definition of a discrete exterior derivative is motivated by the alternative definition of the continuous operator (Definition 2.8). First we define the boundary operator in the discrete case.

Definition 2.41. The k**th boundary operator** denoted by ∂_k takes a primal k-chain to its primal $(k-1)$-chain boundary. It is defined by its action on an oriented k-simplex:

$$\partial_k[v_0, v_1, \cdots, v_k] := \sum_{i=0}^{k}(-1)^i[v_0, \cdots, \widehat{v_i}, \cdots, v_k]$$

where $\widehat{v_i}$ indicates that v_i is omitted. The primal boundary operator is represented as a matrix of size $|\mathcal{C}_{k-1}| \times |\mathcal{C}_k|$ so that the action of ∂_k on a k-chain c is the usual matrix multiplication $\partial_k c$. $\Diamond$

Definition 2.42. The k**th discrete exterior derivative** of a primal k-cochain w is the transpose of the $(k+1)$st boundary operator:

$$\mathbb{D}_k = \partial_{k+1}^T.$$

This is also referred to in the literature as the **coboundary operator**. It is represented as a matrix of size $|\mathcal{C}_{k+1}| \times |\mathcal{C}_k|$ so that the action of $\mathbb{D}_k$ on a primal k-cochain w is the usual matrix multiplication $\mathbb{D}_k \mathrm{w} := \partial_{k+1}^T \mathrm{w}$. $\Diamond$

The discrete exterior derivative satisfies the discrete version of Stokes' theorem.

Lemma 2.43. *Let* w *be a primal k-cochain and $c \in C_{k+1}$ any primal $(k+1)$-chain. Then*

$$\int_c \mathbb{D}_k w = \int_{\partial_{k+1} c} w.$$

Proof. By Definition 2.40 we see that

$$\int_{\partial_{k+1} c} w = w^T \partial_{k+1} c = (\partial^T_{k+1} w)^T c = (\mathbb{D}_k w)^T c = \int_c \mathbb{D}_k w.$$

$\square$

We now consider the analogous constructions for dual cochains. Observe that mesh duality allows us to view a dual k-chain $\bar{c}$ as a primal $(n-k)$-chain c. Hence ∂^T_{n-k+1} serves as a boundary operator on dual k-cochains, giving us the following definition.

Definition 2.44. The **kth discrete exterior derivative** of a dual k-cochain $\overline{w}$ is $\mathbb{D}^T_{n-k-1}$, which is equal to ∂_{n-k}. It is represented as a matrix of size $|\overline{C}_{k+1}| \times |\overline{C}_k|$. $\Diamond$

2.5.3 Primal and Dual Projection Maps

The $\mathcal{P}_k$ and $\overline{\mathcal{P}}_k$ maps are deRham projection maps, from k-forms to primal or dual k-cochains. The intuitive definition of the maps is simple enough to describe. For example, $\mathcal{P}_k u$ should be a primal k-cochain whose ith entry represents the integral of the k-form u over the ith primal k-simplex.

To make this precise, however, a choice must be made between ease of definition and the amount of continuity assumed for u. For instance, if

ψ is a 0-form over $\Omega \subset \mathbb{R}^3$, then ψ is properly treated as a distribution as described in Section 2.2.1. Since distributions need not have well-defined point values, the notion of the "integral of ψ over a 0-simplex" has little hope of leading to a simple definition for $\mathcal{P}_0\psi$. Still, from a physical perspective, there is no problem with this notion; if ψ represents an electric potential, it can be measured at an arbitrary point location by a voltmeter or other device appropriate to the scale of Ω.

This issue is one of the dividing lines between the finite element exterior calculus (FEEC) and discrete exterior calculus (DEC) camps (see Section 1.2). In the DEC camp, it is assumed that there is a well-defined value of the integral of a k-form over a k-dimensional primal or dual mesh element. The resulting definitions of $\mathcal{P}_k$ and $\overline{\mathcal{P}}_k$ are simple:

$$\mathcal{P}_k(u) := \left\{ \int_{\sigma_i^k} u \right\}_i \quad \text{and} \quad \overline{\mathcal{P}}_k(u) := \left\{ \int_{\star\sigma_i^{n-k}} u \right\}_i$$

These definitions are not adequate in the FEEC camp since, in that setting, the minimal continuity requirements on u (e.g. H^1 for $k = 0$) are not sufficient to guarantee that $\int_{\sigma_i^k} u$ is well defined.

To deal with this problem, u is L^2-projected to a differential form whose coefficient functions are polynomials of degree at most r. This process is called Clément interpolation[2] and can be used to get optimal order error estimates.

---

[2]In the finite element community, 'interpolation' typically refers to a mapping from a form or function space to a piecewise polynomial space. This can be understood as the composition $\mathcal{I}_k\mathcal{P}_k$ in the terminology of this thesis.

Unfortunately, Clément interpolation lacks certain necessary properties required for stability analysis such as commutativity with the exterior derivative operator. To resolve this, Arnold, Falk and Winther have defined smoothed projection operators which do satisfy these properties [7, 6]. Their approach is based on the tools of Schöberl [81] and was refined by Christensen [27]. The operators take as input a k-form, convolve it with a mollifier function, and restrict it to each mesh element. The output of this smoothing is a k-form with sufficient smoothness to be integrated over the k-simplices of the mesh.

The precise definition of the smoothed interpolation operators will not be given in this thesis as it is not needed for our analysis. Further, extending the definition of the smoothed projection operators to apply on non-simplicial dual meshes is non-trivial. Thus, we will use a slightly more formal definition of the projection maps than the DEC community and assume sufficient regularity on their inputs to ensure they are well-defined. We will also note when it is possible to use the smoothed projections to get the same results with fewer regularity assumptions, at least for primal meshes.

Definition 2.45. Given a k-simplex σ_i^k or dual k-cell $\star\sigma_i^{n-k}$ associated to a primal mesh $K \subset \mathbb{R}^N$, define the **inclusion mapping**

$$\phi : \sigma_i^k \hookrightarrow K, \quad \text{or} \quad \phi : \star\sigma_i^{n-k} \hookrightarrow K.$$

The projection maps of a k-form u on Ω are defined by

$$\mathcal{P}_k(u) := \left\{ \int_{\sigma_i^k} \phi^* u \right\}_i \tag{2.4}$$

$$\overline{\mathcal{P}}_k(u) := \left\{ \int_{\star\sigma_i^{n-k}} \phi^* u \right\}_i \tag{2.5}$$

In words, the ith entry of the cochain is the integral over the ith primal or dual cell of the pullback of u by the appropriate inclusion mapping. $\qquad \diamondsuit$

For example, consider the effect of the mapping $\mathcal{P}_1$ on a 1-form u with respect to a tetrahedral mesh in $\mathbb{R}^3$. The ith entry of $\mathcal{P}_1 u$ is then

$$\{\mathcal{P}_1(u)\}_i = \int_{\sigma_i^k} u^\sharp \cdot \frac{\vec{\sigma_i^k}}{|\sigma_i^k|}.$$

In words, this is the vector proxy of u (denoted $u^\sharp$), projected onto a unit vector in the direction of edge σ_i^1, and integrated over σ_i^1. Hence, the pullback results in a computation of the circulation of u over the edge. Similarly, the pullback of a 2-form u in $\mathbb{R}^3$ to a face yields the flux of u over the face. More examples can be found in Guillemin and Pollack [52, Chapter 4].

2.6   Whitney Interpolation for Primal Meshes

While the deRham maps defined in Section 2.5.3 provide a way to project continuous differential forms to discrete cochains, we also need maps to reconstruct continuous differential forms from cochain data. We call such maps **interpolation maps** and focus in this section on maps from primal cochain spaces to form spaces. We want maps of the form

$$\mathcal{I}_k : \mathcal{C}^k \to \Lambda^k \quad \text{given by} \quad \mathcal{I}_k(\mathrm{w}) := \sum_{\sigma^k \in \mathcal{C}_k} \mathrm{w}(\sigma^k) \mathcal{W}_{\sigma^k}, \tag{2.6}$$

where $\mathcal{W}_{\sigma^k}$ is a basis function associated to the k-simplex σ^k. These basis functions should be defined so that the following natural properties hold.

40

W1. **Conformity in $H\Lambda^k$:** $\mathcal{I}_k(\mathrm{w}) \in H\Lambda^k$

W2. **Local support:** $\operatorname{supp} \mathcal{W}_{\sigma^k} \subseteq \bigcup_{\sigma^n \succ \sigma^k} \sigma^n$

W3. **Interpolation:** $\int_{\sigma_i^k} \phi^*(\mathcal{W}_{\sigma_i^k}) = 1$

W4. **Optimal Convergence:** $\|u - \mathcal{I}_k \mathcal{P}_k u\|_{H\Lambda^k} \leq C\, \mathrm{m_d}$

W5. **Commutativity with exterior derivative:** $d_k \mathcal{I}_k = \mathcal{I}_{k+1} \mathbb{D}_k$

A natural construction for the $\mathcal{W}_{\sigma^k}$ functions was given by Whitney [96]. These functions have proved to be so useful that they are usually called Whitney functions.

Definition 2.46. Let λ_i be the **barycentric function** associated to vertex $\mathbf{v}_i$ in a primal mesh K. More precisely, $\lambda_i : K \to \mathbb{R}$ is the unique function which is linear on each simplex of K satisfying $\lambda_i(\mathbf{v}_j) = \delta_{ij}$. The **Whitney function** $\mathcal{W}_{\sigma^k}$ associated to the k-simplex $\sigma^k := [\mathbf{v}_0, \ldots, \mathbf{v}_k]$ is given by

$$\mathcal{W}_{\sigma^k} := k! \sum_{i=0}^{k} (-1)^i\, \lambda_i\, d\lambda_0 \wedge \ldots \wedge \widehat{d\lambda_i} \wedge \ldots \wedge d\lambda_k \tag{2.7}$$

where $\widehat{d\lambda_i}$ indicates that $d\lambda_i$ is omitted. Note that $d\lambda$ should be interpreted as $d^{\,0}\lambda$ per Definition 2.17 or as ${}^1(\nabla\lambda)$ per Lemma 2.18. $\qquad \diamondsuit$

We write out the Whitney functions explicitly for $n = 3$, our primary application context. Note that $\mathcal{W}_{\sigma^3}$ is the constant function with value $1/|\sigma^3|$.

k	σ^k	$\mathcal{W}_{\sigma^k}$
0	$[\mathbf{v}_0]$	λ_0
1	$[\mathbf{v}_0, \mathbf{v}_1]$	$\lambda_0 \nabla \lambda_1 - \lambda_1 \nabla \lambda_0$
2	$[\mathbf{v}_0, \mathbf{v}_1, \mathbf{v}_2]$	$2(\lambda_0 \nabla \lambda_1 \times \nabla \lambda_2 - \lambda_1 \nabla \lambda_0 \times \nabla \lambda_2 + \lambda_2 \nabla \lambda_0 \times \nabla \lambda_1)$
3	$[\mathbf{v}_0, \mathbf{v}_1, \mathbf{v}_2, \mathbf{v}_3]$	$1/|\sigma^3|$

Table 2.2: Whitney forms W_{σ^k} for $n = 3$.

This is a consequence of the geometric identity

$$\nabla \lambda_i \cdot (\nabla \lambda_j \times \nabla \lambda_k) = \pm \frac{1}{3! |\sigma^3|}$$

where the right side has sign -1 if an odd index was omitted from the scalar triple product and $+1$ otherwise. This reduces the sum in (2.7) to $(1/|\sigma^3|) \sum_i \lambda_i$, which is simply $1/|\sigma^3|$ due to the partition of unity formed by the barycentric functions.

Theorem 2.47. *The Whitney functions satisfy properties W1-W5.*

Proof. Property W2 is immediate. The commutativity property W5 and optimal convergence W4 are discussed in Section 2.7. The conformity property W1 and interpolation property W3 is given by Corollary 4.5. □

Prior Work on Whitney functions

Although Whitney functions were developed out of theoretical considerations [96], it was recognized by Bossavit [16] that they provided a natural means for constructing stable bases for finite element methods, especially the

42

edge elements and face elements that were gaining popularity at that time. Finite element exterior calculus (FEEC) [7] gives a full account of the analogies between spaces of Whitney functions and classical Nédélec [72, 73] and Raviart and Thomas [80] spaces.

Some work has explored the possibility of Whitney functions over non-simplicial elements as we do in this work. Gradinaru and Hiptmair defined Whitney-like functions on rectangular grids using Haar-wavelet approximations [50] and on square-base pyramids by considering the collapse of a cube to a pyramid [51]. Bossavit has given an approach to Whitney forms over standard finite element shapes (hexahedra, triangular prisms, etc.) based on extrusion and conation arguments [21]. The Whitney-like functions we present in Chapter 4 do not use such heuristics and are defined over the convex polyhedra of a dual mesh instead of specific shape types.

2.7 Operator Commutativity

A number of commutativity relations between the continuous and discrete operators will be required for the stability proofs.

Theorem 2.48. *The following commutativity relationships hold. The diagram for each is shown in Figure 2.2.*

   i. $\mathcal{P}_{k+1}d_k = \mathbb{D}_k\mathcal{P}_k$

  ii. $d_k\mathcal{I}_k = \mathcal{I}_{k+1}\mathbb{D}_k$

$iii.$ $\overline{\mathcal{P}}_{k+1}d_k = \mathbb{D}^T_{n-k-1}\overline{\mathcal{P}}_k$

$iv.$ $d_{n-k-1}(*\mathcal{I}_{k+1}\mathbb{M}^{-1}_{k+1}) = (*\mathcal{I}_k\mathbb{M}^{-1}_k)\mathbb{D}^T_k$

$$
\begin{array}{ccc}
\Lambda^k & \xrightarrow{d_k} & \Lambda^{k+1} \\
\downarrow{\scriptstyle\mathcal{P}_k} & & \downarrow{\scriptstyle\mathcal{P}_{k+1}} \\
\mathcal{C}^k & \xrightarrow{\mathbb{D}_k} & \mathcal{C}^{k+1}
\end{array}
\qquad\qquad
\begin{array}{ccc}
\Lambda^k & \xrightarrow{d_k} & \Lambda^{k+1} \\
\uparrow{\scriptstyle\mathcal{I}_k} & & \uparrow{\scriptstyle\mathcal{I}_{k+1}} \\
\mathcal{C}^k & \xrightarrow{\mathbb{D}_k} & \mathcal{C}^{k+1}
\end{array}
$$

(i) $\qquad\qquad\qquad\qquad$ (ii)

$$
\begin{array}{ccc}
\Lambda^k & \xrightarrow{d_k} & \Lambda^{k+1} \\
\downarrow{\scriptstyle\overline{\mathcal{P}}_k} & & \downarrow{\scriptstyle\overline{\mathcal{P}}_{k+1}} \\
\overline{\mathcal{C}}^k & \xrightarrow{\mathbb{D}^T_{n-k-1}} & \overline{\mathcal{C}}^{k+1}
\end{array}
\qquad\qquad
\begin{array}{ccc}
\Lambda^{n-k-1} & \xrightarrow{d_{n-k-1}} & \Lambda^{n-k} \\
\uparrow{\scriptstyle *\mathcal{I}_{k+1}\mathbb{M}^{-1}_{k+1}} & & \uparrow{\scriptstyle *\mathcal{I}_k\mathbb{M}^{-1}_k} \\
\overline{\mathcal{C}}^{n-k-1} & \xrightarrow{\mathbb{D}^T_k} & \overline{\mathcal{C}}^{n-k}
\end{array}
$$

(iii) $\qquad\qquad\qquad\qquad$ (iv)

Figure 2.2: Commutativity diagrams between discrete and continuous operators (see Theorem 2.48).

Proof. **(i)** Let $u \in \Lambda^k$. Then

$$\mathcal{P}_{k+1}d_k u \;=\; \left\{ \int_{\sigma_j^{k+1}} \phi^*(du) \right\}_j \qquad \text{definition of } \mathcal{P}_{k+1}$$

$$=\; \left\{ \int_{\sigma_j^{k+1}} d(\phi^* u) \right\}_j \qquad d \text{ and } \phi^* \text{ commute}$$

$$=\; \left\{ \int_{\partial \sigma_j^{k+1}} \phi^* u \right\}_j \qquad \text{Stokes' theorem}$$

$$=\; \mathbb{D}_k \left\{ \int_{\sigma_i^k} \phi^* u \right\}_i \qquad \text{definition of } \mathbb{D}_k$$

$$=\; \mathbb{D}_k \mathcal{P}_k u \qquad \text{definition of } \mathcal{P}_k.$$

(ii) We prove a particular instance of this result demonstrating all the relevant proof techniques. Fix $n = 2$, $k = 0$ and take the mesh to be a single 2-simplex $\sigma^2 := [\ \mathbf{v}_1 \quad \mathbf{v}_2 \quad \mathbf{v}_3\ ]$. Let $\mathrm{w} \in \mathcal{C}^0$ be represented by $[\ a_1 \quad a_2 \quad a_3\ ]^T$. Thus

$$\mathbb{D}_0 = \begin{pmatrix} -1 & 1 & 0 \\ -1 & 0 & 1 \\ 0 & -1 & 1 \end{pmatrix}.$$

We will show that $d\mathcal{I}_0 = \mathcal{I}_1\mathbb{D}_0$, i.e. that $d^{\,0}(\mathcal{I}_0\mathrm{w}) = {}^1(\mathcal{I}_1\mathbb{D}_0\mathrm{w})$.

$$
\begin{aligned}
{}^1(\mathcal{I}_1\mathbb{D}_0\mathrm{w}) & \\
&= {}^1\mathcal{I}_1 \begin{bmatrix} a_2 - a_1 \\ a_3 - a_1 \\ a_3 - a_2 \end{bmatrix}, && \text{definition of } \mathbb{D}_0 \\[2mm]
&= {}^1((a_2 - a_1)(\lambda_1\nabla\lambda_2 - \lambda_2\nabla\lambda_1) + \cdots), && \text{definition of } \mathcal{I}_1 \\[2mm]
&= {}^1(a_1(\lambda_2\nabla\lambda_1 - \lambda_1\nabla\lambda_2 \\
&\qquad + \lambda_3\nabla\lambda_1 - \lambda_1\nabla\lambda_3 + \cdots), && \text{factor by } a_i \\[2mm]
&= {}^1(a_1(\nabla\lambda_1(\lambda_2 + \lambda_3) - \lambda_1(\nabla\lambda_2 + \nabla\lambda_3)) + \cdots), && \text{collect terms} \\[2mm]
&= {}^1(a_1(\nabla\lambda_1(1 - \lambda_1) - \lambda_1\nabla(1 - \lambda_1)) + \cdots), && \text{partition of 1} \\[2mm]
&= {}^1(a_1\nabla\lambda_1 + a_2\nabla\lambda_2 + a_3\nabla\lambda_3), && \text{simplify} \\[2mm]
&= d^{\,0}(a_1\lambda_1 + a_2\lambda_2 + a_3\lambda_3), && \text{Lemma 2.18} \\[2mm]
&= d^{\,0}(\mathcal{I}_0\mathrm{w}), && \text{definition of } \mathcal{I}_0.
\end{aligned}
$$

The proof for arbitrary n and k values uses the same techniques in a generalized context. The key idea is that the d operator wedges on differentials (see Definition 2.6) while the Whitney operator omits them (see Definition 2.46). Whitney gave the generalized proof in his seminal work [96, Section IV.27]; it can also be found in the finite difference approach of Dodziuk [35] and elsewhere.

(iii) The argument is the same as the proof for part (i), with the appropriate $\overline{\mathcal{P}}$ maps replacing the $\mathcal{P}$ maps and the $\mathbb{D}_{n-k-1}^T$ matrix replacing the $\mathbb{D}_k$ matrix.

(iv) To see why this result holds, we apply $*$ on both sides, yielding

$$(*d_{n-k-1}*)\mathcal{I}_{k+1}\mathbb{M}_{k+1}^{-1} = (\mathcal{I}_k\mathbb{M}_k^{-1})\mathbb{D}_k^T.$$

We remark the formal adjoint of d_k, denoted δ_k, is called the **coderivative** and can be characterized by

$$\delta_k : \Lambda^{k+1} \to \Lambda^k, \quad \delta_k := *d_{n-k-1}*$$

Therefore, part (iv) says that $\delta_k\mathcal{I}_{k+1}\mathbb{M}_{k+1}^{-1} = (\mathcal{I}_k\mathbb{M}_k^{-1})\mathbb{D}_k^T$, i.e., the natural notions of coderivative in the continuous and discrete settings commute with the dual cochain interpolation operator $\mathcal{I}_k\mathbb{M}_k^{-1}$. The proof mimics that of part (ii). $\square$

Remark 2.49. If $\mathcal{P}_k$ is defined instead using the smoothed projection operators (see Section 2.5.3), results (i) and (ii) follow from [7, Theorem 5.9 part 3].

We also have a standard estimate from the literature for the error between $\mathcal{I}_k\mathcal{P}_k$ and the identity map. We state it here in the language of discrete exterior calculus. A proof from a finite difference perspective for arbitrary k can be found in Dodziuk [35, Corollary 3.27] and from a finite element perspective for $0 \leq k \leq 3$ in Ern and Guermond [38, Section 1.5]. If the smoothed projection operators are used, this result also follows from Arnold, Falk and Winther [7, Theorem 5.9].

Theorem 2.50. *Fix a primal mesh K and let u be an element of Λ^k with enough regularity that $\mathcal{P}_k u$ is well-defined. We express this condition by saying*

that u is bounded in some norm $||\cdot||_{\mathcal{P}}$ *on* Λ^k. *Then there exists a constant* C *independent of* $\mathrm{m_d}$ *such that*

$$||u - \mathcal{I}_k \mathcal{P}_k u||_{H\Lambda^k} \leq C \, \mathrm{m_d} \, ||u||_{\mathcal{P}}, \tag{2.8}$$

where $\mathrm{m_d}$ *indicates the maximum diameter of any mesh element in* K.

Remark 2.51. By the definitions of $\mathcal{I}_k$ and $\mathcal{P}_k$, we have that

$$||u - \mathcal{I}_k \mathcal{P}_k u||_{H\Lambda^k} = \left\| u - \sum_{\sigma_i^k \in \mathcal{C}_k} \left(\int_{\sigma_i^k} \phi^* u \right) \mathcal{W}_{\sigma_i^k} \right\|_{H\Lambda^k}$$

Thus, in words, (2.8) says that when the Whitney functions are weighted appropriately by local integrals of u, they converge to u with order $\mathrm{m_d}$.

2.8 Discrete Hodge Stars

A discrete Hodge star $\mathbb{M}$ maps not only between cochains of complementary dimensions (k and $n-k$) but also between cochains on primal meshes and cochains on dual meshes. That is,

$$\mathbb{M} : \mathcal{C}^k \to \overline{\mathcal{C}}^{n-k}$$

This duality in both domain and dimension has been recognized by Bossavit [17], Hiptmair [56], Tonti [89] and others, in various contexts. Unlike the exterior derivative, however, there is no single canonical way to define the discrete Hodge star operator. As a consequence, the choice of an appropriate discrete Hodge star becomes essential to the stability properties of numerical methods where one is needed.

The simplest discrete Hodge star to formulate is called the **diagonal discrete Hodge star**. Since it will serve as our "default" discrete Hodge star, we will denote it by $\mathbb{M}_k$ or $\mathbb{M}_k^{Diag}$ if context is needed. Its entries are given by

$$(\mathbb{M}_k)_{ij} := \frac{|\star \sigma_i^k|}{|\sigma_i^k|} \delta_{ij}. \tag{2.9}$$

Since $\mathbb{M}_k$ is diagonal, we have its inverse immediately:

$$(\mathbb{M}_k^{-1})_{ij} := \frac{|\sigma_i^k|}{|\star \sigma_i^k|} \delta_{ij}. \tag{2.10}$$

Hence, the effect of $\mathbb{M}_k$ on a k-cochain w can be thought of as averaging the value of w over each simplex σ_i^k then scaling those values by the size of the respective dual simplices $\star \sigma^k$.

The primary alternative to $\mathbb{M}_k$ employs Whitney interpolants in its definition and will be referred to as the **Whitney discrete Hodge star**:

$$(\mathbb{M}_k^{Whit})_{ij} := \int_K \mathcal{W}_{\sigma_i^k} \cdot \mathcal{W}_{\sigma_j^k} \tag{2.11}$$

Dodziuk [35] originally proposed the definition of $\mathbb{M}_k^{Whit}$ but it has been called the Galerkin Hodge [19] for its relation to finite element methods, as we discuss in Section 3.5.

Since the basis function $\mathcal{W}_{\sigma_i^k}$ has local support (property W2), $\mathbb{M}_k^{Whit}$ is a sparse matrix. The inverse matrix $(\mathbb{M}_k^{Whit})^{-1}$ may be of full rank, however, making it unsuitable for numerical methods. The topological thresholding technique of He [54] is one approach to alleviating this problem. We will present a direct definition for an inverse discrete Hodge star with guaranteed sparsity in Section 4.2.

Remark 2.52. We have defined our dual meshes using circumcenters of simplices and hence produced orthogonal meshes. This is the natural choice for dual mesh definition from DEC theory [32]. Bossavit has pointed out, however, that switching from $\mathbb{M}_k$ to $\mathbb{M}_k^{Whit}$ should be accompanied by a switch from circumcentric to barycentric dual meshes. While this loses the orthogonality between the meshes, it ensures that σ^k will intersect $\star\sigma^k$ in the ambient space and allows certain geometric identities to work out nicely [19].

Still, it is not evident that the switch from barycentric to circumcentric dual meshes is necessary from a stability standpoint. The 'geometric' Hodge star of Auchmann and Kurz [8], for instance, is like $\mathbb{M}_k^{Whit}$ with a correction factor for the difference between circumcenters and barycenters and is shown by the authors to be equivalent to $\mathbb{M}_k^{Whit}$ in a natural sense. More recently, Hirani and Kalyanaraman [58] used their DEC method for Darcy flow with both $\mathbb{M}_k$ and $\mathbb{M}_k^{Whit}$ over circumcentric dual meshes and found similar numerical results. The importance of the choice of dual simplex centers is an ongoing area of research.

Many other discrete Hodge stars appear in the literature, including the combinatorial discrete Hodge star of Wardetzsky and Wilson [92, 97] and the metrized chain Hodge star of DiCarlo et al. [34]. These discrete Hodges are based on a different type of discrete theory and thus cannot be compared directly to the more common $\mathbb{M}_k$ and $\mathbb{M}_k^{Whit}$ matrices.

The maps defined thus far are summarized in Figure 2.3.
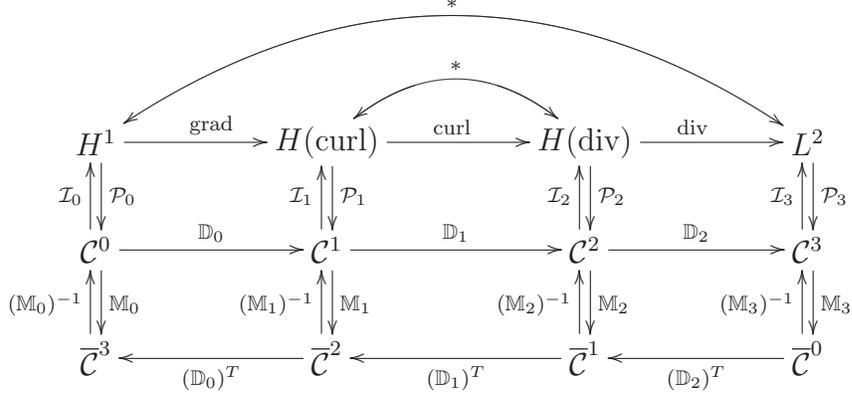
Figure 2.3: The combined DEC and deRham diagram for a contractible domain in $\mathbb{R}^3$.

2.9 Discrete Norms and Inner Products

To define discrete analogues of our continuous norms, we begin by defining a pairing between primal and dual cochains of complementary dimensions. Let $\mathrm{A} \in \mathcal{C}^k$ and $\overline{\mathrm{B}} \in \overline{\mathcal{C}}^{n-k}$. Define

$$< \mathrm{A}, \overline{\mathrm{B}} >=< \overline{\mathrm{B}}, \mathrm{A} >:= \sum_{\sigma_i^k \in \mathcal{C}_k} \mathrm{A}(\sigma_i^k)\overline{\mathrm{B}}(\star\sigma_i^k) \qquad (2.12)$$

As the next lemma shows, this pairing is natural in the way it relates to the discrete exterior derivative operators.

Lemma 2.53. *For any cochains* $\mathrm{A} \in \mathcal{C}^k$, $\overline{\mathrm{B}} \in \overline{\mathcal{C}}^{n-k-1}$, $\left\langle \mathbb{D}_k \mathrm{A}, \overline{\mathrm{B}} \right\rangle = \left\langle \mathrm{A}, \mathbb{D}_k^T \overline{\mathrm{B}} \right\rangle$.

Proof. The proof is a typical linear algebra argument of switching the order

51

of summation.

$$
\begin{aligned}
\langle \mathbb{D}_k \mathrm{A}, \overline{\mathrm{B}} \rangle \;\; &= \;\; \sum_{\sigma_i \in \mathcal{C}^{k+1}} (\mathbb{D}_k \mathrm{A})(\sigma_i^{k+1}) \overline{\mathrm{B}}(\star \sigma_i^{k+1}) \\[2mm]
&= \;\; \sum_{\sigma_i \in \mathcal{C}^{k+1}} \left(\sum_{\sigma_j \in \mathcal{C}^k} (\mathbb{D}_k)_{ij} \mathrm{A}(\sigma_j^k) \right) \overline{\mathrm{B}}(\star \sigma_i^{k+1}) \\[2mm]
&= \;\; \sum_{\sigma_j \in \mathcal{C}^k} \left(\sum_{\sigma_i \in \mathcal{C}^{k+1}} (\mathbb{D}_k)_{ji} \overline{\mathrm{B}}(\star \sigma_i^{k+1}) \right) \mathrm{A}(\sigma_j^k) \\[2mm]
&= \;\; \sum_{\sigma_j \in \mathcal{C}^k} (\mathbb{D}_k^T \overline{\mathrm{B}})(\star \sigma_j^k) \mathrm{A}(\sigma_j^k) \\[2mm]
&= \;\; \left\langle \mathrm{A}, \mathbb{D}_k^T \overline{\mathrm{B}} \right\rangle
\end{aligned}
$$

$$\square$$

Moreover, the pairing allows us to define a discrete norm for the primal and dual cochain spaces.

Definition 2.54. Given $\mathrm{A} \in \mathcal{C}^k$ or $\overline{\mathrm{B}} \in \overline{\mathcal{C}}^k$, define the **cochain norms**

$$
||\mathrm{A}||_{\mathcal{C}^k}^2 := \langle \mathrm{A}, \mathbb{M}_k \mathrm{A} \rangle , \qquad ||\overline{\mathrm{B}}||_{\overline{\mathcal{C}}^k}^2 := \left\langle \mathbb{M}_{n-k}^{-1} \overline{\mathrm{B}}, \overline{\mathrm{B}} \right\rangle , \tag{2.13}
$$

where $\mathbb{M}_k$ is the diagonal discrete Hodge star from (2.9). $\diamondsuit$

The cochain norms are defined using the diagonal discrete Hodge star, but as the next lemma will show, using the Whitney discrete Hodge star results in the same norm up to uniform scaling of the mesh. This is a technical result which will be needed in our stability proofs.

Lemma 2.55. *Let K be a finite primal mesh with $n = 3$. Define a functional $Q_k : \mathcal{C}^k \to \mathbb{R}$ by*

$$Q_k(A) :=< A, \mathbb{M}_k^{Whit} A > \tag{2.14}$$

For any cochains $A \in \mathcal{C}^k$ and $\overline{B} \in \overline{\mathcal{C}}^{n-k}$, the quotients

$$\frac{||A||_{\mathcal{C}^k}^2}{Q_k(A)} \quad and \quad \frac{||\overline{B}||_{\overline{\mathcal{C}}^{3-k}}^2}{Q_k(\mathbb{M}_k^{-1}\overline{B})}$$

are unaffected if K is uniformly scaled by a positive factor $s \in \mathbb{R}$.

Proof. We start with the claim for primal cochains. Let $||\cdot||_{\mathcal{C}^k(sK)}$ denote the cochain norm on the scaled mesh. Observe that

$$||A||_{\mathcal{C}^k(sK)}^2 = \sum_{\sigma_i^k \in \mathcal{C}^k} \frac{s^{3-k}|\star \sigma^k|}{s^k|\sigma^k|} A(\sigma_i^k)^2 = s^{3-2k}||A||_{\mathcal{C}^k}^2. \tag{2.15}$$

It suffices to show that the entries of $\mathbb{M}_k^{Whit}$ also scale as s^{3-2k}. Note that by the chain rule we have

$$\nabla\left(\lambda_i\left(\frac{x}{s}\right)\right) = \frac{1}{s}\left(\nabla\lambda_i\right)\left(\frac{x}{s}\right). \tag{2.16}$$

Recalling Table 2.2, we see that $\mathcal{W}_{\sigma^k}$ has exactly k terms of the type $\nabla\lambda_i$ appearing in each summand of its expression. Let $(\mathbb{M}_{k,s}^{Whit})_{ij}$ denote the ijth entry of $\mathbb{M}_k^{Whit}$ on the scaled mesh. Then

$$
\begin{aligned}
(\mathbb{M}_{k,s}^{Whit})_{ij} &= \int_{sK} \frac{1}{s^k}\mathcal{W}_{\sigma_i^k}\left(\frac{x}{s}\right) \cdot \frac{1}{s^k}\mathcal{W}_{\sigma_j^k}\left(\frac{x}{s}\right) \\
&= \frac{s^3}{s^{2k}}\int_K \mathcal{W}_{\sigma_i^k}(x) \cdot \mathcal{W}_{\sigma_j^k}(x) \qquad = s^{3-2k}(\mathbb{M}_k^{Whit})_{ij},
\end{aligned}
$$

as desired. For the dual cochain claim, we have that

$$||\overline{B}||^2_{\overline{C}^{3-k}(sK)} = \sum_{\sigma_i^k \in \mathcal{C}^k} \frac{s^k|\sigma^k|}{s^{3-k}|\star\sigma^k|}\overline{B}(\star\sigma_i^k)^2 = s^{2k-3}||\overline{B}||^2_{\overline{C}^{3-k}}. \qquad (2.17)$$

To show that the denominator scales the same way, observe that

$$Q_k(\mathbb{M}_k^{-1}\overline{B}) = (\mathbb{M}_k^{-1}\overline{B})^T\mathbb{M}_k^{Whit}(\mathbb{M}_k^{-1}\overline{B}).$$

Thus, the value of $Q_k(\mathbb{M}_k^{-1}\overline{B})$ scales as $s^{2k-3}s^{3-2k}s^{2k-3} = s^{2k-3}$, as desired. $\quad\square$

We note that Lemma 2.55 holds for any n by a similar argument, using the generalized definition of Whitney forms given in Definition 2.46.

2.10   Generalized Barycentric Interpolation

Since we are interested in defining Whitney-like interpolation functions for dual cochains, we first survey prior work on generalizing the Whitney 0-forms, i.e. barycentric functions. Since there are many ways these can be generalized, we first list all the properties we could require and then discuss which are essential in the context of dual discretization methods.

Definition 2.56. Let $\mathcal{T}$ be an n-dimensional cell of the dual mesh (i.e. a polygon in 2D or a polyhedron in 3D) with vertices $\mathbf{v}_1, \ldots, \mathbf{v}_N$. A set of functions $\overline{\lambda}_i : \mathcal{T} \to \mathbb{R}$, $i = 1, \ldots, N$ are called **barycentric coordinates** on $\mathcal{T}$ if they satisfy the following properties.

B1. **Non-negative**: $\overline{\lambda}_i \geq 0$.

B2. **Linear Completeness**: For any linear function $L : \mathcal{T} \to \mathbb{R}$,

$$L = \sum_{i=1}^{N} L(\mathbf{v}_i)\overline{\lambda}_i.$$

B3. **Partition of unity:** $\displaystyle\sum_{i=1}^{N} \overline{\lambda}_i \equiv 1.$

B4. **Linear precision:** $\displaystyle\sum_{i=1}^{N} \mathbf{v}_i\overline{\lambda}_i(\mathbf{x}) = \mathbf{x}.$

B5. **Interpolation:** $\overline{\lambda}_i(\mathbf{v}_j) = \delta_{ij}.$

B6. **Boundary agreement**: If x lies on an edge (facet) and $\mathbf{v}_i$ is not a vertex of the edge (facet) then $\overline{\lambda}_i(x) = 0$.

B7. **Invariance:** $\lambda_i(\mathbf{x}) = \lambda_i^T(T(\mathbf{x}))$, where $T : \mathbb{R}^n \to \mathbb{R}^n$ is a composition of rotation, translation, and uniform scaling transformations and $\{\overline{\lambda}_i^T\}$ are the corresponding functions on $T\mathcal{T}$.

Remark 2.57. The invariance property B7 is included to allow estimates over the class of convex sets with diameter one to be immediately extended to generic sizes since translation, rotation and uniform scaling operations can be easily passed through Sobolev norms (see Section 3.6). At the expense of requiring uniform bounds over a class of diameter-one domains rather than a single reference element, complications associated with handling non-affine mappings between reference and physical elements are avoided [5].

It suffices to satisfy only properties B1, B2, B6, and B7 in order to achieve the rest of the properties as the following proposition shows.

Proposition 2.58. *In 2D or 3D, the properties B1-B5 are related as follows:*

- *B2 ⇔ (B3 and B4)*

- *(B1 and B2) ⇒ B5*

Proof. Given B2, setting $L \equiv 1$ implies B3 and setting $L(\mathbf{x}) = \mathbf{x}$ yields B4. For the converse, we prove the 2D case first. Assuming B3 and B4 hold and let $L(x, y) = ax + by + c$ where $a, b, c \in \mathbb{R}$ are constants. Let $\mathbf{v}_i$ have coordinates $(\mathbf{v}_i^x, \mathbf{v}_i^y)$. Then

$$\sum_{i=1}^n L(\mathbf{v}_i)\lambda_i(x, y) = \sum_{i=1}^n (a\mathbf{v}_i^x + b\mathbf{v}_i^y + c)\lambda_i(\mathbf{x})$$

$$= a \left(\sum_{i=1}^n \mathbf{v}_i^x \lambda_i(\mathbf{x}) \right) + b \left(\sum_{i=1}^n \mathbf{v}_i^y \lambda_i(\mathbf{x}) \right) + c \left(\sum_{i=1}^n \lambda_i(\mathbf{x}) \right)$$

$$= ax + by + c = L(x, y).$$

The 3D case is similar. A proof that B1 and B2 imply B5 can be found in [95, Section 2.4]. □

As we will discuss below, there are many papers on generalized barycentric functions satisfying some or all of properties B1-B7. It is important to note that the results in Chapter 4 on constructing dual Whitney-like functions and discrete inverse Hodge stars do *not* depend on which definition of $\overline{\lambda}_i$ is selected, so long as the properties are satisfied. In this context, property B6 is essential since Corollary 2.35 requires that the value of $\overline{\lambda}_i$ at the intersection of two elements be independent of the element used to compute it.

To show an optimal convergence estimate, however, it is necessary to have an estimate of $\nabla \overline{\lambda}_i$ over the interior of the polygon or polytope. Such estimates require assumptions about the shape regularity of dual mesh elements (see Section 2.11) and are not amenable to proof from Definition 2.56 alone. Still, optimal convergence estimates are possible as we will prove for the Sibson functions, defined below. With a slight modification required for unusual geometries, Milbradt and Pick [70] have shown these functions satisfy all the conditions of Definition 2.56 in 2D and 3D. Further, the functions are defined in 2D and 3D, are reasonable to implement, and are more stable against bad geometry in 2D than the more well-known Wachspress functions. A proof of optimal convergence estimates for other coordinate definitions, including the Wachspress and Harmonic functions, can be found in our paper [48].
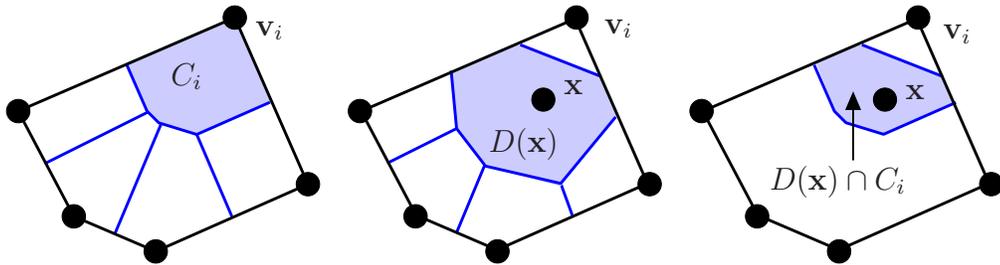
Figure 2.4: Geometric calculation of a Sibson coordinate. C_i is the area of the Voronoi region associated to vertex $\mathbf{v}_i$ inside $\mathcal{T}$. $D(\mathbf{x})$ is the area of the Voronoi region associated to $\mathbf{x}$ if it is added to the vertex list. The quantity $D(\mathbf{x}) \cap C_i$ is exactly $D(\mathbf{x})$ if $\mathbf{x} = \mathbf{v}_i$ and decays to zero as $\mathbf{x}$ moves away from $\mathbf{v}_i$, with value identically zero at all vertices besides $\mathbf{v}_i$.

We define the Sibson coordinates in 2D but the 3D case is analogous

with volume measurements replacing area measurements. Let $\mathbf{x}$ be a point inside a polyhedral cell $\mathcal{T}$ of a dual mesh in $\mathbb{R}62$. Let P denote the set of vertices $\{\mathbf{v}_i\}$ and define

$$P' = P \cup \{\mathbf{x}\} = \{\mathbf{v}_1, \ldots, \mathbf{v}_N, \mathbf{x}\}.$$

We denote the **Voronoi cell** associated to a point $\mathbf{p}$ in a pointset Q by

$$V_Q(\mathbf{p}) := \{\mathbf{y} \in \mathcal{T} \ : \ |\mathbf{y} - \mathbf{p}| < |\mathbf{y} - \mathbf{q}| \ , \ \forall \mathbf{q} \in Q \setminus \{\mathbf{p}\}\} \, .$$

Note that these Voronoi cells have been restricted to $\mathcal{T}$ and are thus always of finite size. We fix the notation

$$
\begin{aligned}
C_i \quad &:= \quad |V_P(\mathbf{v}_i)| = |\{\mathbf{y} \in \mathcal{T} \ : \ |\mathbf{y} - \mathbf{v}_i| < |\mathbf{y} - \mathbf{v}_j| \ , \ \forall j \neq i\}| \\
&= \quad \text{area of cell for } \mathbf{v}_i \text{ in Voronoi diagram on the points of } P, \\
D(\mathbf{x}) \quad &:= \quad |V_{P'}(\mathbf{x})| = |\{\mathbf{y} \in \mathcal{T} \ : \ |\mathbf{y} - \mathbf{x}| < |\mathbf{y} - \mathbf{v}_i| \ , \ \forall i\}| \\
&= \quad \text{area of cell for } \mathbf{x} \text{ in Voronoi diagram on the points of } P'.
\end{aligned}
$$

By a slight abuse of notation, we also define

$$D(\mathbf{x}) \cap C_i := |V_{P'}(\mathbf{x}) \cap V_P(\mathbf{v}_i)|.$$

The notation is shown in Figure 2.4.

Definition 2.59. The Sibson coordinate function associated to vertex $\mathbf{v}_i$ is

$$\overline{\lambda}_i(\mathbf{x}) := \frac{D(\mathbf{x}) \cap C_i}{D(\mathbf{x})} \qquad \text{or, equivalently,} \qquad \overline{\lambda}_i(\mathbf{x}) = \frac{D(\mathbf{x}) \cap C_i}{\sum_{j=1}^N D_j(\mathbf{x}) \cap C_j}.$$

$\Diamond$

It has been shown that the Sibson functions are C^∞ on $\mathcal{T}$ except at the vertices $\mathbf{v}_i$ where they are C^0 and on circumcircles of Delaunay triangles where they are C^1 [84, 41]. Since the finite set of vertices are the only points at which the function is not C^1, we conclude that $\overline{\lambda}_i \in H^1(\Omega)$.

We now discuss prior work on generalized barycentric functions in 2D and then in 3D.

2.10.1 Generalized Barycentric Interpolation in 2D

Many generalizations of barycentric functions on 2D polygons have emerged in the literature. The Wachspress functions [91, 43] are rational functions constructed explicitly based on the areas of certain triangles within $\mathcal{T}$. The Sibson functions [84], also called the natural neighbor or natural element coordinates [86], are also constructed explicitly, as described above. The Harmonic functions [95, 26] are defined as the solution to Laplace's equation over $\mathcal{T}$ with certain piecewise linear boundary data. These three types are discussed and analyzed in detail in our paper [48].

Other generalizations include maximum entropy [85], metric [69], discrete harmonic [77] and mean value coordinates [42]. Of these, the mean value coordinates are of particular interest since they appear to have well-behaved gradients for a large class of polygons. Additional comparisons of barycentric functions can be found in the survey papers of Cueto et al. [28] and Sukumar and Tabarraei [87].

2.10.2 Generalized Barycentric Interpolation in 3D

As noted earlier, the Sibson functions [84] are defined in any dimension and have been considered for use in finite element methods by Milbradt and Pick [70]. The definition of Harmonic functions also holds any dimension and thus extends to 3D, although implementing them presents a separate challenge. Approaches along these lines have been considered by Christensen [26], Euler [39], Warren et al. [95] and Hormann and Sukumar [62]. Floater [44] has extended mean value coordinates to 3D in the particular case of star-shaped polyhedra with triangular facets. Warren [93] also presented an approach extending the notions of the Wachspress functions to convex polytopes in arbitrary dimensions, but no explicit formulation of how to compute the functions is given.

If rational functions are desired, a result from Warren [94] shows that the Wachspress functions are the unique, lowest degree rational barycentric functions over polygons. Likewise, his functions in 3D [93] are the unique, lowest degree rational barycentric functions over polytopes. For finite element applications, however, the λ_i need not be rational. Moreover, as we have shown in our paper [48], the Wachspress functions require stricter shape regularity requirements to achieve optimal order convergence estimates than either the Sibson or Harmonic functions. This makes them somewhat less desirable for use in the finite element type applications considered here and explains why we have focused on the Sibson functions.

2.11   Generalized Shape Regularity Conditions

In this section, we discuss generalizations of shape regularity conditions to convex 2D polygons. These will be used in Section 3.6 to prove an optimal order convergence estimate for the Sibson functions.

Let $n = 2$ and let $\mathcal{T}$ be a 2-cell in the dual mesh, i.e. a convex polygon. Denote the interior angle at $\mathbf{v}_i \in \mathcal{T}$ by β_i. The largest distance between two points in $\mathcal{T}$ (the diameter of $\mathcal{T}$) is denoted $\mathrm{diam}(\mathcal{T})$ and the radius of the largest inscribed circle is denoted $\rho(\mathcal{T})$. The center of this circle is denoted $\mathbf{c}$ and is selected arbitrarily when no unique circle exists. The **aspect ratio** (or chunkiness parameter) γ is the ratio of the diameter to the radius of the largest inscribed circle, i.e.

$$\gamma := \frac{\mathrm{diam}(\mathcal{T})}{\rho(\mathcal{T})}.$$

We will consider the following geometric conditions.

G1. **Bounded aspect ratio:** There exists $\gamma^* \in \mathbb{R}$ such that $\gamma < \gamma^*$.

G2. **Minimum edge length:**   There exists $d_* \in \mathbb{R}$ such that $|\mathbf{v}_i - \mathbf{v}_j| > d_* > 0$ for all $i \neq j$ with $\mathbf{v}_i, \mathbf{v}_j \in \mathcal{T}$.

G3. **Maximum interior angle:** There exists $\beta^* \in \mathbb{R}$ such that $\beta_i < \beta^* < \pi$ for all i.

G4. **Minimum interior angle:** There exists $\beta_* \in \mathbb{R}$ such that $\beta_i > \beta_* > 0$ for all i.

G5. **Maximum vertex count:** There exists $n^* \in \mathbb{R}$ such that $n < n^*$.

For triangles, G4 and G3 are the only two important geometric restrictions since G5 holds trivially and G1⇔G4⇒G2. For general polygons, the relationships between these conditions are more complicated; for example, a polygon satisfying G1 may have vertices which are arbitrarily close to each other and thus might not satisfy G5.

Proposition 2.61 below specifies when the first three geometric assumptions (G1-G3) imply the last two. To prove it, we will need the following result.

Proposition 2.60. *Let $|\mathcal{T}|$ denote the area of a convex polygon $\mathcal{T}$ and $|\partial \mathcal{T}|$ its perimeter. If $\mathrm{diam}(\mathcal{T}) = 1$, then*

   i. $|\mathcal{T}| < \pi/4$,

  ii. $|\partial \mathcal{T}| \leq \pi$,

 iii. $\mathcal{T}$ is contained in a ball of radius no larger than $1/\sqrt{2}$, and

 iv. If convex polygon Υ is contained in $\mathcal{T}$, then $|\partial \Upsilon| \leq |\partial \mathcal{T}|$.

The first three statements are the isodiametric inequality, a corollary to Barbier's theorem, and Jung's theorem, respectively. The last statement is a technical result along the same lines. See [37, 98, 82] for more details.

Proposition 2.61. *The following implications hold.*

   i. $G1 \Rightarrow G4$

ii. (G2 or G3) ⇒ G5

Proof. G1 ⇒ G4: If β_i is an interior angle, then $\rho(\Omega) \leq \sin(\beta_i/2)$ (see Figure 2.5). Thus $\gamma > \frac{1}{\sin(\beta_i/2)}$. We conclude that $\beta_i > 2\arcsin\frac{1}{\gamma^*}$. Note that $\gamma^* \geq 2$ so this is well-defined.
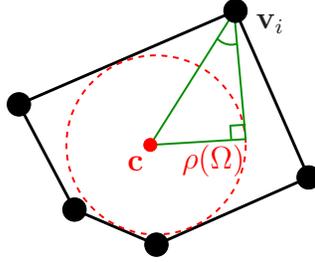
Figure 2.5: Proof that G1 ⇒ G4. The upper angle in the triangle is $\leq \beta_i/2 \leq \pi/2$ and the hypotenuse is $\leq \operatorname{diam}(\Omega) = 1$. Thus $\rho(\Omega) \leq \sin(\beta_i/2)$.

G2 ⇒ G5: By Jung's theorem (Proposition 2.60(3)), there exists $\mathbf{x} \in \Omega$ such that $\Omega \subset B(\mathbf{x}, 1/\sqrt{2})$. By G2, $\{B(\mathbf{v}_i, d_*/2)\}_{i=1}^n$ is a set of disjoint balls. Thus $B(\mathbf{x}, 1/\sqrt{2} + d_*/2)$ contains all of these balls. Comparing the areas of $\bigcup_{i=1}^n B(\mathbf{v}_i, d_*/2)$ and $B(\mathbf{x}, 1/\sqrt{2} + d_*/2)$ gives $n\frac{\pi d_*^2}{4} < \pi(\frac{1}{\sqrt{2}} + d_*/2)^2$, so $n < \frac{(\sqrt{2}+d_*)^2}{d_*^2}$.

G3 ⇒ G5: Since Ω is convex, $\sum_{i=1}^n \beta_i = \pi(n-2)$. So $n\beta^* \geq \pi(n-2)$. Thus $n \leq \frac{2\pi}{\pi-\beta^*}$.

$\square$

2.12 Generalized Interpolation in Sobolev Spaces

In this section we state some classic results related to interpolation in Sobolev spaces that will be used in the proof of discretization stability using Sibson functions in Section 3.6.

Definition 2.62. Let $n = 2$ and let $\{\mathbf{v}_i\}$ be the vertices of a dual mesh. Let $\overline{\lambda}_i$ denote the Sibson coordinate function associated to $\mathbf{v}_i$, defined piecewise over the dual mesh cells adjacent to $\mathbf{v}_i$ (see Definition 2.59). Then the **Sibson dual interpolation operator** is

$$\overline{\mathcal{I}}_0 : \overline{\mathcal{C}}^0 \to \overline{\Lambda}^0 \quad \text{given by} \quad \overline{\mathcal{I}}_0(\overline{\mathbf{w}}) := \sum_i \overline{\mathbf{w}}(\mathbf{v}_i)\overline{\lambda}_i \qquad (2.18)$$

$\Diamond$

For the rest of this section, we will use the abbreviated notation

$$I := \overline{\mathcal{I}}_0 \overline{\mathcal{P}}_0.$$

This coincides with the standard notation of interpolation in the finite element literature.

We start with the Bramble-Hilbert lemma, originally given in [22], but stated in a modern form for the particular case of H^1 estimates for convex domains of diameter 1.

Lemma 2.63 (Bramble-Hilbert [90, 29]). *Let $\mathcal{T}$ be a convex polygon with diameter 1. For all $u \in H^2(\mathcal{T})$, there exists a first order polynomial p_u such that $\|u - p_u\|_{H^1(\mathcal{T})} \leq C_{BH} \, |u|_{H^2(\mathcal{T})}$.*

We emphasize that the constant C_{BH} is uniform over all convex sets of diameter 1.

Lemma 2.64. *Let $\mathcal{T}$ be a convex polygon with diameter* 1*. Suppose that the following estimate holds*

$$\|Iu\|_{H^1(\mathcal{T})} \leq C_I \|u\|_{H^2(\mathcal{T})}, \quad \forall u \in H^1(\mathcal{T}) \tag{2.19}$$

Then for all $u \in H^2(\mathcal{T})$,

$$\|u - Iu\|_{H^1(\mathcal{T})} \leq (1 + C_I)\sqrt{1 + C_{BH}^2}\, |u|_{H^2(\mathcal{T})}.$$

Proof. Let p_u be the polynomial given in Lemma 2.63 which closely approximates u. By linear completeness of the $\{\overline{\lambda}_i\}$ functions, $Ip_u = p_u$, yielding the estimate

$$\|u - Iu\|_{H^1(\mathcal{T})} \leq \|u - p_u\|_{H^1(\mathcal{T})} + \|I(u - p_u)\|_{H^1(\mathcal{T})}$$
$$\leq (1 + C_I)\|u - p_u\|_{H^2(\mathcal{T})} \leq (1 + C_I)\sqrt{1 + C_{BH}^2}\, |u|_{H^2(\mathcal{T})}.$$

$\square$

Corollary 2.65. *Let $\mathrm{diam}(\mathcal{T}) \leq 1$. If estimate (2.19) holds, then for all $u \in H^2(\mathcal{T})$,*

$$\|u - Iu\|_{H^1(\mathcal{T})} \leq (1 + C_I)\sqrt{1 + C_{BH}^2}\, \mathrm{diam}(\mathcal{T})\, |u|_{H^2(\mathcal{T})}.$$

Proof. This follows from the standard scaling properties of Sobolev norms since the invariance property B7 (see Section 2.10) allows for a change of variables to a unit diameter domain. We remark that the L^2-component of the H^1-norm satisfies a stronger estimate containing an extra power of $\mathrm{diam}(\mathcal{T})$. $\square$

Lemma 2.66. *Under G1 and G5, estimate (2.19) holds whenever there exists a constant C_λ such that*

$$||\bar{\lambda}_i||_{H^1(\mathcal{T})} \leq C_\lambda. \qquad (2.20)$$

Proof. This follows almost immediately from the Sobolev embedding theorem; see [2, 66]:

$$||Iu||_{H^1(\mathcal{T})} \leq \sum_{i=1}^n |u(\mathbf{v}_i)| \, ||\lambda_i||_{H^1(\mathcal{T})} \leq n^* C_\lambda \, ||u||_{C^0(\overline{\mathcal{T}})} \leq n^* \, C_\lambda \, C_s \, ||u||_{H^2(\mathcal{T})},$$

where C_s is the Sobolev embedding; i.e., $||u||_{C^0(\overline{\mathcal{T}})} \leq C_s \, ||u||_{H^2(\mathcal{T})}$ for all $u \in H^2(\mathcal{T})$. The constant C_s is independent of the domain $\mathcal{T}$ since the boundaries of all polygons satisfying G1 are uniformly Lipschitz [66]. $\square$

Finally, we state a particular instance of the Poincaré inequality which we will use in our proof of stability. A proof can be found in, e.g. [40]

Theorem 2.67 (Poincaré Inequality)**.** *Let Ω be a bounded domain. Then for any $u \in H^1(\Omega)$ with $u = 0$ on $\partial\Omega$,*

$$||u||_{L^2} \leq C|u|_{H^1}$$

for some constant C dependent on Ω but independent of u.

We close this section by noting that $|u|_{H^1}$ and $||\nabla u||_{[L^2]^3}$ are different expressions for the same quantity.

66

Chapter 3

Discretization Stability of Dual Methods

While DEC terminology suggests discretization approaches for many types of PDEs, we focus in this section only on problems deriving from a generalized problem $d * du = f$. These problems encompass many famous PDE problems including Poisson's equation and a magnetostatics problem. We begin by describing the dual discretization methodology for the generalized problem and stating the discretization stability result.

3.1 Generic methodology

Consider the abstract problem of solving

$$-d * du = f \tag{3.1}$$

for $u \in \Lambda^k$, given $f \in \overline{\Lambda}^n$. For any n, the $k = 0$ instance of (3.1) is an exterior calculus description of

$$-\text{div grad } u = f,$$

the standard Poisson problem. Likewise, the $k = n - 1$ instance of (3.1) is a description of

$$-\text{grad div } u = f.$$

For $n = 3$, the $k = 1$ instance of (3.1) is a description of

$$-\text{curl curl } \vec{u} = \vec{f}, \tag{3.2}$$

a type of eddy-current problem and similar to the magnetostatics problem discussed in Section 3.2.

Taking (3.1) as the result of Step I from the generic approach outlined in Section 1.1, we linearize the problem by introducing an intermediary variable $v \in \overline{\Lambda}^{n-k-1}$ defined by

$$*v := -du \tag{3.3}$$

This results in the linear system

$$\begin{pmatrix} * & d_k \\ d_{n-k-1} & 0 \end{pmatrix} \begin{pmatrix} v \\ u \end{pmatrix} = \begin{pmatrix} 0 \\ f \end{pmatrix}. \tag{3.4}$$

The primal and dual formulations in this setting are

- u-**Primal Formulation:** $u \in \Lambda^k$, $v \in \overline{\Lambda}^{n-k-1}$ and $f \in \overline{\Lambda}^{n-k}$

- u-**Dual Formulation:** $u \in \overline{\Lambda}^k$, $v \in \Lambda^{n-k-1}$ and $f \in \Lambda^{n-k}$

In a sense, this is a false dichotomy since Λ^k and $\overline{\Lambda}^k$ are the same space (recall $\overline{\Lambda}^k := *\Lambda^{n-k}$ and $*$ is an isometry). However, when we apply the appropriate primal or dual projection operators to u, v, and f we end up with distinct discretizations and different linear systems.

- u-**Primal Discretization:** $\text{U} \in \mathcal{C}^k$, $\overline{\text{V}} \in \overline{\mathcal{C}}^{n-k-1}$ and $\overline{\text{F}} \in \overline{\mathcal{C}}^{n-k}$

$$\begin{pmatrix} \mathbb{M}_{k+1}^{-1} & \mathbb{D}_k \\ \mathbb{D}_k^T & 0 \end{pmatrix} \begin{pmatrix} \overline{\text{V}} \\ \text{U} \end{pmatrix} = \begin{pmatrix} 0 \\ \overline{\text{F}} \end{pmatrix} \tag{3.5}$$

68
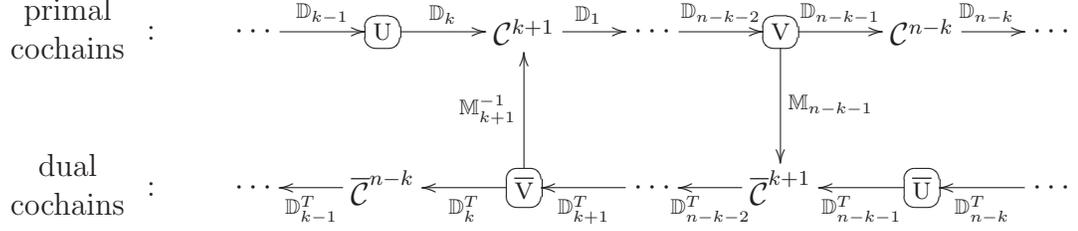
Figure 3.1: Portion of a generic primal and dual cochain diagram showing the natural duality between the variables and operators of systems (3.5) and (3.6). Discretizations of the variables are written in place of the primal or dual cochain spaces to which they belong.

- u-**Dual Discretization:** $\overline{\mathrm{U}} \in \overline{\mathcal{C}}^k$, $\mathrm{V} \in \mathcal{C}^{n-k-1}$ and $\mathrm{F} \in \mathcal{C}^{n-k}$

$$
\begin{pmatrix} \mathbb{M}_{n-k-1} & \mathbb{D}^T_{n-k-1} \\ \mathbb{D}_{n-k-1} & 0 \end{pmatrix} \begin{pmatrix} \mathrm{V} \\ \overline{\mathrm{U}} \end{pmatrix} = \begin{pmatrix} 0 \\ \mathrm{F} \end{pmatrix} \tag{3.6}
$$

We show in Figure 3.1 how these two discretizations fit into a generic cochain diagram in a natural and complementary fashion.

We now treat our DEC-inspired discretization techniques with a FEEC-inspired analysis of convergence. A method is said to have **discretization stability** if it can be shown to have an **optimal convergence estimate**. We will focus on "h-estimates" which dictate how fast the error between the continuous and discrete solutions to the PDE goes to zero as the size of maximum width domain element goes to zero.[1] Since the I_k interpolants are linear, the optimal convergence rate should be linear as well.

---

[1] Throughout this work, we use the notation $\mathrm{m_d}$ instead of the traditional h to avoid confusion with the h variable in the magnetostatics problem.

We now state a general conjecture about primal and dual discretization stability and which we will prove for various problems in the case $n = 3$ in subsequent sections.

Conjecture 3.1. *Consider the problem (3.4) with Dirichlet or Neumann boundary conditions over a contractible, compact domain Ω in $\mathbb{R}^n$ with primal and dual domain meshes of a finite number of elements. Let m_d denote the maximum diameter of a mesh element and assume the mesh elements have bounded aspect ratio. Let $||\cdot||_{\mathcal{P}_k}$, $||\cdot||_{\mathcal{P}_{n-k-1}}$ be norms on Λ^k and Λ^{n-k}, respectively, such that $||u||_{\mathcal{P}_k}, ||v||_{\mathcal{P}_{n-k-1}} < \infty$ implies u and v have enough regularity for $\mathcal{P}_k u$ and $\mathcal{P}_{n-k-1} v$ to be well-defined.*

- *u-**Primal Stability:** Let $(\mathrm{U}, \overline{\mathrm{V}})$ be a solution pair to (3.5). There exists a constant C dependent on $|\Omega|$ and $||u||_{\mathcal{P}_k}$ but independent of m_d, such that*

$$||\mathcal{I}_k \mathrm{U} - u||_{H\Lambda^k} + \left|\left|*\mathcal{I}_{k+1}\mathbb{M}_{k+1}^{-1}\overline{\mathrm{V}} - v\right|\right|_{H\Lambda^{n-k-1}} \leq C\, m_d.$$

- *u-**Dual Stability:** Let $(\overline{\mathrm{U}}, \mathrm{V})$ be a solution pair to (3.6). There exists a constant C dependent on $|\Omega|$ and $||v||_{\mathcal{P}_{n-k}}$ but independent of m_d, such that*

$$||\mathcal{I}_{n-k-1}\mathrm{V} - v||_{H\Lambda^{n-k-1}} + \left|\left|*\mathcal{I}_{n-k}\mathbb{M}_{n-k}^{-1}\overline{\mathrm{U}} - u\right|\right|_{H\Lambda^k} \leq C\, m_d.$$

This implies that both primal and dual methods are stable with the optimal order error estimate.

70

3.2   Example: Magnetostatics

This section begins by casting a magnetostatics problem similar to the generic problem (3.1) into the language of DEC. The primal stability result and accompanying proof technique is attributed to Bossavit [18, 20]. We explain the approach in much more detail here than is given in his work so that it can be adapted easily to the equivalent dual formulation as well as instances of the generic problem (3.1).

3.2.1   Magnetostatics - Continuous Problem

The magnetostatics problem is characterized by Gauss's law for magnetism, a constitutive relationship, and Ampère's law, respectively,

$$\text{div } b = 0, \quad *b = h, \quad \text{curl } h = j. \tag{3.7}$$

Here, j is a given current density and b and h both represent the magnetic field. It is assumed that the domain Ω is a compact, contractible 3-manifold with boundary Γ written as a disjoint union $\Gamma^e \cup \Gamma^h$ such that $\hat{n} \cdot b = 0$ on Γ^e and $\hat{n} \times h = 0$ on Γ^h.

Translated to exterior calculus, the equations become

$$db = 0, \quad *b = h, \quad dh = j$$

where b and j are 2-forms, and h is a 1-form. We use b as the indicator of primal or dual treatment since b is typically discretized as a primal 2-cochain.

Remark 3.2. Note that over contractible domains, div $b = 0$ means there exists $a \in \Lambda^1$ such that curl $a = b$ by exactness of the deRham sequence. If

we consider relabeling $h \mapsto u$, $a \mapsto v$, the magnetostatics problem has the constraint $dv = *u$ (or, equivalently, $*dv = u$) while the generic problem (3.1) has $*v = du$. This analogy hints at why the proof techniques can be adapted.

3.2.2 Magnetostatics - Stability of Primal Discretization

Treating b as an element of Λ^2, the discretization of (3.7) is

$$\mathbb{D}_2 \mathrm{B} = 0, \quad \mathbb{M}_2 \mathrm{B} = \overline{\mathrm{H}}, \quad \mathbb{D}_1^T \overline{\mathrm{H}} = \overline{\mathrm{J}} \tag{3.8}$$

Two mixed systems similar to (3.5) and (3.6) are available to solve for a solution pair $(\mathrm{B}, \overline{\mathrm{H}}) \in \mathcal{C}^2 \times \overline{\mathcal{C}}^1$. The first is

$$\begin{pmatrix} -\mathbb{M}_2 & \mathbb{D}_2^T \\ \mathbb{D}_2 & 0 \end{pmatrix} \begin{pmatrix} \mathrm{B} \\ \overline{\mathrm{P}} \end{pmatrix} = \begin{pmatrix} -\overline{\mathrm{H}}_0 \\ 0 \end{pmatrix}. \tag{3.9}$$

In this system, $\overline{\mathrm{H}}_0 \in \overline{\mathcal{C}}^1$ is any dual 1-cochain satisfying $\mathbb{D}_1^T \overline{\mathrm{H}}_0 = \overline{\mathrm{J}}$ and $\overline{\mathrm{H}}$ is defined by $\overline{\mathrm{H}} := \overline{\mathrm{H}}_0 + \mathbb{D}_2^T \overline{\mathrm{P}}$. Thus $\mathbb{D}_1^T \overline{\mathrm{H}} = \mathbb{D}_1^T (\overline{\mathrm{H}}_0 + \mathbb{D}_2^T \overline{\mathrm{P}}) = \overline{\mathrm{J}}$ is assured.

The second mixed system is

$$\begin{pmatrix} -\mathbb{M}_2^{-1} & \mathbb{D}_1 \\ \mathbb{D}_1^T & 0 \end{pmatrix} \begin{pmatrix} \overline{\mathrm{H}} \\ \mathrm{A} \end{pmatrix} = \begin{pmatrix} 0 \\ \overline{\mathrm{J}} \end{pmatrix}. \tag{3.10}$$

In this system, B is defined by $\mathrm{B} := \mathbb{D}_1 \mathrm{A}$, so that $\mathbb{D}_2 \mathrm{B} = \mathbb{D}_2 \mathbb{D}_1 \mathrm{A} = 0$. The choice between (3.9) and (3.10) is irrelevant with regards to discretization stability but will make a difference in regards to numerical stability (see Chapter 4).

The boundary conditions are enforced by requiring certain entries of B and $\overline{\mathrm{H}}$ to be zero. If $\partial\Omega$ is a subset of the primal mesh, then for any $\sigma_j^2 \in \Gamma^e$, assign $\mathrm{B}(\sigma^2) := 0$ and for any $\sigma_j^2 \in \Gamma^h$, assign $\overline{\mathrm{H}}(\star\sigma^2) := 0$. If $\partial\Omega$ is a subset

of the dual mesh, then for any $\star\sigma_j^2 \in \Gamma^e$, assign $\overline{\mathrm{H}}(\star\sigma^2) := 0$ and for any $\star\sigma_j^2 \in \Gamma^h$, assign $\mathrm{B}(\sigma_j^2) := 0$. These constraints can be incorporated into the eventual linear system used to solve the discrete problem.

To get the desired convergence estimates, we have to assume a certain amount of regularity on b. The typical assumption is that b lies in $[H^1]^3$ and div b lies in H^1. For readability, we define a unique norm for this context:

$$||b||_{[H^1]^3, H^1} := ||b||_{[H^1]^3} + ||\mathrm{div}\ b||_{H^1}.$$

We also have to assume that the input data j is known to a high degree of accuracy. This type of assumption is essential to any numerical method as one cannot expect an error estimate on the solution better than the error estimate on the input. Hence, it should suffice to assume that the error is $O(\mathrm{m_d})$. For simplicity, however, we assume that

$$\overline{\mathrm{J}} - \overline{\mathcal{P}}_2 j \equiv 0. \tag{3.11}$$

These assumptions allow for the following stability estimate.

Theorem 3.3. *Bossavit [18, 20] Let Ω be a contractible, compact domain in $\mathbb{R}^3$ with primal and dual domain meshes of a finite number of elements. Let $\mathrm{m_d}$ denote the maximum diameter of a mesh element and assume the mesh elements have bounded aspect ratio.. Let $(\mathrm{B}, \overline{\mathrm{H}})$ be a solution pair to (3.8). There exists a constant C dependent on $||b||_{[H^1]^3, H^1}$ but independent of $\mathrm{m_d}$, such that*

$$||\mathcal{I}_2 \mathrm{B} - b||_{H\Lambda^2} + \left||\ast\mathcal{I}_2 \mathbb{M}_2^{-1} \overline{\mathrm{H}} - h\right||_{H\Lambda^1} \leq C\, \mathrm{m_d}.$$

This implies that the method is stable with the optimal order error estimate.

Proof. The maps involved in proving the stability results are summarized in the following diagram.

$$
\begin{array}{lll}
\text{primal forms} & \boxed{b} & \\
& \quad \Big\uparrow \,\, \Big\downarrow \quad \searrow{}^{*} & \\
& \mathcal{I}_2 \,\, \mathcal{P}_2 \quad \boxed{h} & \text{dual forms} \\
& & \\
\text{primal cochains} & \boxed{\mathrm{B}} \qquad \overline{\mathcal{P}}_1 & \\
& \mathbb{M}_2^{-1} \,\, \mathbb{M}_2 & \\
& \boxed{\overline{\mathrm{H}}} & \text{dual cochains}
\end{array}
$$
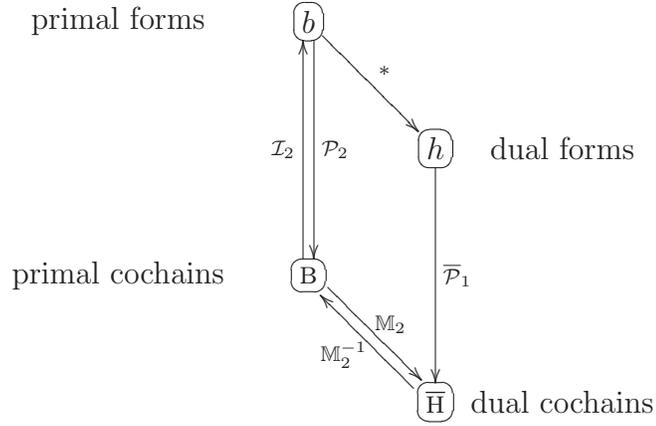
To simplify the presentation of the material, we will prove that

$$
\left\| \mathcal{I}_2 \mathrm{B} - b \right\|_{H\Lambda^2}^2 + \left\| * \mathcal{I}_2 \mathbb{M}_2^{-1} \overline{\mathrm{H}} - h \right\|_{H\Lambda^1}^2 \leq C \, \mathrm{m}_{\mathrm{d}}^2,
$$

from which the theorem follows.

$$
\left\| \mathcal{I}_2 \mathrm{B} - b \right\|_{H\Lambda^2}^2 + \left\| * \mathcal{I}_2 \mathbb{M}_2^{-1} \overline{\mathrm{H}} - h \right\|_{H\Lambda^1}^2
$$

$$\leq \;\; ||\mathcal{I}_2\mathrm{B} - \mathcal{I}_2\mathcal{P}_2 b||^2_{H\Lambda^2} + \left|\left|*\mathcal{I}_2\mathbb{M}_2^{-1}\overline{\mathrm{H}} - *\mathcal{I}_2\mathbb{M}_2^{-1}\overline{\mathcal{P}}_1 h\right|\right|^2_{H\Lambda^1}$$

$$+ C\,||b||^2_{[H^1]^3, H^1}\; \mathrm{m}_\mathrm{d}^2 \qquad \text{by Lemma 3.5}$$

$$= \;\; ||\mathcal{I}_2(\mathrm{B} - \mathcal{P}_2 b)||^2_{H\Lambda^2} + \left|\left|*\mathcal{I}_2\mathbb{M}_2^{-1}(\overline{\mathrm{H}} - \overline{\mathcal{P}}_1 h)\right|\right|^2_{H\Lambda^1}$$

$$+ C\,||b||^2_{[H^1]^3, H^1}\; \mathrm{m}_\mathrm{d}^2 \qquad \text{by linearity}$$

$$\leq \;\; \frac{1}{\alpha^2}\left(||\mathrm{B} - \mathcal{P}_2 b||^2_{\tilde{\mathcal{C}}^2} + \left|\left|\overline{\mathrm{H}} - \overline{\mathcal{P}}_1 h\right|\right|^2_{\tilde{\mathcal{C}}^1}\right) + C\,||b||^2_{[H^1]^3, H^1}\; \mathrm{m}_\mathrm{d}^2 \;\; \text{by Lemma 3.7}$$

$$= \;\; \frac{1}{\alpha^2}\left|\left|(\mathbb{M}_2\mathcal{P}_2 - \overline{\mathcal{P}}_1*)b\right|\right|^2_{\tilde{\mathcal{C}}^1} + C\,||b||^2_{[H^1]^3, H^1}\; \mathrm{m}_\mathrm{d}^2 \qquad \text{by Lemma 3.8}$$

$$\leq \;\; C\,||b||_{[H^1]^3, H^1}\left(||b||_{[H^1]^3, H^1}\,|\Omega| + 1\right)\mathrm{m}_\mathrm{d}^2 \qquad \text{by Lemma 3.9}$$

Note that per convention, the C value in the last step may not be the same as in previous steps. The largest C value required for any of the steps suffices as a general constant. $\qquad\square$

We first need a technical lemma related to our regularity assumption.

Lemma 3.4. *Under the assumptions of Theorem 3.3, for any 2-simplex $\sigma_i^2 \in \mathcal{C}_2$,*

$$\left|\frac{|\sigma_i^2|}{|\star\sigma_i^2|}\left(\int_{\star\sigma_i^2}\phi^*(*b)\right) - \int_{\sigma_i^2}\phi^*b\right| \leq ||b||_{[H^1]^3, H^1}\,|\sigma_i^2|\,\mathrm{m}_\mathrm{d}$$

Proof. Without loss of generality, fix a 2D coordinate system x for $\star\sigma_i^2$ and a 1D coordinate system y for σ_i^2 with origin $\mathbf{z} = \sigma_i^2 \cap \star\sigma_i^2$ as shown in Figure 3.2. Since σ_i^2 and $\star\sigma_i^2$ are orthogonal, we can write b in coordinates as

$$b(x)dx := \phi^*(*b) \quad \text{and} \quad b(y)dy := \phi^*b$$
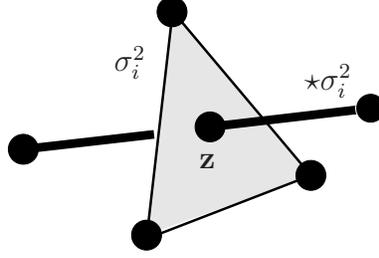
Figure 3.2: In $n = 3$, a primal 2-simplex σ_i^2 and its orthogonal dual edge $\star\sigma_i^2$ intersecting at point $\mathbf{z}$.

We then have that

$$\frac{|\sigma_i^2|}{|\star\sigma_i^2|} \left(\int_{\star\sigma_i^2} \phi^*(*b) \right) - \int_{\sigma_i^2} \phi^* b$$

$$= \frac{|\sigma_i^2|}{|\star\sigma_i^2|} \left(\int_{\star\sigma_i^2} b(x) - b(\mathbf{z}) + b(\mathbf{z})dx \right) - \int_{\sigma_i^2} b(y)dy$$

$$\leq \frac{|\sigma_i^2|}{|\star\sigma_i^2|} \int_{\star\sigma_i^2} ||b||_{[H^1]^3,H^1} |x - \mathbf{z}|dx + |\sigma_i^2| b(\mathbf{z}) - \int_{\sigma_i^2} b(y)dy$$

$$\leq \frac{|\sigma_i^2|}{|\star\sigma_i^2|} \int_{\star\sigma_i^2} ||b||_{[H^1]^3,H^1} |x - \mathbf{z}|dx + \int_{\sigma_i^2} ||b||_{[H^1]^3,H^1} |\mathbf{z} - y|dy$$

$$\leq |\sigma_i^2| ||b||_{[H^1]^3,H^1} \operatorname{diam}(\star\sigma_i^2) + |\sigma_i^2| ||b||_{[H^1]^3,H^1} \operatorname{diam}(\sigma_i^2)$$

$$\leq ||b||_{[H^1]^3,H^1} |\sigma_i^2| \, \mathrm{m_d}$$

$\square$

Lemma 3.5. *Under the assumptions of Theorem 3.3, there exists a constant C such that*

$$||b - \mathcal{I}_2\mathcal{P}_2 b||_{H\Lambda^2} \leq C \, \mathrm{m_d} \, ||b||_{[H^1]^3,H^1} \tag{3.12}$$

$$\left|\left|h - *\mathcal{I}_2\mathbb{M}_2^{-1}\overline{\mathcal{P}}_1 h\right|\right|_{H\Lambda^1} \leq C \, \mathrm{m_d} \, ||b||_{[H^1]^3,H^1} \tag{3.13}$$

76

Proof. Note that (3.12) is the result of Theorem 2.50 for $k = 2$. For (3.13), we have that

$$\left\|h - *\mathcal{I}_2 \mathbb{M}_2^{-1} \overline{\mathcal{P}}_1 h\right\|_{H\Lambda^1} = \left\|h - * \sum_{\sigma_i^2 \in \mathcal{C}_2} \frac{|\sigma_i^2|}{|\star\sigma_i^2|} \left(\int_{\star\sigma_i^2} \phi^* h\right) \mathcal{W}_{\sigma_i^2}\right\|_{H\Lambda^1}$$

Since $**$ is the identity, we factor out $*$ (which changes the norm to $H\Lambda^2$) and write the integrand in terms of b. This yields

$$\cdots = \left\|b - \sum_{\sigma_i^2 \in \mathcal{C}_2} \frac{|\sigma_i^2|}{|\star\sigma_i^2|} \left(\int_{\star\sigma_i^2} \phi^*(*b)\right) \mathcal{W}_{\sigma_i^2}\right\|_{H\Lambda^2}$$

We now add and subtract $(\int_{\sigma_i^2} \phi^* b)\mathcal{W}_{\sigma_i^2}$ inside the summation so that we can apply Lemma 3.4 and use our result from (3.12):

$$\cdots = \left\|b - \sum_{\sigma_i^2 \in \mathcal{C}_2} \left(\int_{\sigma_i^2} \phi^* b\right) \mathcal{W}_{\sigma_i^2}\right.$$

$$\left. - \sum_{\sigma_i^2 \in \mathcal{C}_2} \left(\frac{|\sigma_i^2|}{|\star\sigma_i^2|} \int_{\star\sigma_i^2} \phi^*(*b) - \int_{\sigma_i^2} \phi^* b\right) \mathcal{W}_{\sigma_i^2}\right\|_{H\Lambda^2}$$

$$\leq \ C \, \mathrm{m_d} \left\|b\right\|_{[H^1]^3, H^1} + \left\|\sum_{\sigma_i^2 \in \mathcal{C}_2} \left\|b\right\|_{[H^1]^3, H^1} |\sigma_i^2| \, \mathrm{m_d} \mathcal{W}_{\sigma_i^2}\right\|_{H\Lambda^2}$$

$$\leq \ C \, \mathrm{m_d} \left\|b\right\|_{[H^1]^3, H^1} + \left\|b\right\|_{[H^1]^3, H^1} \, \mathrm{m_d} \sum_{\sigma_i^2 \in \mathcal{C}_2} |\sigma_i^2| \left\|\mathcal{W}_{\sigma_i^2}\right\|_{H\Lambda^2}$$

To bound the summation on the right, we observe that the $\mathcal{W}_{\sigma_i^2}$ functions have compact support (recall property W5 from Section 2.6). Hence, the summation is bounded by a constant depending only on $|\Omega|$, from which we conclude

$$\left\|h - *\mathcal{I}_2 \mathbb{M}_2^{-1} \overline{\mathcal{P}}_1 h\right\|_{H\Lambda^1} \leq C \, \mathrm{m_d} \left\|b\right\|_{[H^1]^3, H^1}$$

77

$\square$

Remark 3.6. The last step in the previous proof says that $I_k\mathcal{P}_k$ is bounded in operator norm. Related results can be found in many other contexts, including Bossavit's computation of integrals of Whitney forms [19], and bounds on interpolation error from finite element theory, e.g. [23, Section 4.4] and [7].

Lemma 3.7. *Under the assumptions of Theorem 3.3, there exists a constant* $\alpha > 0$ *independent of* $\mathrm{m_d}$ *such that*

$$\alpha||\mathcal{I}_2(\mathrm{B} - \mathcal{P}_2 b)||_{H\Lambda^2} \leq ||\mathrm{B} - \mathcal{P}_2 b||_{\mathcal{C}^2}, \tag{3.14}$$

$$\alpha\left|\left|*\mathcal{I}_2\mathbb{M}_2^{-1}(\overline{\mathrm{H}} - \overline{\mathcal{P}}_1 h)\right|\right|_{H\Lambda^1} \leq \left|\left|\overline{\mathrm{H}} - \overline{\mathcal{P}}_1 h\right|\right|_{\overline{\mathcal{C}}^1} \tag{3.15}$$

Proof. Observe that $d\mathcal{I}_2(\mathrm{B} - \mathcal{P}_2 b) = \mathcal{I}_3\mathbb{D}_2(\mathrm{B} - \mathcal{P}_2 b) = -\mathcal{I}_3\mathbb{D}_2\mathcal{P}_2 b$ and $\mathbb{D}_2\mathcal{P}_2 b = \mathcal{P}_3 db = 0$, by Theorem 2.48*i* and *ii*. This gives us

$$||\mathcal{I}_2(\mathrm{B} - \mathcal{P}_2 b)||_{H\Lambda^2} = ||\mathcal{I}_2(\mathrm{B} - \mathcal{P}_2 b)||_{[L^2]^3} + ||d\mathcal{I}_2(\mathrm{B} - \mathcal{P}_2 b)||_{L^2} = ||\mathcal{I}_2(\mathrm{B} - \mathcal{P}_2 b)||_{[L^2]^3}.$$

Hence, it suffices to prove (3.14) with the $[L^2]^3$ norm on the left side.

Similarly, by Theorem 2.48*iii* and *iv*, we have that $d*\mathcal{I}_2\mathbb{M}_2^{-1}(\overline{\mathrm{H}} - \overline{\mathcal{P}}_1 h) = (*\mathcal{I}_1\mathbb{M}_1^{-1})\mathbb{D}_1^T(\overline{\mathrm{H}} - \overline{\mathcal{P}}_1 h)$ and $\mathbb{D}_1^T\overline{\mathrm{H}} - \mathbb{D}_1^T\overline{\mathcal{P}}_1 h = \overline{\mathrm{J}} - \overline{\mathcal{P}}_2 j$. The quantity $\overline{\mathrm{J}} - \overline{\mathcal{P}}_2 j$ is zero since we assume (3.11). This yields

$$\begin{aligned}
\left|\left|*\mathcal{I}_2\mathbb{M}_2^{-1}(\overline{\mathrm{H}} - \overline{\mathcal{P}}_1 h)\right|\right|_{H\Lambda^1} &= \left|\left|*\mathcal{I}_2\mathbb{M}_2^{-1}(\overline{\mathrm{H}} - \overline{\mathcal{P}}_1 h)\right|\right|_{[L^2]^3} \\
&\quad + \left|\left|d*\mathcal{I}_2\mathbb{M}_2^{-1}(\overline{\mathrm{H}} - \overline{\mathcal{P}}_1 h)\right|\right|_{[L^2]^3} \\
&= \left|\left|*\mathcal{I}_2\mathbb{M}_2^{-1}(\overline{\mathrm{H}} - \overline{\mathcal{P}}_1 h)\right|\right|_{[L^2]^3}.
\end{aligned}$$

Hence, it suffices to prove (3.15) with the $[L^2]^3$ norm on the left side.

Let $A \in \mathcal{C}^2$ and recall Lemma 2.55. A binomial expansion gives the equality

$$||\mathcal{I}_2 A||^2_{[L^2]^3} = \int_\Omega \left| \sum_{\sigma_i^2 \in \mathcal{C}_2} A(\sigma_i^2) \mathcal{W}_{\sigma_i^2} \right|^2 = \, < A, \mathbb{M}_2^{Whit} A > =: Q_2(A).$$

Hence Lemma 2.55 and the bounded aspect ratio assumption allow us to conclude that there exists a uniform bound

$$\frac{||B - \mathcal{P}_2 b||^2_{\mathcal{C}^2}}{||\mathcal{I}_2(B - \mathcal{P}_2 b)||^2_{[L^2]^3}} \geq \alpha^2,$$

for some constant $\alpha > 0$ dependent on the element shape quality parameters but not the size or orientation of the element.

The proof for (3.15) is nearly the same once we parse the notation. Note that $*\mathcal{I}_2$ means $*^2(\mathcal{I}_2)$ which by Lemma 2.18 is the same as $^1(\mathcal{I}_2)$. We observe that $||^1(\mathcal{I}_2)||_{[L^2]^3} = ||^2(\mathcal{I}_2)||_{[L^2]^3}$ since the components of the vector proxies for $^1(\mathcal{I}_2)$ and $^2(\mathcal{I}_2)$ are the same. Therefore

$$\left|\left| *\mathcal{I}_2 \mathbb{M}_2^{-1}(\overline{H} - \overline{\mathcal{P}}_1 h) \right|\right|^2_{[L^2]^3} = Q_2(\mathbb{M}_2^{-1}(\overline{H} - \overline{\mathcal{P}}_1 h))$$

Again by Lemma 2.55, we have a uniform bound

$$\frac{\left|\left| \overline{H} - \overline{\mathcal{P}}_1 h \right|\right|^2_{\overline{\mathcal{C}}^1}}{\left|\left| *\mathcal{I}_2 \mathbb{M}_2^{-1}(\overline{H} - \overline{\mathcal{P}}_1 h) \right|\right|^2_{[L^2]^3}} \geq \alpha^2,$$

for some α with the same dependencies as the primal case. $\qquad\square$

Lemma 3.8. *Under the assumptions of Theorem 3.3,*

$$||B - \mathcal{P}_2 b||^2_{\mathcal{C}^2} + \left|\left| \overline{H} - \overline{\mathcal{P}}_1 h \right|\right|^2_{\overline{\mathcal{C}}^1} = \left|\left| (\mathbb{M}_2 \mathcal{P}_2 - \overline{\mathcal{P}}_1 *) b \right|\right|^2_{\overline{\mathcal{C}}^1} \qquad (3.16)$$

Proof. First we show that the right side equals the left side plus an additional term involving the discrete inner product. We then show that this inner product is zero, yielding the result.

$$\left|\left|(\mathbb{M}_2\mathcal{P}_2 - \overline{\mathcal{P}}_1*)b\right|\right|^2_{\overline{\mathcal{C}}^1}$$

$$= \left\langle (\mathbb{M}_2\mathcal{P}_2 - \overline{\mathcal{P}}_1*)b, \mathbb{M}_2^{-1}((\mathbb{M}_2\mathcal{P}_2 - \overline{\mathcal{P}}_1*)b) \right\rangle \qquad \text{by Definition 2.54}$$

$$= \left\langle \mathbb{M}_2\mathcal{P}_2 b - \mathbb{M}_2\textsc{b}, \mathbb{M}_2^{-1}(\mathbb{M}_2\mathcal{P}_2 b - \mathbb{M}_2\textsc{b}) \right\rangle$$

$$+ \left\langle \mathbb{M}_2\textsc{b} - \overline{\mathcal{P}}_1 * b, \mathbb{M}_2^{-1}(\mathbb{M}_2\textsc{b} - \overline{\mathcal{P}}_1 * b) \right\rangle$$

$$+ \left\langle \mathbb{M}_2\mathcal{P}_2 b - \mathbb{M}_2\textsc{b}, \mathbb{M}_2^{-1}(\mathbb{M}_2\textsc{b} - \overline{\mathcal{P}}_1 * b) \right\rangle$$

$$+ \left\langle \mathbb{M}_2\textsc{b} - \overline{\mathcal{P}}_1 * b, \mathbb{M}_2^{-1}(\mathbb{M}_2\mathcal{P}_2 b - \mathbb{M}_2\textsc{b}) \right\rangle \qquad \text{by adding } \pm\mathbb{M}_2\textsc{b}$$

$$= \left\langle \mathbb{M}_2(\mathcal{P}_2 b - \textsc{b}), \mathcal{P}_2 b - \textsc{b} \right\rangle$$

$$+ \left|\left|\overline{\textsc{h}} - \overline{\mathcal{P}}_1 * b\right|\right|^2_{\overline{\mathcal{C}}^1}$$

$$+ \left\langle \mathbb{M}_2(\mathcal{P}_2 b - \textsc{b}), \textsc{b} - \mathbb{M}_2^{-1}\overline{\mathcal{P}}_1 * b \right\rangle$$

$$+ \left\langle \overline{\textsc{h}} - \overline{\mathcal{P}}_1 * b, \mathcal{P}_2 b - \textsc{b} \right\rangle \qquad \text{since } \overline{\textsc{h}} := \mathbb{M}_2\textsc{b}$$

$$= ||\textsc{b} - \mathcal{P}_2 b||^2_{\mathcal{C}^2} + \left|\left|\overline{\textsc{h}} - \overline{\mathcal{P}}_1 h\right|\right|^2_{\overline{\mathcal{C}}^1} - 2\left\langle \textsc{b} - \mathcal{P}_2 b, \overline{\textsc{h}} - \overline{\mathcal{P}}_1 h \right\rangle \quad \text{since } h := *b$$

It thus suffices to show that

$$\left\langle \textsc{b} - \mathcal{P}_2 b, \overline{\textsc{h}} - \overline{\mathcal{P}}_1 h \right\rangle = 0. \tag{3.17}$$

Observe that

$$\mathbb{D}_2(\textsc{b} - \mathcal{P}_2 b) = -\mathbb{D}_2\mathcal{P}_2 b = -\mathcal{P}_3 db = 0,$$

by the enforcement of the discrete equation $\mathbb{D}_2\mathrm{B} = 0$, Theorem 2.48$i$, and the continuous equation. By exactness, there exists $\mathrm{A} \in \mathcal{C}^1$ such that $\mathbb{D}_1\mathrm{A} = \mathrm{B} - \mathcal{P}_2 b$. Using Lemma 2.53, we have that

$$\left\langle \mathrm{B} - \mathcal{P}_2 b, \overline{\mathrm{H}} - \overline{\mathcal{P}}_1 h \right\rangle = \left\langle \mathbb{D}_1\mathrm{A}, \overline{\mathrm{H}} - \overline{\mathcal{P}}_1 h \right\rangle = \left\langle \mathrm{A}, \mathbb{D}_1^T(\overline{\mathrm{H}} - \overline{\mathcal{P}}_1 h) \right\rangle = \left\langle \mathrm{A}, \overline{\mathrm{J}} - \mathbb{D}_1^T\overline{\mathcal{P}}_1 h \right\rangle$$

By Theorem 2.48iii and the continuous equation $dh = j$, the right entry becomes $\overline{\mathrm{J}} - \overline{\mathcal{P}}_2 j$. Since we assume (3.11), this entry is zero and the entire inner product is zero, as desired. $\qquad\square$

Lemma 3.9. *Under the assumptions of Theorem 3.3,*

$$\left\| (\mathbb{M}_2\mathcal{P}_2 - \overline{\mathcal{P}}_1\ast)b \right\|_{\overline{\mathcal{C}}^1}^2 \leq \|b\|_{[H^1]^3, H^1}^2 \, |\Omega| \, \mathrm{m_d} \tag{3.18}$$

Proof. We write out the left side explicitly to derive the estimate.

$$\left\| (\mathbb{M}_2\mathcal{P}_2 - \overline{\mathcal{P}}_1\ast)b \right\|_{\overline{\mathcal{C}}^1}^2$$

$$= \sum_{\sigma_i^2 \in \mathcal{C}_2} \frac{|\sigma_i^2|}{|\star\sigma_i^2|} \left(\frac{|\star\sigma_i^2|}{|\sigma_i^2|} \int_{\sigma_i^2} \phi^\ast b - \int_{\star\sigma_i^2} \phi^\ast(\ast b) \right)^2 \quad \text{by definition}$$

$$= \sum_{\sigma_i^2 \in \mathcal{C}_2} \frac{|\star\sigma_i^2|}{|\sigma_i^2|} \left(\int_{\sigma_i^2} \phi^\ast b - \frac{|\sigma_i^2|}{|\star\sigma_i^2|} \int_{\star\sigma_i^2} \phi^\ast(\ast b) \right)^2$$

$$\leq \sum_{\sigma_i^2 \in \mathcal{C}_2} \frac{|\star\sigma_i^2|}{|\sigma_i^2|} \|b\|_{[H^1]^3, H^1}^2 \, |\sigma_i^2|^2 \, \mathrm{m_d} \quad \text{by Lemma 3.4}$$

$$\leq \|b\|_{[H^1]^3, H^1}^2 \, |\Omega| \, \mathrm{m_d}$$

$$\square$$
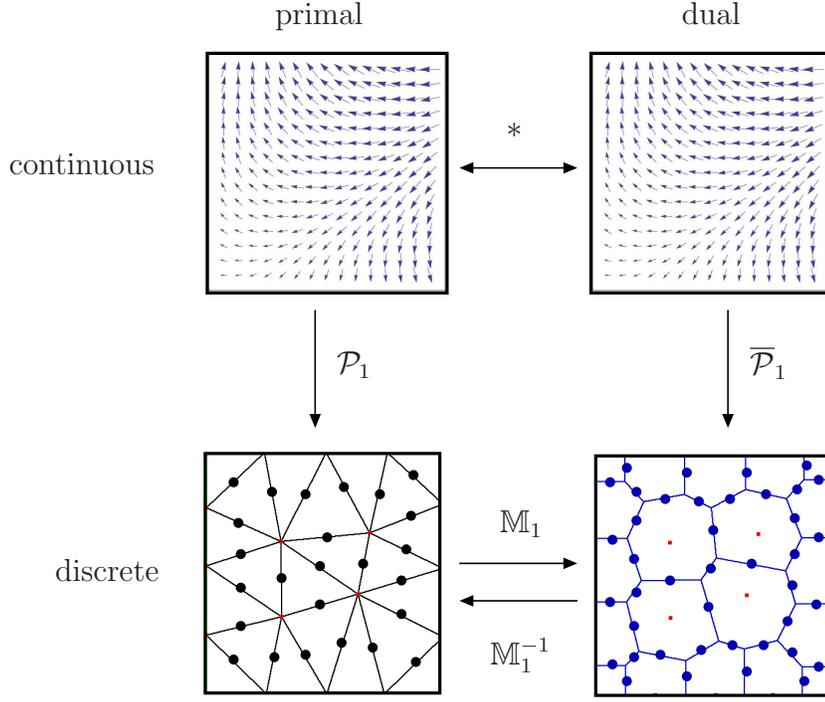
Figure 3.3: This diagram in 2D shows the relations between the projection and Hodge star operators. The dots indicate where degrees of freedom are assigned in the case of $k = 1$, $n = 2$, i.e. primal and dual mesh edges. All the discretization stability proofs rely on an estimate of $\mathbb{M}\mathcal{P} - \overline{\mathcal{P}}*$ or $\mathbb{M}^{-1}\overline{\mathcal{P}} - \mathcal{P}*$ in an appropriate norm.

3.2.3   Magnetostatics - Stability of Dual Discretization

The crucial estimate in the primal discretization case was the estimate (3.18) of $\mathbb{M}_2\mathcal{P}_2 - \overline{\mathcal{P}}_1*$. As Figure 3.3 suggests, an analagous estimate should hold for $\mathbb{M}_2^{-1}\overline{\mathcal{P}}_2 - \overline{\mathcal{P}}_1*$. This estimate will be used to prove the discretization stability of the dual formulation, namely, treating b as an element of $\overline{\Lambda}^2$. The discretization of (3.7) becomes

$$\mathbb{D}_0^T\overline{\mathrm{B}} = 0, \quad \overline{\mathrm{B}} = \mathbb{M}_1\mathrm{H}, \quad \mathbb{D}_1\mathrm{H} = \mathrm{J}. \tag{3.19}$$

82

Again, two mixed systems are available to solve for a solution pair is $(\overline{B}, H) \in \overline{\mathcal{C}}^2 \times \mathcal{C}^1$. The first is

$$\begin{pmatrix} -\mathbb{M}_1^{-1} & \mathbb{D}_0 \\ \mathbb{D}_0^T & 0 \end{pmatrix} \begin{pmatrix} \overline{B} \\ P \end{pmatrix} = \begin{pmatrix} -H_0 \\ 0 \end{pmatrix}. \tag{3.20}$$

In this system, $H_0 \in \mathcal{C}^1$ is any primal 1-cochain satisfying $\mathbb{D}_1 H_0 = J$ and H is defined by $H := \mathbb{M}_1^{-1}\overline{B}$. Thus $\mathbb{D}_1 H = \mathbb{D}_1(H_0 + \mathbb{D}_0 P) = J$ is assured. The second is

$$\begin{pmatrix} -\mathbb{M}_1 & \mathbb{D}_1^T \\ \mathbb{D}_1 & 0 \end{pmatrix} \begin{pmatrix} H \\ \overline{A} \end{pmatrix} = \begin{pmatrix} 0 \\ J \end{pmatrix}, \tag{3.21}$$

where $\overline{B}$ is defined by $\overline{B} := \mathbb{D}_1^T \overline{A}$ so that $\mathbb{D}_0^T \overline{B} = \mathbb{D}_0^T \mathbb{D}_1^T \overline{A} = 0$. As in the primal case, the choice between (3.20) and (3.21) only makes a difference in regards to numerical stability (see Chapter 4).

The boundary conditions can be enforced in an analogous fashion to the primal case. Our estimates will be cast in terms of an energy on h. We define the norm

$$||h||_{[H^1]^3,[H^1]^3} := ||h||_{[H^1]^3} + ||\mathrm{curl}\, h||_{[H^1]^3}.$$

As in the primal case, we also assume that the input current density j is approximated exactly, i.e.

$$J - \mathcal{P}_2 j \equiv 0. \tag{3.22}$$

We then have the same type of stability estimate as in the primal case.

Theorem 3.10. *Let Ω be a contractible, compact domain in $\mathbb{R}^3$ with primal and dual domain meshes of a finite number of elements. Let m_d denote the*

83

maximum diameter of a mesh element and assume the mesh elements have bounded aspect ratio. Let $(\overline{B}, H)$ be a solution pair to (3.19). There exists a constant C dependent on $||h||_{[H^1]^3,[H^1]^3}$ but independent of m_d such that

$$||\mathcal{I}_1 H - h||_{H\Lambda^1} + \left|\left|*\mathcal{I}_1\mathbb{M}_1^{-1}\overline{B} - b\right|\right|_{H\Lambda^2} \leq C\, m_d.$$

This implies that the method is stable with the optimal order error estimate.

Proof. The proof technique is similar to that of the primal-formulated problem.

$$||\mathcal{I}_1 H - h||_{H\Lambda^1}^2 + \left|\left|*\mathcal{I}_1\mathbb{M}_1^{-1}\overline{B} - b\right|\right|_{H\Lambda^2}^2$$

$$\leq\ ||\mathcal{I}_1 H - \mathcal{I}_1\mathcal{P}_1 h||_{H\Lambda^1}^2 + \left|\left|*\mathcal{I}_1\mathbb{M}_1^{-1}\overline{B} - *\mathcal{I}_1\mathbb{M}_1^{-1}\overline{\mathcal{P}}_2 b\right|\right|_{H\Lambda^2}^2$$

$$+ C\,||h||_{[H^1]^3,[H^1]^3}^2\ m_d^2 \qquad \text{by Lemma 3.12}$$

$$=\ ||\mathcal{I}_1(H - \mathcal{P}_1 h)||_{H\Lambda^1}^2 + \left|\left|*\mathcal{I}_1\mathbb{M}_1^{-1}(\overline{B} - \overline{\mathcal{P}}_2 b)\right|\right|_{H\Lambda^2}^2$$

$$+ C\,||h||_{[H^1]^3,[H^1]^3}^2\ m_d^2 \qquad \text{by linearity}$$

$$\leq\ \frac{1}{\alpha^2}\left(||H - \mathcal{P}_1 h||_{\mathcal{C}^1}^2 + \left|\left|\overline{B} - \overline{\mathcal{P}}_2 b\right|\right|_{\overline{\mathcal{C}}^2}^2\right) + C\,||h||_{[H^1]^3,[H^1]^3}^2\ m_d^2 \quad \text{by Lemma 3.13}$$

$$=\ \frac{1}{\alpha^2}\left|\left|(\mathbb{M}_1\mathcal{P}_1 - \overline{\mathcal{P}}_2*)h\right|\right|_{\overline{\mathcal{C}}^2}^2 + C\,||h||_{[H^1]^3,[H^1]^3}^2\ m_d^2 \qquad \text{by Lemma 3.14}$$

$$\leq\ C\,||h||_{[H^1]^3,[H^1]^3}\left(||h||_{[H^1]^3,[H^1]^3}\,|\Omega| + 1\right)m_d^2 \qquad \text{by Lemma 3.15}$$

$$\square$$

We need a corresponding technical lemma for the regularity assumption on h.
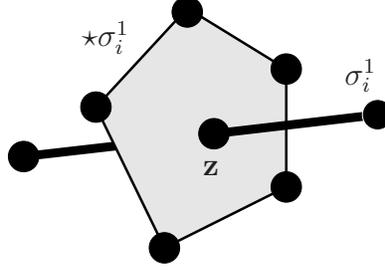
Figure 3.4: In $n = 3$, a primal 1-simplex σ_i^1 and its orthogonal dual face $\star\sigma_i^1$ intersecting at point $\mathbf{z}$.

Lemma 3.11. *Under the assumptions of Theorem 3.10, for any $\sigma_i^1 \in \mathcal{C}_1$,*

$$\left| \frac{|\sigma_i^1|}{|\star\sigma_i^1|} \left(\int_{\star\sigma_i^1} \phi^*(\star h) \right) - \int_{\sigma_i^1} \phi^* h \right| \leq ||h||_{[H^1]^3,[H^1]^3} \, |\sigma_i^1| \, \mathrm{m_d}$$

The proof is analogous to that of Lemma 3.4 by using coordinate systems for σ_i^1 and $\star\sigma_i^1$, as shown in Figure 3.4.

Lemma 3.12. *Under the assumptions of Theorem 3.10, there exists a constant C such that*

$$||h - \mathcal{I}_1 \mathcal{P}_1 h||_{H\Lambda^1} \leq C \, \mathrm{m_d} \, ||h||_{[H^1]^3,[H^1]^3} \tag{3.23}$$

$$\left|\left| b - \star\mathcal{I}_1 \mathbb{M}_1^{-1} \overline{\mathcal{P}}_2 b \right|\right|_{H\Lambda^2} \leq C \, \mathrm{m_d} \, ||h||_{[H^1]^3,[H^1]^3} \tag{3.24}$$

Note that (3.13) is the result of Theorem 2.50 for $k = 1$. The rest of the proof is analogous to that of Lemma 3.5.

Lemma 3.13. *Under the assumptions of Theorem 3.10, there exists a constant $\alpha > 0$ independent of $\mathrm{m_d}$ such that*

$$\alpha ||\mathcal{I}_1 (\mathrm{H} - \mathcal{P}_1 h)||_{H\Lambda^1} \leq ||\mathrm{H} - \mathcal{P}_1 h||_{\mathcal{C}^1}, \tag{3.25}$$

$$\alpha \left|\left| \star\mathcal{I}_1 \mathbb{M}_1^{-1} (\overline{\mathrm{B}} - \overline{\mathcal{P}}_2 b) \right|\right|_{H\Lambda^2} \leq \left|\left| \overline{\mathrm{B}} - \overline{\mathcal{P}}_2 b \right|\right|_{\overline{\mathcal{C}}^2} \tag{3.26}$$

85

The proof is analogous to that of Lemma 3.7.

Lemma 3.14. *Under the assumptions of Theorem 3.10,*

$$||\mathrm{H} - \mathcal{P}_1 h||^2_{\mathcal{C}^1} + \left|\left|\overline{\mathrm{B}} - \overline{\mathcal{P}}_2 b\right|\right|^2_{\overline{\mathcal{C}}^2} = \left|\left|(\mathbb{M}_1 \mathcal{P}_1 - \overline{\mathcal{P}}_2 *)h\right|\right|^2_{\overline{\mathcal{C}}^2} \qquad (3.27)$$

The proof is analogous to that of Lemma 3.8

Lemma 3.15. *Under the assumptions of Theorem 3.10,*

$$\left|\left|(\mathbb{M}_1 \mathcal{P}_1 - \overline{\mathcal{P}}_2 *)h\right|\right|_{\overline{\mathcal{C}}^2} \leq ||h||^2_{[H^1]^3,[H^1]^3} |\Omega| \, \mathrm{m_d}$$

The proof is analogous to that of Lemma 3.9

Remark 3.16. It is worth noting that this 'dual' approach to discretizing the magnetostatics problem has been considered before. The thesis work of M. Barton [10] (described in [11]) gave some theoretical and practical justification for the approach and modern papers in electrical engineering still point to [11] as a seminal work. Bossavit gives additional theoretical analysis and justification in [17, Chapter 6].

Our purpose in revisiting the topic here is to show how this dual formulation can be treated in a generic and unified way with the terminology of DEC, suggesting how a similar treatment can be applied to other PDE problems. Moreover, the proof of the dual stability theorem is almost identical to the primal stability proof in our generalized language. ◇

3.3 Example: Poisson Equation

3.3.1 Poisson Equation - Continuous Problem

We now look at how similar techniques can be applied to a classical PDE problem: Poisson's equation. With Dirichlet boundary conditions, the problem is

$$\begin{cases} \Delta u & = & f & \text{in } \Omega \\ u & = & 0 & \text{on } \partial\Omega \end{cases} \tag{3.28}$$

We consider solving for u given f over a compact, contractible 3-manifold Ω embedded in $\mathbb{R}^3$ with boundary denoted $\Gamma := \partial\Omega$. Translated to exterior calculus, the equation over Ω becomes

$$d * du = f$$

where u is a 0-form and f is a (dual) 3-form.[2] To write this equation as a linear system, we introduce an auxiliary variable s and solve

$$\begin{aligned} *du & = s, \\ ds & = f. \end{aligned} \tag{3.29}$$

We now examine the primal and dual discretizations of (3.29) and their stability properties.

3.3.2 Poisson Equation - Stability of Primal Discretization

Treating u as an element of Λ^0, the discretization of (3.29) is

$$\mathbb{M}_1 \mathbb{D}_0 \mathsf{U} = \bar{\mathsf{S}}, \quad \mathbb{D}_0^T \bar{\mathsf{S}} = \bar{\mathsf{F}}. \tag{3.30}$$

---

[2]We note that, formally, the equation is $(\delta d + d\delta)u = f$ where f is treated as a 0-form, but our treatment here is equivalent and simpler for exposition.

Thus a solution pair is $(\mathrm{U}, \overline{\mathrm{S}}) \in \mathcal{C}^0 \times \overline{\mathcal{C}}^2$. In this case, the general linear system (3.5) is written

$$\begin{pmatrix} \mathbb{M}_1^{-1} & \mathbb{D}_0 \\ \mathbb{D}_0^T & 0 \end{pmatrix} \begin{pmatrix} \overline{\mathrm{S}} \\ \mathrm{U} \end{pmatrix} = \begin{pmatrix} 0 \\ \mathrm{F} \end{pmatrix} \tag{3.31}$$

Our DEC treatment reveals, by analogy to the magnetostatics problem, an equivalent linear system,

$$\begin{pmatrix} \mathbb{M}_1 & \mathbb{D}_1^T \\ \mathbb{D}_1 & 0 \end{pmatrix} \begin{pmatrix} \mathrm{Q} \\ \overline{\mathrm{G}} \end{pmatrix} = \begin{pmatrix} \overline{\mathrm{S}}_0 \\ 0 \end{pmatrix}. \tag{3.32}$$

In this system, $\overline{\mathrm{S}}_0$ is any dual cochain satisfying $\mathbb{D}_0^T \overline{\mathrm{S}}_0 = \mathrm{F}$ and $\overline{\mathrm{S}}$ is defined by $\overline{\mathrm{S}} := \mathbb{M}_1 \mathrm{Q}$. The first equation implies $\mathbb{D}_0^T \overline{\mathrm{S}} = \mathbb{D}_0^T (\overline{\mathrm{S}}_0 - \mathbb{D}_1^T \overline{\mathrm{G}}) = \mathrm{F}$, since $\mathbb{D}_0^T \mathbb{D}_1^T = 0$. By exactness of the discrete primal cochain sequence, $\mathbb{D}_1 \mathrm{Q} = 0$ implies that there exists a unique $\mathrm{U} \in \mathcal{C}^0$ such that $\mathbb{D}_0 \mathrm{U} = \mathrm{Q}$; the uniqueness of U comes from enforcement of the boundary conditions. Hence $\overline{\mathrm{S}} = \mathbb{M}_1 \mathbb{D}_0 \mathrm{U}$ and the same solution pair $(\mathrm{U}, \overline{\mathrm{S}})$ is recovered. As before, the choice between (3.31) and (3.32) only makes a difference in regards to numerical stability (see Chapter 4).

We assume that $u \in H^1$ and $\nabla u \in [H^1]^3$. For readability, we define the norm:

$$\|u\|_{H^1,[H^1]^3} := \|u\|_{H^1} + \|\nabla u\|_{[H^1]^3}$$

We assume the domain boundary Γ is a collection of primal mesh faces and incorporate the constraints $\mathrm{U}(\sigma^0) := 0$ for $\sigma^0 \subset \Gamma$. We also assume the input data is known exactly, i.e.

$$\overline{\mathrm{F}} - \overline{\mathcal{P}}_3 f \equiv 0. \tag{3.33}$$

The stability result is as follows.

Theorem 3.17. *Let Ω be a contractible, compact domain in $\mathbb{R}^3$ with primal and dual domain meshes of a finite number of elements. Let $\mathrm{m_d}$ denote the maximum diameter of a mesh element and assume the mesh elements have bounded aspect ratio. Let $(\mathrm{U}, \overline{\mathrm{S}})$ be a solution pair to (3.30). There exists a constant C dependent on $\|u\|_{H^1,[H^1]^3}$ but independent of $\mathrm{m_d}$, such that*

$$\|\mathcal{I}_0 \mathrm{U} - u\|_{H\Lambda^0} + \left\|*\mathcal{I}_1 \mathbb{M}_1^{-1}\overline{\mathrm{s}} - s\right\|_{H\Lambda^2} \leq C\,\mathrm{m_d}.$$

This implies that the method is stable with the optimal order error estimate.

Proof. The maps involved in proving the stability results are summarized in the following diagram.
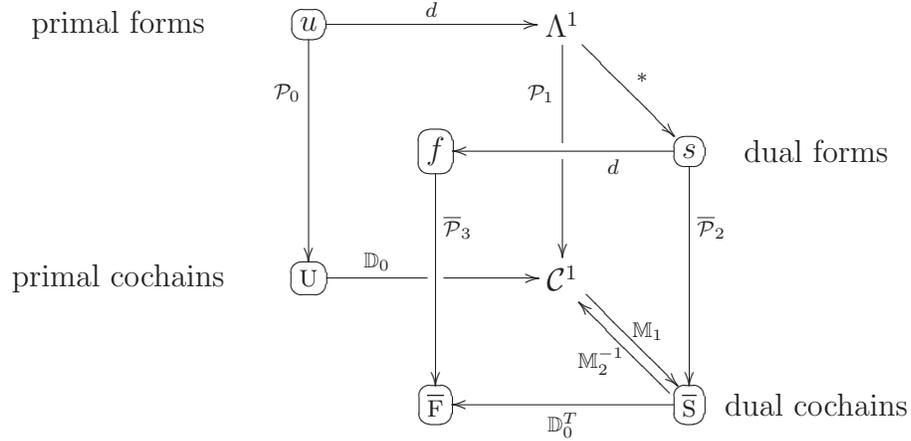
To simplify the presentation of the material, we will prove that

$$\|\mathcal{I}_0 \mathrm{U} - u\|^2_{H\Lambda^0} + \left\|*\mathcal{I}_1 \mathbb{M}_1^{-1}\overline{\mathrm{s}} - s\right\|^2_{H\Lambda^2} \leq C\,\mathrm{m_d^2},$$

from which the theorem follows.

89

$$||\mathcal{I}_0\mathrm{U} - u||^2_{H\Lambda^0} + ||*\mathcal{I}_1\mathbb{M}_1^{-1}\overline{\mathrm{S}} - s||^2_{H\Lambda^2}$$

$$\leq \quad ||\mathcal{I}_0\mathrm{U} - \mathcal{I}_0\mathcal{P}_0 u||^2_{H\Lambda^0} + ||*\mathcal{I}_1\mathbb{M}_1^{-1}\overline{\mathrm{S}} - *\mathcal{I}_1\mathbb{M}_1^{-1}\overline{\mathcal{P}}_2 s||^2_{H\Lambda^2}$$

$$+ C\,||u||^2_{H^1,[H^1]^3}\,\mathrm{m}_\mathrm{d}^2 \quad \text{by Lemma 3.19}$$

$$= \quad ||\mathcal{I}_0(\mathrm{U} - \mathcal{P}_0 u)||^2_{H\Lambda^0} + ||*\mathcal{I}_1\mathbb{M}_1^{-1}(\overline{\mathrm{S}} - \overline{\mathcal{P}}_2 s)||^2_{H\Lambda^2}$$

$$+ C\,||u||^2_{H^1,[H^1]^3}\,\mathrm{m}_\mathrm{d}^2 \quad \text{by linearity}$$

$$\leq \quad \frac{1}{\alpha^2}\left(||\mathbb{D}_0(\mathrm{U} - \mathcal{P}_0 u)||^2_{\mathcal{C}^1} + ||\overline{\mathrm{S}} - \overline{\mathcal{P}}_2 s||^2_{\overline{\mathcal{C}}^2}\right)$$

$$+ C\,||u||^2_{H^1,[H^1]^3}\,\mathrm{m}_\mathrm{d}^2 \quad \text{by Lemma 3.20}$$

$$= \quad \frac{1}{\alpha^2}||(\mathcal{P}_1 * -\mathbb{M}_1^{-1}\overline{\mathcal{P}}_2)s||^2_{\mathcal{C}^1} + C\,||u||^2_{H^1,[H^1]^3}\,\mathrm{m}_\mathrm{d}^2 \quad \text{by Lemma 3.21}$$

$$\leq \quad C\,||u||_{H^1,[H^1]^3}\left(||u||_{H^1,[H^1]^3}\,|\Omega| + 1\right)\mathrm{m}_\mathrm{d}^2 \quad \text{by Lemma 3.22}$$

$$\square$$

We first need a technical lemma related to our regularity assumption.

Lemma 3.18. *Under the assumptions of Theorem 3.17, for any 2-simplex* $\sigma_i^2 \in \mathcal{C}_2$,

$$\left|\frac{|\sigma_i^1|}{|\star\sigma_i^1|}\left(\int_{\star\sigma_i^1}\phi^*(*du)\right) - \int_{\sigma_i^1}\phi^*(du)\right| \leq ||u||_{H^1,[H^1]^3}\,|\sigma_i^1|\,\mathrm{m}_\mathrm{d}$$

Proof. Observe that $ddu = 0$ implies $||du||_{[H^1]^3,[H^1]^3} = ||du||_{[H^1]^3} \leq ||u||_{H^1,[H^1]^3}$.
Hence, the proof is identical to that of Lemma 3.11, with h replaced by du. $\square$

Lemma 3.19. *Under the assumptions of Theorem 3.17, there exists a constant C such that*

$$||u - \mathcal{I}_0 \mathcal{P}_0 u||_{H\Lambda^0} \le C \, \mathrm{m_d} \, ||u||_{H^1, [H^1]^3} \tag{3.34}$$

$$\left|\left|s - *\mathcal{I}_1 \mathbb{M}_1^{-1} \overline{\mathcal{P}}_2 s\right|\right|_{H\Lambda^1} \le C \, \mathrm{m_d} \, ||u||_{H^1, [H^1]^3} \tag{3.35}$$

Proof. First note that (3.34) holds by Theorem 2.50 for $k = 0$. By the same theorem for $k = 1$, we have that

$$||du - \mathcal{I}_1 \mathcal{P}_1 du||_{H\Lambda^1} \le C \, \mathrm{m_d} \, ||du||_{[H^1]^3, [H^1]^3} \le C \, \mathrm{m_d} \, ||u||_{H^1, [H^1]^3} \tag{3.36}$$

since $ddu = 0$ implies $||du||_{[H^1]^3, [H^1]^3} = ||du||_{[H^1]^3} \le ||u||_{H^1, [H^1]^3}$. Thus, the proof of (3.35) proceeds exactly as the proof of (3.24) from Lemma 3.12 by replacing h by du and b by s. $\square$

Lemma 3.20. *Under the assumptions of Theorem 3.17, there exists a constant $\alpha > 0$ independent of $\mathrm{m_d}$ such that*

$$\alpha ||\mathcal{I}_0 (\mathrm{u} - \mathcal{P}_0 u)||_{H\Lambda^0} \le ||\mathbb{D}_0 (\mathrm{u} - \mathcal{P}_0 u)||_{\mathcal{C}^1}, \tag{3.37}$$

$$\alpha \left|\left| *\mathcal{I}_1 \mathbb{M}_1^{-1} (\overline{\mathrm{s}} - \overline{\mathcal{P}}_2 s) \right|\right|_{H\Lambda^2} \le \left|\left| \overline{\mathrm{s}} - \overline{\mathcal{P}}_2 s \right|\right|_{\overline{\mathcal{C}}^2} \tag{3.38}$$

Proof. The subtle difference between this proof and its counterparts from the magnetostatics examples is that the two variables involved (u and s) are not related just by a $*$ relation. However, we can use the Poincaré Inequality to bound u in terms of its gradient $\nabla u \ (= du)$ and proceed in a similar fashion. For (3.37), we have

$$||\mathcal{I}_0 (\mathrm{u} - \mathcal{P}_0 u)||_{H\Lambda^0} = ||\mathcal{I}_0 (\mathrm{u} - \mathcal{P}_0 u)||_{L^2} + ||d\mathcal{I}_0 (\mathrm{u} - \mathcal{P}_0 u)||_{[L^2]^3}$$

91

by the definition of $||\cdot||_{H\Lambda^0}$. Observe that U and u are both identically zero on $\partial\Omega$ and hence $\mathcal{I}_0(\mathrm{U} - \mathcal{P}_0 u) = 0$ on $\partial\Omega$, as well.[3] Thus, by the Poincaré inequality (Theorem 2.67), we have

$$||\mathcal{I}_0(\mathrm{U} - \mathcal{P}_0 u)||_{H\Lambda^0} \leq (C+1)||d\mathcal{I}_0(\mathrm{U} - \mathcal{P}_0 u)||_{[L^2]^3}$$

By the commutativity of d and $\mathcal{I}$ (Theorem 2.48ii), we have

$$||\mathcal{I}_0(\mathrm{U} - \mathcal{P}_0 u)||_{H\Lambda^0} \leq (C+1)||\mathcal{I}_1 \mathbb{D}_0(\mathrm{U} - \mathcal{P}_0 u)||_{[L^2]^3}$$

The proof is now analogous to that of Lemma 3.7; we use the nice refinement assumption and Lemma 2.55 to conclude that

$$\frac{||\mathbb{D}_0(\mathrm{U} - \mathcal{P}_0 u)||^2_{\mathcal{C}^1}}{||\mathcal{I}_1 \mathbb{D}_0(\mathrm{U} - \mathcal{P}_0 u)||^2_{[L^2]^3}} \geq \alpha^2,$$

for some constant $\alpha > 0$ dependent on the element shape quality parameters but not the size or orientation of the element. The proof for (3.38) is analogous to that of Lemma 3.7 $\hfill\square$

Lemma 3.21. *Under the assumptions of Theorem 3.17,*

$$||\mathbb{D}_0(\mathrm{U} - \mathcal{P}_0 u)||^2_{\mathcal{C}^1} + \left|\left|\overline{\mathrm{S}} - \overline{\mathcal{P}}_2 s\right|\right|^2_{\overline{\mathcal{C}}^2} = \left|\left|(\mathcal{P}_1 * -\mathbb{M}_1^{-1}\overline{\mathcal{P}}_2)s\right|\right|^2_{\mathcal{C}^1} \tag{3.39}$$

The proof is analogous to that of Lemma 3.8

Lemma 3.22. *Under the assumptions of Theorem 3.17,*

$$\left|\left|(\mathcal{P}_1 * -\mathbb{M}_1^{-1}\overline{\mathcal{P}}_2)s\right|\right|_{\mathcal{C}^1} \leq ||u||^2_{H^1,[H^1]^3} |\Omega|\, \mathrm{m_d}$$

The proof is analogous to that of Lemma 3.9.

---

[3]Note that even if non-Dirichlet boundary conditions were used, we can proceed so long as we can assume that $\mathrm{U} = \mathcal{P}_0 u$ on $\partial\Omega$.

3.3.3 Poisson Equation - Stability of Dual Discretization

Treating u as an element of $\overline{\Lambda}^0$, the discretization of (3.29) is

$$\mathbb{M}_2^{-1}\mathbb{D}_2^T\overline{\mathrm{U}} = \mathrm{S}, \quad \mathbb{D}_2\mathrm{S} = \mathrm{F}. \tag{3.40}$$

Thus a solution pair is $(\overline{\mathrm{U}}, \mathrm{S}) \in \overline{\mathcal{C}}^0 \times \mathcal{C}^2$. The general linear system (3.6) is written

$$\begin{pmatrix} \mathbb{M}_2 & \mathbb{D}_2^T \\ \mathbb{D}_2 & 0 \end{pmatrix} \begin{pmatrix} \mathrm{S} \\ \overline{\mathrm{U}} \end{pmatrix} = \begin{pmatrix} 0 \\ \mathrm{F} \end{pmatrix} \tag{3.41}$$

Again, we have an equivalent linear system,

$$\begin{pmatrix} -\mathbb{M}_2^{-1} & \mathbb{D}_1 \\ \mathbb{D}_1^T & 0 \end{pmatrix} \begin{pmatrix} \overline{\mathrm{Q}} \\ \mathrm{G} \end{pmatrix} = \begin{pmatrix} -\mathrm{S}_0 \\ 0 \end{pmatrix}. \tag{3.42}$$

where $\mathrm{S}_0 \in \mathcal{C}^2$ is a primal 2-cochain satisfying $\mathbb{D}_2\mathrm{S}_0 = \mathrm{F}$ and $\overline{\mathrm{U}}$ is a solution to $\mathbb{D}_2^T\overline{\mathrm{U}} = -\overline{\mathrm{Q}}$. Define $\mathrm{S} := \mathbb{M}_2^{-1}\overline{\mathrm{Q}}$ so that $\mathbb{D}_2\mathrm{S} = \mathbb{D}_2(\mathbb{M}_2^{-1}\overline{\mathrm{Q}}) = \mathbb{D}_2(\mathrm{S}_0 + \mathbb{D}_1\mathrm{G}) = \mathrm{F}$. As before, the choice between (3.41) and (3.42) only makes a difference in regards to numerical stability (see Chapter 4).

We assume that $s \in [H^1]^3$ and div $s \in H^1$. We assume the domain boundary Γ is a collection of dual mesh faces and incorporate the constraints $\overline{\mathrm{U}}(\star\sigma^3) := 0$ for $\star\sigma^3 \subset \Gamma$. We also assume the input data is known exactly, i.e.

$$\mathrm{F} - \mathcal{P}_3 f \equiv 0. \tag{3.43}$$

The stability result is as follows.

Theorem 3.23. *Let Ω be a contractible, compact domain in $\mathbb{R}^3$ with primal and dual domain meshes of a finite number of elements. Let m_d denote*

93

the maximum diameter of a mesh element and assume that we have a nice refinement technique. Let $(\overline{\mathrm{U}}, \mathrm{S})$ *be a solution pair to (3.40). There exists a constant C dependent on $||u||_{H^1, [H^1]^3}$ but independent of* $\mathrm{m_d}$*, such that*

$$\left|\left|*\mathcal{I}_3\mathbb{M}_3^{-1}\overline{\mathrm{U}} - u\right|\right|_{H\Lambda^0} + ||\mathcal{I}_2\mathrm{S} - s||_{H\Lambda^2} \leq C\, \mathrm{m_d}.$$

This implies that the method is stable with the optimal order error estimate.

Proof. The proof is very similar to the previous stability proofs, differing only in the first step. Observe that $\overline{\mathrm{U}} = u = 0$ on Γ so the Poincaré inequality (Theorem 2.67) implies

$$\left|\left|*\mathcal{I}_3\mathbb{M}_3^{-1}\overline{\mathrm{U}} - u\right|\right|_{H\Lambda^0} \leq C\left|\left|\nabla(*\mathcal{I}_3\mathbb{M}_3^{-1}\overline{\mathrm{U}} - u)\right|\right|_{[L^2]^3}$$

By Theorem 2.48(iv) and the interpretation of ∇ as d_0, we can equate

$$\left|\left|\nabla(*\mathcal{I}_3\mathbb{M}_3^{-1}\overline{\mathrm{U}} - u)\right|\right|_{[L^2]^3} = \left|\left|*\mathcal{I}_2\mathbb{M}_2^{-1}\mathbb{D}_2^T\overline{\mathrm{U}} - du\right|\right|_{[L^2]^3}$$

The claim is now almost identical to the magnetostatics primal stability result by the identifications

$$s \to b, \quad \mathrm{S} \to \mathrm{B}, \quad du \to h, \quad \mathbb{D}_2^T\overline{\mathrm{U}} \to \overline{\mathrm{H}}.$$

There is a small difference in that we have $\mathbb{D}_2\mathrm{S} = \mathrm{F}$ instead of $\mathbb{D}_2\mathrm{B} = 0$ and we have $\mathbb{D}_1^T(\mathbb{D}_2^T\overline{\mathrm{U}}) = 0$ instead of $\mathbb{D}_1^T\overline{\mathrm{H}} = \overline{\mathrm{J}}$. However, these differences only matter in two places in the proof which we can easily dispatch. First, in the beginning of Lemma 3.7, our assumption that $\mathrm{F} - \mathcal{P}_3f = 0$ lets us reduce the $H\Lambda^2$ norm

to an $[L^2]^3$ norm (instead of it being immediate from the equations). Second, to prove equation (3.17), we use the fact that

$$\overline{\mathrm{H}} - \overline{\mathcal{P}}_1 h = \mathbb{D}_2^T \overline{\mathrm{U}} - \overline{\mathcal{P}}_1 du = \mathbb{D}_2^T (\overline{\mathrm{U}} - \overline{\mathcal{P}}_0 u)$$

and proceed using Lemma 2.53 in the same manner. Therefore, the proof goes through in exactly the same way. □

3.4 Example: Darcy Flow

We now consider a simplified Darcy flow problem which has previously been considered as an application of DEC theory by Hirani et al. [58, 60]. Under the assumption of no external body force, the problem on $\Omega \subset \mathbb{R}^3$ is

$$\begin{cases} f + \dfrac{k}{\mu}\nabla p & = & 0 & \text{in } \Omega, \\ \operatorname{div} f & = & \phi & \text{in } \Omega, \\ f \cdot \hat{n} & = & \psi & \text{on } \partial\Omega, \end{cases} \tag{3.44}$$

The goal is to solve for volumetric flux f and pressure p given ϕ and ψ satisfying the compatibility condition $\int_\Omega \phi d\Omega = \int_{\partial\Omega} \psi d\Gamma$. We assume for simplicity of presentation that the ratio k/μ of permeability to viscosity is 1.

We take $p \in \Lambda^0$ and $f \in \Lambda^2$ since they are operated on by grad $= d_0$ and div $= d_2$, respectively. The first equation requires a Hodge star for the summation to make sense, yielding the system

$$\begin{aligned} f + *dp & = 0, \\ df & = \phi. \end{aligned} \tag{3.45}$$

By the correspondence $f \mapsto s$ and $p \mapsto u$, we can recognize (3.45) as the Poisson problem (3.29) with Neumann instead of Dirichlet boundary condi-

tions. This problem does not have a unique solution unless some additional constraint is imposed, e.g. partial Dirichlet boundary data. With such a constraint, a Poincaré estimate still holds for p (the analogue of u) and hence all our analysis from Section 3.3 carries over to this problem.

The method proposed by Hirani et al. [58, 60] gives a primal discretization of f as $\mathrm{F} \in \mathcal{C}^2$ and a dual discretization of p as $\overline{\mathrm{P}} \in \overline{\mathcal{C}}^0$. Thus, their approach is the same as the dual discretization of the mixed Poisson equation presented in Section 3.3.3 and achieves the same stability estimates. Our methodology thus reveals an alternate discretization, namely, f as $\overline{\mathrm{F}} \in \overline{\mathcal{C}}^2$ and p as $\mathrm{P} \in \mathcal{C}^0$, with stability guaranteed by the analysis in Section 3.3.2.

The important message from this example is the evident arbitrariness of 'primal' and 'dual' monikers. While a primal discretization of u was the first consideration when discretizing Poisson's equation, a primal discretization of v was the first consideration when discretizing the Darcy flow equation. This, we contend, provides evidence that the toolkit of DEC will be useful in identifying alternative discretization methods for many PDEs beyond those considered in this thesis.

3.5 Discretization Stability with the Whitney Hodge Star

It is almost possible to claim that the linear systems presented thus far maintain their discretization stability results if $\mathbb{M}_k$ is replaced with $\mathbb{M}_k^{Whit}$, mutatis mutandis. As we have discussed in Remark 2.52, this type of change

96

$$
\begin{array}{ccc}
\Lambda^k & \xrightarrow{\quad * \quad} & \overline{\Lambda}^{n-k} \\
\Big\uparrow{\scriptstyle \mathcal{I}_k} & & \Big\downarrow{\scriptstyle \overline{\mathcal{P}}_{n-k}} \\
\mathcal{C}^k & \xrightarrow{\quad \mathbb{M}_k \quad} & \overline{\mathcal{C}}^{n-k}
\end{array}
$$

Figure 3.5: Certain maps between cochain and form spaces are shown, indicating how definitions of the discrete Hodge star $\mathbb{M}_k$ can be motivated as approximations to the composed map $\overline{\mathcal{P}}_{n-k} * \mathcal{I}_k$.

is typically accompanied by a switch from circumcentric to barycentric dual meshes. In this case, it has been shown by Bossavit [19] that the analogues of all the Lemmas in Section 3.2.2 hold and hence Theorem 3.3 holds as well. Thus, the all the subsequent examples depending on the primal magnetostatics proof hold as well. The end result of such analysis is a fact already well known in the finite element community, namely, that the appropriate use of Whitney elements produces stable mixed methods [24, 7].

Rather than reproving these well-known results in a lengthy exposition, we will show how the definitions of $\mathbb{M}_k$ and $\mathbb{M}_k^{Whit}$ can be seen as different attempts at discretizing the composed map $\overline{\mathcal{P}}_{n-k} * \mathcal{I}_k$ as shown in Figure 3.5. This will shed light on why two seemingly unrelated operator discretizations can both result in stable methodologies. It will also motivate why the inverse discrete Hodge star we define in Section 4.2 should be a good proxy for the inverse of either of either $\mathbb{M}_k$ or $\mathbb{M}_k^{Whit}$.

First we define an approximation of $\overline{\mathcal{P}}_{n-k}$ which we will call $\overline{\mathcal{P}}_{n-k}^g$ where the g is meant to stand for 'geometric.' Definition 2.45 tells us that evaluating $\overline{\mathcal{P}}_{n-k} * u$ for some $u \in \Lambda^k$ requires the computation of integrals of $*u$ over each

dual $n - k$ cell in the mesh. Finding a closed form expression of these integrals for arbitrary u and arbitrary mesh geometry is implausible. If u is reasonably smooth, however, we can estimate the integrals by assuming

$$\frac{1}{|\star \sigma_i^k|} \int_{\star \sigma_i^k} \phi^*(*u) \approx \frac{1}{|\sigma_i^k|} \int_{\sigma_i^k} \phi^* u,$$

i.e. that $*u$ has the same average value over $\star \sigma_i^k$ that u has over σ_i^k. Thus, we define

$$\mathcal{P}_{n-k}^g * u := \left\{ \frac{|\star \sigma_i^k|}{|\sigma_i^k|} \int_{\sigma_i^k} \phi^* u \right\}_i$$

Observe that for $\mathrm{U} \in \mathcal{C}^k$, the value $\mathrm{U}(\sigma_i^k)$ is meant to represent the integral of u over σ_i^k. Thus, we can view $\mathbb{M}_k^{Diag} \mathrm{U}$ as

$$\mathbb{M}_k^{Diag} \mathrm{U} = \left\{ \frac{|\star \sigma_i^k|}{|\sigma_i^k|} \mathrm{U}(\sigma_i^k) \right\}_i = \overline{\mathcal{P}}_{n-k}^g * \mathcal{I}_k \mathrm{U} \approx \overline{\mathcal{P}}_{n-k} * \mathcal{I}_k \mathrm{U}. \tag{3.46}$$

To see $\mathbb{M}_k^{Whit}$ as a similar composition, we first define an approximation of $\mathcal{P}_k$ which we will call $\mathcal{P}_k^s$ where the s is meant to stand for 'smoothed.' Define

$$\mathcal{P}_k^s(u) := \left\{ |\sigma_i^k| \frac{\displaystyle\int u \mathcal{W}_{\sigma_i^k}}{\displaystyle\int \mathcal{W}_{\sigma_i^k}} \right\}_i$$

The integrals are over Ω. Note that $\mathcal{P}_k^s$ is exactly $\mathcal{P}_k$ on constant functions and can be expected to give a good approximation of $\mathcal{P}_k$ for arbitrary u by the properties of Whitney functions. We will make use of the geometric identity

$$|\star \sigma_i^k| = \int \mathcal{W}_{\sigma_i^k} \tag{3.47}$$

which holds over barycentric meshes, as was shown by Bossavit [19].

98

Lemma 3.24. *For any* $\mathrm{U} \in \mathcal{C}^k$,

$$\mathbb{M}_k^{Whit}\mathrm{U} = \overline{\mathcal{P}}_{n-k}^g * \mathcal{I}_k \mathcal{P}_k^s \mathcal{I}_k \mathrm{U}$$

Proof. The proof is a matter of picking through the definitions. Denote $\mathrm{U}(\sigma_j^k)$ by U_j and $\mathcal{W}_{\sigma_j^k}$ by $\mathcal{W}_j$. Observe that

$$\mathcal{P}_k^s \mathcal{I}_k \mathrm{U} = \left\{ |\sigma_i^k| \frac{\int \left(\sum_j \mathrm{U}_j \mathcal{W}_j \right) \mathcal{W}_i}{\int \mathcal{W}_i} \right\}_i$$

Thus,

$$\mathcal{I}_k \mathcal{P}_k^s \mathcal{I}_k \mathrm{U} = \sum_i \left(|\sigma_i^k| \frac{\int \left(\sum_j \mathrm{U}_j \mathcal{W}_j \right) \mathcal{W}_i}{\int \mathcal{W}_i} \right) \mathcal{W}_i$$

$$= \sum_{i,j} \frac{\int \mathcal{W}_i \mathcal{W}_j}{\int \mathcal{W}_i} \mathrm{U}_i |\sigma_i^k| \mathcal{W}_i$$

Hence,

$$\overline{\mathcal{P}}_{n-k}^g * \mathcal{I}_k \mathcal{P}_k^s \mathcal{I}_k \mathrm{U} = \left\{ \mathrm{U}_i| \star \sigma_i^k| \sum_j \frac{\int \mathcal{W}_i \mathcal{W}_j}{\int \mathcal{W}_i} \right\}_i$$

$$= \left\{ \sum_j \int \mathcal{W}_i \mathcal{W}_j \mathrm{U}_i \right\}_i$$

$$= \mathbb{M}_k^{Whit} \mathrm{U}.$$

Note that this last chain of equalities used the geometric identity (3.47). $\quad\square$

99

Since $\mathcal{P}_k^s \mathcal{I}_k \approx 1$, we can use Lemma 3.24 to conclude

$$\mathbb{M}_k^{Whit} U \approx \overline{\mathcal{P}}_{n-k}^g * \mathcal{I}_k U = \mathbb{M}_k^{Diag} U$$

and thus, by (3.46), $\mathbb{M}_k^{Whit} U \approx \overline{\mathcal{P}}_{n-k} * \mathcal{I}_k U$, as well.

The definition of a discrete Hodge is by no means canonical and many plausible choices for their definition may provide for discretization stability in these types of mixed methods. In this section, however, we have seen that the most used definitions of $\mathbb{M}_k$ both provide an approximation of $\overline{\mathcal{P}}_{n-k} * \mathcal{I}_k$. Hence, this approximation property can be used as a criterion to motivate alternate definitions of $\mathbb{M}_k$ and of its inverse. This will be discussed further in Section 4.2.

3.6 Discretization Stability with Generalized Barycentric Interpolation

In all of our analysis thus far, we have used the composed operator

$$*\mathcal{I}_{n-k}\mathbb{M}_{n-k}^{-1} : \overline{\mathcal{C}}^k \to \overline{\Lambda}^k \tag{3.48}$$

as a shortcut for defining an interpolation operator on the dual cochain spaces. This has had the advantage of allowing us to leverage many established results on the I_k operators in our stability proofs. The drawback, however, is that writing the operator out in a simple closed form (in preparation for subsequent implementation in code, for instance) is rather difficult due to the presence of the $*$ operator.

As we will show, (3.48) is neither the only nor the optimal definition for a dual cochain interpolation operator. We will construct explicit interpolation operators $\overline{\mathcal{I}}_k$ for dual k-cochains and show that they achieve the same optimal convergence estimate. The results in this section are for $\overline{\mathcal{I}}_0$ with $n = 2$, taken from my paper [48]. A construction of $\overline{\mathcal{I}}_k$ with $n = 3$ for $0 \leq k \leq 3$ will be given in Chapter 4.

To show a standard optimal convergence estimate for the $\overline{\mathcal{I}}_0$ operator with the Sibson functions, we will make use of the definitions and results given in Sections 2.10, 2.11, and 2.12.

Theorem 3.25. *Assuming conditions G1 and G2, the optimal convergence estimate holds for $\overline{\mathcal{I}}_0$ using the Sibson generalized barycentric interpolation functions. That is, there exists a constant C independent of $\mathrm{m_d}$ such that*

$$\left\lVert u - \overline{\mathcal{I}}_0\overline{\mathcal{P}}_0 u \right\rVert_{H^1(\mathcal{T})} \leq C \operatorname{diam}(\mathcal{T})|u|_{H^2(\mathcal{T})}, \quad \forall u \in H^2(\mathcal{T}). \qquad (3.49)$$

Proof. Again, we will use the abbreviated notation

$$I := \overline{\mathcal{I}}_0\overline{\mathcal{P}}_0.$$

By Corollary 2.65, it suffices to prove estimate (2.19). By Lemma 2.66, it suffices to prove (2.20). By Lemma 3.29, (2.20) holds. Hence, the rest of this section is devoted to proving Lemma 3.29. □

We begin with a technical property of domains satisfying conditions G1 and G2.

101
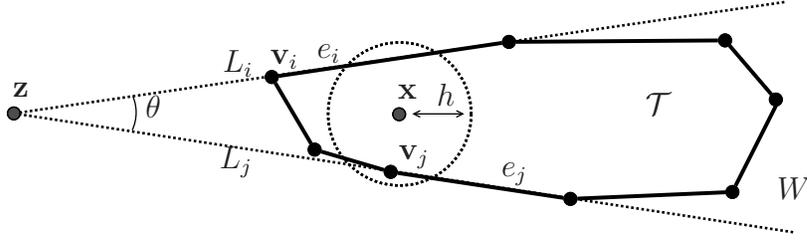
Figure 3.6: Notation for proof of Proposition 3.26.

Proposition 3.26. *Under G1 and G2, there exists $h_* > 0$ such that for all $x \in \mathcal{T}$, $B(x, h_*)$ does not intersect any three edges or any two non-adjacent edges of $\mathcal{T}$.*

Proof. Let $\mathbf{x} \in \mathcal{T}$, $h \in (0, d_*/2)$, and suppose that two disjoint edges of $\mathcal{T}$, e_i and e_j, intersect $B(\mathbf{x}, h)$. Let L_i and L_j be the lines containing e_i and e_j and let θ be the angle between these lines; see Figure 3.6. We first consider the case where L_i and L_j are not parallel and define $\mathbf{z} = L_i \cap L_j$.

Let $\mathbf{v}_i$ and $\mathbf{v}_j$ be the endpoints of e_i and e_j nearest to $\mathbf{z}$. Since $h < d_*/2$ both $\mathbf{v}_i$ and $\mathbf{v}_j$ cannot live in $B(\mathbf{x}, h)$; without loss of generality assume that $\mathbf{v}_i \notin B(\mathbf{x}, h)$. Since $\operatorname{dist}(\mathbf{v}_j, L_i) < 2h$,

$$\sin \theta < 2h/ \left| \mathbf{z} - \mathbf{v}_j \right|. \tag{3.50}$$

Let W be the sector between L_i and L_j containing x. Now $\mathcal{T} \subset B(\mathbf{v}_j, 1) \cap W \subset B(\mathbf{z}, 1 + |\mathbf{z} - \mathbf{v}_j|) \cap W$. It follows that $\rho(\mathcal{T}) \leq (1 + |\mathbf{v}_j - \mathbf{z}|) \sin \theta$. Using (3.50) and G1,

$$\frac{1}{\gamma^*} \leq \frac{2h}{|\mathbf{z} - \mathbf{v}_j|}(1 + |\mathbf{z} - \mathbf{v}_j|) \leq 2h \left(\frac{1}{d_*} + 1 \right)$$

102

where the final inequality holds because by G2 $|\mathbf{z} - \mathbf{v}_j| \geq |\mathbf{v}_i - \mathbf{v}_j| \geq d_*$. Thus

$$h > \frac{d_*}{2\gamma^*(1 + d_*)}. \tag{3.51}$$

Estimate (3.51) holds in the limiting case: when L_i and L_j are parallel. In this case $\mathcal{T}$ must be contained in a strip of width $2h$ which for small h violates the aspect ratio condition.

The triangle is the only polygon with three or more pairwise non-adjacent edges. So it remains to find a suitable h_* so that $B(\mathbf{x}, h_*)$ does not intersect all three edges of the triangle. For a triangle, $\rho(\mathcal{T})$ is the radius of the smallest circle touching all three edges. Since under G1 $\rho(\mathcal{T}) \geq 1/\gamma^*$, $B(\mathbf{x}, \frac{1}{2\gamma^*})$ intersects at most two edges. Thus $h_* = \frac{d_*}{2\gamma^*(1+d_*)}$ is sufficiently small to satisfy the proposition in all cases. $\qquad\square$

Proposition 3.26 is a useful tool for proving a lower bound on $D(\mathbf{x})$, the area of the Voronoi cell of $\mathbf{x}$ intersected with $\mathcal{T}$.

Proposition 3.27. *Under G1 and G2, there exists $D_* > 0$ such that $D(\boldsymbol{x}) > D_*$.*

Proof. Let h_* be the constant in Proposition 3.26. We consider two cases, based on whether the point $\mathbf{x}$ is near any vertex of $\mathcal{T}$, as shown in Figure 3.7 (left).

<u>Case 1</u>: There exists $\mathbf{v}_i$ such that $\mathbf{x} \in B(\mathbf{v}_i, h_*/2)$.

Consider the sector of $B(\mathbf{x}, h_*/2)$ specified by segments which are parallel to the edges of $\mathcal{T}$ containing $\mathbf{v}_i$, as shown in Figure 3.7 (right). This
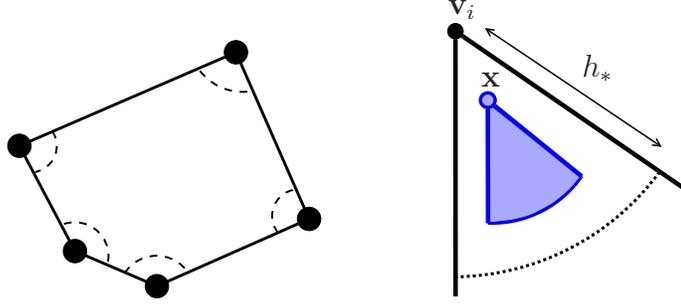
Figure 3.7: The proof of Proposition 3.27 has two cases based on whether $\mathbf{x}$ is within $h_*/2$ of some $\mathbf{v}_i$ or not. When $\mathbf{x}$ is within $h_*/2$ of $\mathbf{v}_i$, the shaded sector shown on the right is contained in $V_{P'}(\mathbf{x}) \cap \mathcal{T}$.

sector must be contained in $\mathcal{T}$ by Proposition 3.26 and in the Voronoi cell of $\mathbf{x}$ by choice of $h_* < d_*$. Thus by G4 (using Proposition 2.61(1)) $D(\mathbf{x}) \geq \beta_* h_*^2/8$.

<u>Case 2</u>: For all $\mathbf{v}_i$, $\mathbf{x} \notin B(\mathbf{v}_i, h_*/2)$.

In this case, $B(\mathbf{x}, h_*/4) \cap \mathcal{T} \subset V_{P'}(\mathbf{x})$. If $B(\mathbf{x}, h_*/4)$ intersects zero or one boundary edge of $\mathcal{T}$, then $D(\mathbf{x}) \geq \pi h_*^2/32$. Otherwise $B(\mathbf{x}, h_*/4)$ intersects two adjacent boundary edges. By G4, $D(\mathbf{x}) \geq \beta_* h_*^2/32$. $\qquad\square$

General formulas for the gradient of the area of a Voronoi cell are well-known and can be used to bound the gradients of $D(\mathbf{x})$ and $D(\mathbf{x}) \cap C_i$.

Proposition 3.28. $|\nabla D(\boldsymbol{x})| \leq \pi$ and $|\nabla(D(\boldsymbol{x}) \cap C_i)| \leq 1$.

Proof. The gradient of the area of a Voronoi region is known to be

$$\nabla D(\mathbf{x}) = \sum_{j=1}^{n} \frac{\mathbf{v}_j - \mathbf{x}}{|\mathbf{v}_j - \mathbf{x}|} F_j,$$

104

where F_j is the length of the segment separating the Voronoi cells of $\mathbf{x}$ and $\mathbf{v}_j$ [75, 76]. Then applying Proposition 2.60 gives

$$|\nabla D(\mathbf{x})| \leq \sum_{i=1}^{n} F_i \leq |\partial \mathcal{T}| \leq \pi.$$

Similarly,

$$\nabla(D(\mathbf{x}) \cap C_i) = \frac{\mathbf{v}_i - \mathbf{x}}{|\mathbf{v}_i - \mathbf{x}|} F_i,$$

and since $F_i \leq \mathrm{diam}(\mathcal{T})$, $|\nabla(D(\mathbf{x}) \cap C_i)| \leq 1$. $\qquad\square$

Propositions 3.27 and 3.28 give estimates for the key terms needed to prove (2.20), i.e. a uniform bound on the H^1 norm of the $\overline{\lambda}_i$ functions.

Lemma 3.29. *Under G1 and G2, (2.20) holds for the Sibson coordinates.*

Proof. $\left|\nabla\overline{\lambda}_i\right|$ is estimated by applying Propositions 3.27 and 3.28:

$$
\begin{aligned}
\left|\nabla\overline{\lambda}_i\right| &\leq \frac{|\nabla(D(\mathbf{x}) \cap C_i)|}{D(\mathbf{x})} + \frac{(D(\mathbf{x}) \cap C_i) |\nabla D(\mathbf{x})|}{D(\mathbf{x})^2} \leq \frac{|\nabla(D(\mathbf{x}) \cap C_i)| + |\nabla D(\mathbf{x})|}{D(\mathbf{x})} \\
&\leq \frac{1 + \pi}{D_*}.
\end{aligned}
$$

Integrating this estimate completes the result. $\qquad\square$

We conclude with a remark on why Theorem 3.25 implies a similar estimate over an entire Ω. Suppose Ω is a mesh of a finite number of elements denoted by $\mathcal{T}$. Squaring both sides of (3.49) and summing over the elements yields

$$\sum_{\mathcal{T}} \left\|u - \overline{\mathcal{I}}_0\overline{\mathcal{P}}_0 u\right\|_{H^1(\mathcal{T})}^2 \leq C^2 \sum_{\mathcal{T}} \mathrm{diam}(\mathcal{T})^2 |u|_{H^2(\mathcal{T})}^2, \quad \forall u \in H^2(\mathcal{T}).$$

Letting m_d denote the maximum diameter of all $\mathcal{T} \in \Omega$, we have that

$$\sum_{\mathcal{T}} \left|\left| u - \overline{\mathcal{I}}_0 \overline{\mathcal{P}}_0 u \right|\right|_{H^1(\mathcal{T})}^2 \leq C^2 \; m_d^2 \sum_{\mathcal{T}} |u|_{H^2(\mathcal{T})}^2, \quad \forall u \in H^2(\mathcal{T}).$$

The sums are now of integrals whose domains are disjoint with union Ω (recall Definition 2.14). Given this observation, we can rewrite and square root both sides to get the global estimate

$$\left|\left| u - \overline{\mathcal{I}}_0 \overline{\mathcal{P}}_0 u \right|\right|_{H^1(\Omega)} \leq C \; m_d |u|_{H^2(\Omega)}, \quad \forall u \in H^2(\Omega).$$

Chapter 4

Numerical Stability of Dual Methods

In Chapter 3, we explained how to construct primal and dual discretizations of the same PDE and showed that both resulted in optimal convergence estimates as the size of the maximum mesh element shrinks. This begs the question of how implementation concerns might guide the choice of one method over the other. Recalling the generic systems (3.5) and (3.6) from Section 3.1, both have similar structures. However, they may have vastly different numerical properties depending on whether the diagonal Hodge star $\mathbb{M}_k$ or the Whitney Hodge star $\mathbb{M}_k^{Whit}$ is used.

While the matrices $\mathbb{M}$ and $\mathbb{M}^{-1}$ are both diagonal and thus result in fast solvers, they yield a very coarse approximation of the metric information encoded by $*$. This means a very fine mesh may be needed to get sufficiently accurate results with $\mathbb{M}$. The richer approximation power of $\mathbb{M}^{Whit}$ provides for a better approximation of metric information, but $\mathbb{M}^{Whit}$ is only sparse and $(\mathbb{M}^{Whit})^{-1}$ may be dense. Hence there is a tradeoff between computational efficiency and accuracy in choosing between the diagonal and Whitney discrete Hodge stars, with one choice (viz. $(\mathbb{M}^{Whit})^{-1}$) essentially untenable.

To allow for an accurate alternative to $\mathbb{M}^{-1}$ and a sparse alternative to

107

$(\mathbb{M}^{Whit})^{-1}$, we introduce a new discrete Hodge star based on the generalized barycentric functions $\overline{\lambda}_i$ defined in Section 2.10. To motivate the definition, we begin by proposing a set of functions analogous to the Whitney forms but defined relative to a dual mesh.

4.1 Whitney-like Interpolation Functions for Dual Meshes

We define the dual Whitney-like interpolant of a dual k-cochain $\overline{\mathrm{w}} \in \overline{\mathcal{C}}^k$ to be

$$\overline{\mathcal{I}}_k(\overline{\mathrm{w}}) := \sum_{\star\sigma^{n-k}\in\overline{\mathcal{C}}_k} \overline{\mathrm{w}}(\star\sigma^{n-k})\overline{\mathcal{W}}_{\star\sigma^{n-k}}. \tag{4.1}$$

where $\overline{\mathcal{W}}_{\star\sigma^{n-k}}$ is a basis function associated to the k-dimensional element $\star\sigma^{n-k}$ in the dual mesh. We now define these dual basis functions in 2D and 3D.

Definition 4.1. Let $n = 2$. The **Whitney-like function** $\overline{\mathcal{W}}_{\star\sigma^{2-k}}$ associated to the k-dimensional element $\star\sigma^{2-k}$ in a dual mesh is defined as follows.

- **Dual Vertices**. The function associated to a dual vertex $\star\sigma^2 := \mathbf{v}_i$ is

$$\overline{\mathcal{W}}_{\star\sigma^2} := \overline{\lambda}_i,$$

  where $\overline{\lambda}_i$ is any barycentric function satisfying Definition 2.56. An example is the Sibson functions given in Definition 2.59.

- **Dual Edges**. The function associated to an oriented dual edge $\star\sigma^1 := [\mathbf{v}_i, \mathbf{v}_j]$ is the vector-valued function

$$\overline{\mathcal{W}}_{\star\sigma^1} := \overline{\lambda}_i\nabla\overline{\lambda}_j - \overline{\lambda}_j\nabla\overline{\lambda}_i$$

- **Dual Cells**. The scalar-valued function associated to the polygon $\star\sigma^0$ is a constant function on the element:

$$\overline{\mathcal{W}}_{\star\sigma^0} := \chi_{\star\sigma^0} = \begin{cases} 1/|\star\sigma^0| & \text{on } \star\sigma^0 \\ 0 & \text{otherwise} \end{cases}$$

$\diamond$

Definition 4.2. Let $n = 3$. The **Whitney-like function** $\overline{\mathcal{W}}_{\star\sigma^{3-k}}$ associated to the k-dimensional element $\star\sigma^{3-k}$ in a dual mesh is defined as follows.

- **Dual Vertices**. The function associated to a dual vertex $\star\sigma^3 := \overline{\mathbf{v}}_i$ is

$$\overline{\mathcal{W}}_{\star\sigma^3} := \overline{\lambda}_i,$$

  where $\overline{\lambda}_i$ is any barycentric function satisfying Definition 2.56. An example is the Sibson functions given in Definition 2.59.

- **Dual Edges**. The function associated to an oriented dual edge $\star\sigma^2 := [\overline{\mathbf{v}}_i, \overline{\mathbf{v}}_j]$ is the vector-valued function

$$\overline{\mathcal{W}}_{\star\sigma^2} := \overline{\lambda}_i \nabla \overline{\lambda}_j - \overline{\lambda}_j \nabla \overline{\lambda}_i$$

- **Dual Faces**. Consider a dual face $\star\sigma^1$ with m vertices $\{\overline{\mathbf{v}}_0, \ldots, \overline{\mathbf{v}}_{m-1}\}$. Partition the face canonically into triangles by adding a vertex $\overline{\mathbf{c}}$ at the centroid of the face vertices and adding the edges $[\overline{\mathbf{c}}, \overline{\mathbf{v}}_i]$. Define 2-simplices $\tau_i := [\overline{\mathbf{c}}, \overline{\mathbf{v}}_i, \overline{\mathbf{v}}_{i+1}]$, indices taken mod m. Define 3-simplices by connecting the τ_i to the endpoint of σ^1 inside the polyhedron. Define

$$\overline{\mathcal{W}}_{\star\sigma^1} := \sum_{i=0}^{m-1} \frac{|\tau_i|}{|\star\sigma^1|} \mathcal{W}_{\tau_i} \chi_{\tau_i},$$

109

where χ_{τ_i} is the characteristic function on τ_i (1 on τ_i, 0 otherwise) and

$$\mathcal{W}_{\tau_i} := 2 \left(\lambda_{\overline{\mathbf{c}}} \nabla \lambda_i \times \nabla \lambda_{i+1} - \lambda_i \nabla \lambda_{\overline{\mathbf{c}}} \times \nabla \lambda_{i+1} + \lambda_{i+1} \nabla \lambda_{\overline{\mathbf{c}}} \times \nabla \lambda_i \right).$$

Note that $\mathcal{W}_{\tau_i}$ is the Whitney 2-form associated to face τ_i of a tetrahedron and that these tetrahedra partition the entire polyhedra. An example is shown in Figure 4.1.

- **Dual Cells**. The scalar-valued function associated to a dual cell $\star\sigma^0$ is a constant function on the cell:

$$\overline{\mathcal{W}}_{\star\sigma^0} := \chi_{\star\sigma^0} = \left\{ \begin{array}{rl} 1/|\star\sigma^0| & \text{on } \star\sigma^0 \\ 0 & \text{otherwise} \end{array} \right.$$

$\lozenge$

The analogy to the primal Whitney functions is made precise by the following Lemma.

Lemma 4.3. *If $\star\sigma^0$ is a simplex, the dual Whitney functions associated to its subsimplices are identical to the Whitney functions.*

Proof. The generalized barycentric functions reduce to barycentric functions on simplices. Hence the result follows immediately from the definitions. $\square$

Moreover, many of the properties of Whitney functions can be recovered for dual Whitney functions.
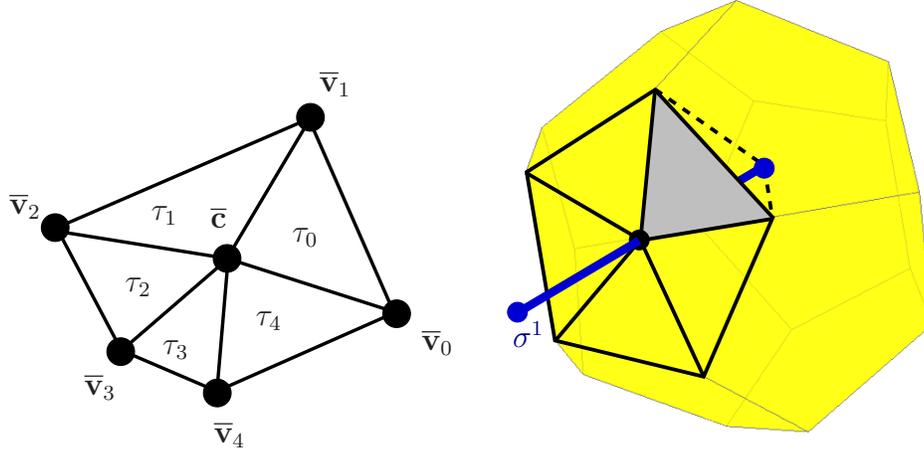
Figure 4.1: Sample computation of a Whitney-like form associated to a dual face $\star\sigma^1$ with vertices $\overline{\mathbf{v}}_i$. By adding the centroid $\overline{\mathbf{c}}$, we have a canonical decomposition of $\star\sigma^1$ into triangles τ_i. A weighted sum of the primal Whitney function associated with each τ_i is constructed to define the function for the face. As shown on the right, each τ_i, e.g. the shaded triangle, forms a tetrahedron by connecting its vertices to the vertex of σ^1 interior to the polyhedron. Note that in general $\overline{\mathbf{c}}$ need not be the same as $\sigma^1 \cap \star\sigma^1$.

Theorem 4.4. *Let $\overline{\lambda}_i$ denote any set of generalized barycentric functions satisfying Definition 2.56. Then the associated Whitney-like functions satisfy properties analogous to properties W1-W3 of the Whitney functions. More precisely, the following conditions hold for $n = 2$ or 3 with $0 \le k \le n$.*

$\overline{\text{W}}$1. **Conformity in $H\Lambda^k$:** $\overline{\mathcal{I}}_k(\overline{\text{w}}) \in H\Lambda^k$

$\overline{\text{W}}$2. **Local support:** $\text{supp } \overline{\mathcal{W}}_{\star\sigma^k} \subseteq \bigcup_{\star\sigma^0 \succ \star\sigma^k} \star\sigma^0$

$\overline{\text{W}}$3. **Interpolation:** $\displaystyle\int_{\star\sigma_i^k} \phi^*(\overline{\mathcal{W}}_{\star\sigma_i^k}) = 1$

The following property holds for $k = 0$ when $n = 2$, using Sibson coordinates.

$\overline{\mathrm{W}}$4. **Optimal Convergence:** $\left\|u - \overline{\mathcal{I}}_k \overline{\mathcal{P}}_k u\right\|_{H\Lambda^k} \leq C\, \mathrm{m_d}$

Proof. The partition of unity property is property B3 in Section 2.10. The local support property is immediate by construction and is discussed further in Section 4.2. The optimal convergence property is the result of Theorem 3.25.

To prove the conformity property, we will use the results and notation of Section 2.4 and Lemma 4.6 given below. We take $n = 3$ since similar arguments suffice to prove conformity in $n = 2$. Figure 4.2 motivates the proof.

(a)   (b)
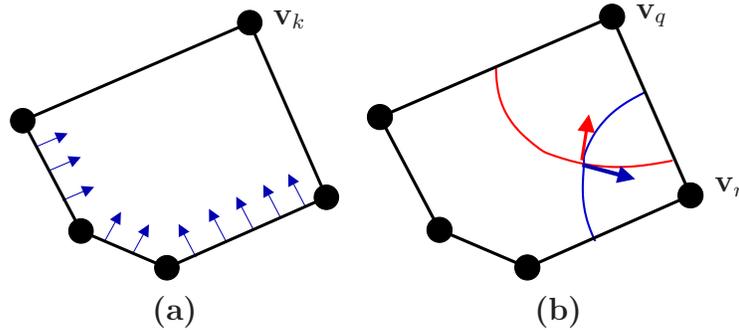
Figure 4.2: Proof of the conformity property in cases $k = 1$ and $k = 2$. In **(a)**, we depict the observation that on any face not containing $\mathbf{v}_k$, $\overline{\lambda}_k$ is identically 0 and hence $\nabla \overline{\lambda}_k$ is orthogonal. In **(b)**, we depict, similarly, how $\nabla \overline{\lambda}_q$ and $\nabla \overline{\lambda}_r$ lie in the same plane as a face containing $\mathbf{v}_q$ and $\mathbf{v}_r$; their cross product will be a portion of the normal component of the two form associated to the face and thus is agreed upon by two polyhedra sharing the polygon.

$\overline{\mathbf{W}}$1, **k=0:** We need to show $u \in H^1$ for

$$u := \overline{\mathcal{I}}_0(\overline{\mathrm{w}}) = \sum_i \overline{\mathrm{w}}(\star \sigma_i^3)\overline{\lambda}_i,$$

112

where $\overline{\mathrm{w}}$ is an arbitrary dual 0-cochain. Let $F := \star\sigma^1$ be an arbitrary dual face such that $F = \star\sigma_1^3 \cap \star\sigma_2^3$. By Corollary 2.35, it suffices to show that $u_1 \equiv u_2$ on F. By Lemma 4.6, u_1 and u_2 only depend on the vertices $\mathbf{v}_j \in F$. Since u_1 and u_2 are computed by the summation of the same coefficients and coordinate functions for any $\mathbf{x} \in F$, they are identical on F.

$\overline{\mathbf{W}}1$, $\mathbf{k=1}$: We need to show $\vec{z} \in H(\text{curl})$ for

$$\vec{z} := \overline{\mathcal{I}}_1(\overline{\mathrm{w}}) = \sum_i \overline{\mathrm{w}}(\star\sigma_i^2)\overline{\mathcal{W}}_{\star\sigma_i^2},$$

where $\overline{\mathrm{w}}$ is an arbitrary dual 1-cochain. Let $F := \star\sigma^1$ be an arbitrary dual face as before. By Corollary 2.37, it suffices to show $T_F(\vec{z}_1) = T_F(\vec{z}_2)$ where $T_F(\vec{z}_i)$ is the tangential component of $\vec{z}_i$ on F. Note that the $\overline{\mathcal{W}}_{\star\sigma^2}$ functions are comprised of terms of form $\overline{\lambda}_p \nabla \overline{\lambda}_q$ where $\star\sigma^2 = [\mathbf{v}_p, \mathbf{v}_q]$. By Lemma 4.6, if $\mathbf{v}_p$ is not a vertex of F then the term is zero on F and if $\mathbf{v}_q$ is not a vertex of F then the term is orthogonal to F. Therefore, $\overline{\mathcal{W}}_{\star\sigma^2}$ contributes to $T_F(\vec{z}_i)$ if and only if $\star\sigma^2$ is an edge of F. By the $k = 0$ case, the values of $\overline{\lambda}_i$ agree on F, meaning $T_F(\vec{z}_1) = T_F(\vec{z}_2)$.

$\overline{\mathbf{W}}1$, $\mathbf{k=2}$: We need to show that $\vec{z} \in H(\text{div})$ for

$$\vec{z} := \overline{\mathcal{I}}_2(\overline{\mathrm{w}}) = \sum_i \overline{\mathrm{w}}(\star\sigma_i^1)\overline{\mathcal{W}}_{\star\sigma_i^1},$$

where $\overline{\mathrm{w}}$ is an arbitrary dual 2-cochain. Let $F := \star\sigma^1$ be an arbitrary dual face as before. By Corollary 2.37, it suffices to show $N_F(\vec{z}_1) = N_F(\vec{z}_2)$ where $N_F(\vec{z}_i)$ is the normal component of $\vec{z}_i$ on F. Note that the $\overline{\mathcal{W}}_{\star\sigma^1}$ functions are comprised of terms of form

$$\xi_{p,q,r} := \overline{\lambda}_p \nabla \overline{\lambda}_q \times \nabla \overline{\lambda}_r$$

113

where p, q, r are vertices on some face (2-cell) of the mesh. In our definition of $\overline{\mathcal{W}}_{\star\sigma^1}$, the $\overline{\lambda}_i$ functions in $\xi_{p,q,r}$ are actually standard barycentric functions over a tetrahedron inside the polyhedron; this was chosen to ensure that the interpolation property holds and effectively reduces the conformity proof to the primal case. As we will now show, however, such reduction is not necessary to prove conformity; we only need that the $\overline{\lambda}_i$ are some type of generalized barycentric functions within the polygon.

Denote the vertices of F by $\{\mathbf{v}_j\}_{j \in J}$. We will show that $\xi_{p,q,r}$ has a non-zero normal component on F only if $p, q, r \in J$. If $p \notin J$ then $\overline{\lambda}_p = 0$ on F by Lemma 4.6, making $\xi_{p,q,r} = 0$ on F, as well. If $p \in J$ but $q, r \notin J$, then $\nabla\overline{\lambda}_q$ and $\nabla\overline{\lambda}_r$ are both orthogonal to F on F by Lemma 4.6. Hence, their cross product is zero and again $\xi_{p,q,r} = 0$ on F. If $p, q \in J$ but $r \notin J$ then again $\nabla\overline{\lambda}_r \perp F$ on F. Since $\nabla\overline{\lambda}_q \times \nabla\overline{\lambda}_r \perp \nabla\overline{\lambda}_r$, we conclude that $\xi_{p,q,r} \in F$ on F, meaning it has no normal component. The same argument holds for the case $p, r \in J$, $q \notin J$. The only remaining case is $p, q, r \in J$, proving our claim.

Since $\xi_{p,q,r}$ is only a term of $\overline{\mathcal{W}}_{\star\sigma^1}(= \overline{\mathcal{W}}_F)$, we conclude that $N_F(\vec{z}_i)$ is determined by $\overline{\mathcal{W}}_{\star\sigma^1}$ alone. By the $k = 0$ case, the values of $\overline{\lambda}_i$ agree on F, meaning $N_F(\vec{z}_1) = N_F(\vec{z}_2)$.

$\overline{\mathbf{W}}1$, $\mathbf{k=3}$: We observe that $\overline{\mathcal{I}}_3(\overline{\mathbf{w}})$ is piecewise constant over each dual cell $\star\sigma^0$. Since $\overline{\mathbf{w}}$ is finite-valued and we have a finite number of cells, $\overline{\mathcal{I}}_3(\overline{\mathbf{w}}) \in L^2 = H\Lambda^3$.

Now we address the interpolation property. Again we take $n = 3$ since

114

the $n = 2$ proofs are essentially identical.

$\overline{\mathbf{W}}3$, $\mathbf{k=0}$: We must show that $\overline{\lambda}_i$ evaluated at the ith dual vertex is 1, which is immediate from property B5 in Section 2.10. In notation,

$$\int_{\star\sigma_i^3} \phi^*(\mathcal{W}_{\star\sigma_i^3}) = \overline{\lambda}_i(\star\sigma_i^3) = 1.$$

$\overline{\mathbf{W}}3$, $\mathbf{k=1}$: Without loss of generality, suppose e_{ij} is an edge oriented from dual vertex $\overline{\mathbf{v}}_i$ to dual vertex $\overline{\mathbf{v}}_j$. Observe that

$$\int_{e_{ij}} \overline{\lambda}_i \nabla \overline{\lambda}_j = \frac{1}{|e_{ij}|} \int_{e_{ij}} \overline{\lambda}_i (\nabla \overline{\lambda}_j \cdot \vec{e}_{ij}),$$

where $\vec{e}_{ij}$ is the vector in the direction of e_{ij} with length $|e_{ij}|$. On e_{ij},

$$\nabla \overline{\lambda}_j \cdot \vec{e}_{ij} = T(\nabla \overline{\lambda}_j) \cdot \vec{e}_{ij} = |T(\nabla \overline{\lambda}_j)||\vec{e}_{ij}|, \tag{4.2}$$

where $T(\nabla \overline{\lambda}_j)$ is the tangential projection of $\nabla \overline{\lambda}_j$ on e_{ij}. Further, on e_{ij}, $T(\nabla \overline{\lambda}_j)$ is the same as the derivative of $\overline{\lambda}_j$ in the direction of e_{ij}. Since $\overline{\lambda}_j$ is the linear function satisfying $\overline{\lambda}_j(\overline{\mathbf{v}}_k) = \delta_{jk}$ on e_{ij} (by the boundary agreement property B6 from Section 2.10), we have that $T(\nabla \overline{\lambda}_j) = 1/|e_{ij}|$. Therefore (4.2) is equal to 1 and, by similar reasoning, we have that

$$\int_{e_{ij}} \overline{\lambda}_i \nabla \overline{\lambda}_j - \overline{\lambda}_j \nabla \overline{\lambda}_i = \frac{1}{|e_{ij}|} \int_{e_{ij}} \overline{\lambda}_i + \overline{\lambda}_j = \frac{1}{|e_{ij}|} \int_{e_{ij}} 1 = 1.$$

Letting $\star\sigma_k^2 := e_{ij}$, we have shown that

$$\int_{\star\sigma_k^2} \phi^*(\mathcal{W}_{\star\sigma_k^2}) = 1,$$

$\overline{\mathbf{W}}3$, $\mathbf{k=2:}$ We first prove the primal version of this case. Consider a tetrahedron σ^3 defined by a face σ^2 and vertex $\mathbf{v}$. Let $\hat{n}$ denote the outward normal to σ^3 on σ^2. By geometric arguments [17, page 141], it follows that

$$\mathcal{W}_{\sigma^2} \cdot \hat{n} = \frac{\text{alt}(\sigma^2,\mathbf{v})}{3|\sigma^3|},$$

where $\text{alt}(\sigma^2,\mathbf{v})$ denotes the altitude of σ^3 from σ^2 to $\mathbf{v}$. Using the standard volume equation $|\sigma^3| = |\sigma^2|\text{alt}(\sigma^2,\mathbf{v})/3$, we have that

$$\int_{\sigma^2} \mathcal{W}_{\sigma^2} \cdot \hat{n} = \int_{\sigma^2} \frac{1}{|\sigma^2|} = 1,$$

as desired. For a dual face $\star\sigma^1$ decomposed into triangles τ_i,

$$\int_{\star\sigma^1} \overline{\mathcal{W}}_{\star\sigma^1} \cdot \hat{n} = \sum_{i=0}^{m-1} \frac{|\tau_i|}{|\star\sigma^1|} \int_{\tau_i} \mathcal{W}_{\tau_i} \cdot \hat{n} = \sum_{i=0}^{m-1} \frac{|\tau_i|}{|\star\sigma^1|} = 1,$$

since the τ_i partition $\star\sigma^1$.

$\overline{\mathbf{W}}3$, $\mathbf{k=3:}$ Let $\overline{\mathbb{U}} \in \overline{\mathcal{C}}^3$. Then

$$\{\overline{\mathcal{P}}_3 \overline{\mathcal{I}}_3 \overline{\mathbb{U}}\}_i = \int_{\star\sigma_i^0} \phi^*(\mathcal{W}_{\star\sigma_i^0}) = \int_{\star\sigma_i^0} \frac{1}{|\star\sigma_i^0|} = 1$$

$\square$

Corollary 4.5. *The Whitney functions on a primal mesh satisfy the interpolation property W3 and the conformity property W1.*

Proof. By Lemma 4.3, Theorem 4.4 suffices as a proof for Whitney functions on a primal mesh. $\square$

Lemma 4.6. *Let $\star\sigma^0$ be a cell in a dual mesh and $F := \star\sigma^1$ a codimension one face. Denote the vertices of F by $\{v_j\}_{j \in J}$. Let v_i be any vertex of $\star\sigma^0$. If $i \notin J$ then $\overline{\lambda}_i \equiv 0$ on F and $\nabla\overline{\lambda}_i$ is normal to F on F, pointing inward.*

Proof. The first statement is a consequence of the boundary agreement property B6 from Definition 2.56 in Section 2.10. This implies F is part of the zero level set of $\overline{\lambda}_i$, from which it follows that $\nabla\overline{\lambda}_i$ is orthogonal to F on F. It points inward since the support of $\overline{\lambda}_i$ has support in $\star\sigma^0$ but not on the other side of F. $\qquad\square$

Remark 4.7. It seems unlikely that a commutativity property between the exterior derivative and the $\overline{\overline{\mathcal{I}}}_k$ operator will hold. This is due to the fact that the proof of W5 relies strongly on the fact that a k-dimensional cell in a primal mesh is a simplex and hence has $k + 1$ vertices. Since dual cells certainly do not have this property, we cannot expect a similar result for them. This lies in contrast to some claims in the literature that the exterior derivative and Whitney-like operators commute over rectangular meshes - they do not. The lack of commutativity makes proofs of discretization stability using $\overline{\overline{\mathcal{I}}}_k$ more difficult, but not impossible, as exhibited by Theorem 3.25.

4.2 $\left(\mathbb{M}_k^{Dual}\right)^{-1}$: A Sparse Inverse Discrete Hodge Star

We use the dual interpolants to define a dual discrete Hodge star by

$$\left(\mathbb{M}_k^{Dual}\right)^{-1}{}_{ij} := \left(\overline{\mathcal{W}}_{\star\sigma_i^k}, \overline{\mathcal{W}}_{\star\sigma_j^k}\right). \qquad (4.3)$$

The inner product here is the standard integration of scalar or vector valued functions over the dual domain $\star K$. For instance, in the case $k = 3$, we have

$$((\mathbb{M}_3^{Dual})^{-1})_{ij} := \left(\overline{\mathcal{W}}_{\star \sigma_i^3}, \overline{\mathcal{W}}_{\star \sigma_j^3} \right) = \int_{\star K} \overline{\lambda}_i \overline{\lambda}_j.$$

The formulation for other k values will similarly involve integrals of the $\overline{\lambda}_i$ functions. A comparison of $\mathbb{M}_k^{Diag}$, $\mathbb{M}_k^{Whit}$ and $\left(\mathbb{M}_k^{Dual} \right)^{-1}$ is shown in Figure 4.3.

$$\mathbb{M}_1^{Diag} \qquad\qquad \mathbb{M}_1^{Whit} \qquad\qquad \left(\mathbb{M}_1^{Dual} \right)^{-1}$$
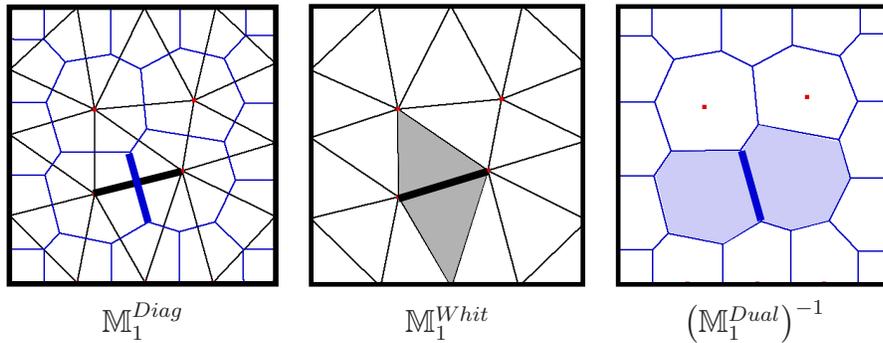
Figure 4.3: The various discrete Hodge stars depend on different aspects of mesh geometry as shown in this 2D examples. The diagonal Hodge star (left) computes ratios of sizes of primal-dual element pairs. The Whitney Hodge star (middle) has entries of Whitney functions integrated against each other. The support of a particular $\mathcal{W}_{\sigma_i^1}$ function is shown in grey; the integral of its projection to the bold edge has value 1. The Dual Hodge star (right) that we propose has entries of dual Whitney functions integrated against each other. The support of a particular $\overline{\mathcal{W}}_{\star \sigma_i^1}$ is shown in blue; the integral of its projection to the bold dual edge has value 1.

We note that $\mathbb{M}_k^{Dual}$ may, in the general case, be full, but this is of no concern; the point was to have a sparse *inverse* discrete Hodge star.

Lemma 4.8. $(\mathbb{M}_k^{Dual})^{-1}$ *is sparse.*

Proof. Observe that $\overline{\mathcal{W}}_{\star\sigma^k}$ has localized support by construction. Entry ij of $(\mathbb{M}_k^{Dual})^{-1}$ will be non-zero only if $\star\sigma_i^k$ and $\star\sigma_j^k$ are adjacent. Thus each row of the matrix will have at most as many non-zero entries as $\star\sigma_i^k$ has adjacent $n-k$ cells, meaning the matrix is sparse. $\square$

We now prove a more specific characterization of the sparsity structure of $\mathbb{M}_k^{Whit}$ and $(\mathbb{M}_k^{Dual})^{-1}$ over a mesh K and its dual mesh $\star K$.

Lemma 4.9. *Entry ij in $\mathbb{M}_k^{Whit}$ is non-zero only if there exists $\sigma^n \in K$ such that σ^n has at least one vertex from σ_i^k and one vertex from σ_j^k.*

Proof. Computing entry ij in $\mathbb{M}_k^{Whit}$ involves [12] summing terms of the form

$$\left(\int_K \lambda_1\lambda_2\right)\det\left(V_I^T W_J\right) \tag{4.4}$$

where λ_1, λ_2 are barycentric functions associated to $v_1 \in \sigma_i^k$, $v_2 \in \sigma_j^k$, respectively; I is a list of k vertices from σ_i^k not including v_1; J is a list of k vertices from σ_j^k not including v_2; and V_I, W_J are $n \times k$ matrices. The pth column of V_I is the vector $\nabla\lambda_p$ where λ_p is the barycentric function associated to the pth entry in I. The qth column of W_J is the vector $\nabla\lambda_q$ where λ_q is the barycentric function associated to the qth entry in J.

Observe that the support of the barycentric function associated to vertex v is contained within the n-simplices touching v. Thus, if there is no σ^n with at least one vertex from σ_i^k and one vertex from σ_j^k, the λ_1 and λ_2 appearing in (4.4) will always have disjoint support, making the entry zero. $\square$

Using the same kind of reasoning, we have a similar result for our dual discrete Hodge star.

Lemma 4.10. *Entry ij in $(\mathbb{M}_k^{Dual})^{-1}$ is non-zero only if there exists $\star\sigma^0 \in \star K$ such that $\star\sigma^0$ has at least one vertex from $\star\sigma_i^k$ and one vertex from $\star\sigma_j^k$.*

The number of k-simplices in an n-simplex is $\binom{n+1}{k+1}$ which gives the following corollary.

Corollary 4.11. *Let $A(\sigma^k)$ denote the number of n-simplices in K incident on at least one vertex from σ^k. Then the number of non-zero entries in row i of $\mathbb{M}_k^{Whit}$ or row i of $(\mathbb{M}_k^{Dual})^{-1}$ is at most $\binom{n+1}{k+1} A(\sigma_i^k)$.*

The bound can be sharpened for particular choices of n and k or if additional assumptions are made about K. As stated, however, the corollary provides a simple means for evaluating the computational expense of a particular discretization scheme.

Since $\left(\mathbb{M}_k^{Dual}\right)^{-1}$ was defined in analogy to $\mathbb{M}_k^{Whit}$, it satisfies a scaling property similar to that of $\mathbb{M}_k^{Whit}$.

Lemma 4.12. *Let K be a finite primal mesh with $n = 3$. Define a functional $\overline{Q}_k : \overline{\mathcal{C}}^{3-k} \to \mathbb{R}$ by*

$$\overline{Q}_k(\overline{\mathrm{B}}) := \left\langle (\mathbb{M}_k^{Dual})^{-1}\overline{\mathrm{B}}, \overline{\mathrm{B}} \right\rangle \tag{4.5}$$

For any cochains $\mathrm{A} \in \mathcal{C}^k$ and $\overline{\mathrm{B}} \in \overline{\mathcal{C}}^{3-k}$, the quotients

$$\frac{||\mathrm{A}||_{\mathcal{C}^k}^2}{\overline{Q}_k(\mathbb{M}_k\mathrm{A})} \quad and \quad \frac{||\overline{\mathrm{B}}||_{\overline{\mathcal{C}}^{3-k}}^2}{\overline{Q}_k(\overline{\mathrm{B}})}$$

are unaffected if K is uniformly scaled by a positive factor $s \in \mathbb{R}$.

Proof. The proof closely mimics that of Lemma 2.55. We start with the claim for dual cochains. By (2.17), we have that $||\bar{B}||^2_{\bar{\mathcal{C}}^{3-k}(sK)} = s^{2k-3}||\bar{B}||^2_{\bar{\mathcal{C}}^{3-k}}$. Hence, it suffices to show that $(\mathbb{M}_k^{Dual})^{-1}$ also scales as s^{2k-3}.

Note that the chain rule as stated in (2.16) still applies if the λ_i are replaced by the generalized barycentric functions $\bar{\lambda}_i$. From Definition 4.1, we see that $\overline{\mathcal{W}}_{\star\sigma^0}$ scales as $1/s^3$ since $|\star\sigma_0|$ is a volume measurement. Further, for $k \neq 0$, $\overline{\mathcal{W}}_{\star\sigma^k}$ has exactly $3-k$ terms of the type $\nabla\lambda_i$ appearing in each summand of its expression. Let $(\mathbb{M}_{k,s}^{Dual})^{-1}_{ij}$ denote the ijth entry of $(\mathbb{M}_k^{Dual})^{-1}$ on the scaled mesh and let $0 \leq k \leq 3$. Then

$$(\mathbb{M}_{k,s}^{Dual})^{-1}_{ij} = \int_{sK} \frac{1}{s^{3-k}} \overline{\mathcal{W}}_{\star\sigma_i^k}\left(\frac{x}{s}\right) \cdot \frac{1}{s^{3-k}} \mathcal{W}_{\star\sigma_j^k}\left(\frac{x}{s}\right)$$

$$= \frac{s^3}{s^{2(3-k)}} \int_K \overline{\mathcal{W}}_{\star\sigma_i^k}(x) \cdot \overline{\mathcal{W}}_{\star\sigma_j^k}(x) \qquad = s^{2k-3}(\mathbb{M}_k^{Dual})^{-1}_{ij},$$

as desired. For the primal cochain case, we have from (2.15) that $||A||^2_{\mathcal{C}^k(sK)} = s^{3-2k}||A||^2_{\mathcal{C}^k}$. Observe that

$$\overline{Q}_k(\mathbb{M}_k A) = (\mathbb{M}_k A)^T (\mathbb{M}_k^{Dual})^{-1}(\mathbb{M}_k A).$$

Thus, the value of $\overline{Q}_k(\mathbb{M}_k A)$ scales as $s^{3-2k}s^{2k-3}s^{3-2k} = s^{3-2k}$, as desired. $\square$

This scaling result suggests that we could have defined the cochain norms using $(\mathbb{M}_k^{Dual})^{-1}$ and maintained the stability results. More formally, we have the following result akin to Lemma 3.7.

Lemma 4.13. *Let Ω be a contractible, compact domain in $\mathbb{R}^3$ with primal and dual domain meshes of a finite number of elements. Let $\mathrm{m_d}$ denote*

the maximum diameter of a mesh element and assume that we have a nice refinement technique. Let $\overline{A}$ be a dual k-cochain. There exists a constant $\alpha > 0$ independent of m_d such that

$$\alpha \left|\left|\overline{\mathcal{I}_k \overline{A}}\right|\right|_{L^2} \leq \left|\left|\overline{A}\right|\right|_{\overline{\mathcal{C}}^k},$$

where the norm on the left is interpreted as $[L^2]^3$ if $k = 1$ or 2.

Proof. A binomial expansion gives the equality

$$\left|\left|\overline{\mathcal{I}_k \overline{A}}\right|\right|_{L^2}^2 = \int_\Omega \left|\sum_{\star\sigma_i^{3-k} \in \mathcal{C}_k} \overline{A}(\star\sigma_i^{3-k})\overline{\mathcal{W}}_{\sigma_i^{3-k}}\right|^2 = <\overline{A}, \left(\mathbb{M}_{3-k}^{Dual}\right)^{-1}\overline{A}> =: \overline{Q}_{3-k}(\overline{A}).$$

Hence Lemma 4.12 and the nice refinement assumption allow us to conclude that there exists a uniform bound

$$\frac{\left|\left|\overline{A}\right|\right|_{\overline{\mathcal{C}}^k}^2}{\left|\left|\overline{\mathcal{I}_k \overline{A}}\right|\right|_{L^2}^2} \geq \alpha^2,$$

for some constant α dependent on the element shape quality parameters but not the size or orientation of the element. $\qquad\square$

Lemma 4.13 says that the energy norm on cochains induced by the dual interpolation map $\overline{\mathcal{I}}_k$ is bounded in the same way as the energy norm on cochains induced by the composed map $*\mathcal{I}_{n-k}\mathbb{M}_{n-k}^{-1}$. This was an essential ingredient in our proofs of discretization stability in Chapter 3 and thus provides additional evidence for the naturalness of our approach.

4.3 Improved Condition Numbers with $\left(\mathbb{M}_k^{Dual}\right)^{-1}$

To maintain the numerical stability of a DEC-based method, the discrete Hodge star matrix should have a bounded condition number. Put differently, the entries of the matrix should be roughly the same order of magnitude. This requirement is frequently considered from the context of numerical analysis, but is often absent from the literature on discrete operators.

We first consider the size of entries in the diagonal Hodge star $\mathbb{M}_k$. These depend upon the relative size of dual-primal pairs, i.e. $|\star\sigma^k|/|\sigma_k|$, suggesting that geometric criteria on primal elements alone will not be sufficient to control the condition number of the discrete Hodge star matrix. We show some examples in Figures 4.4 and 4.5.

<center>(a)   (b)   (c)</center>
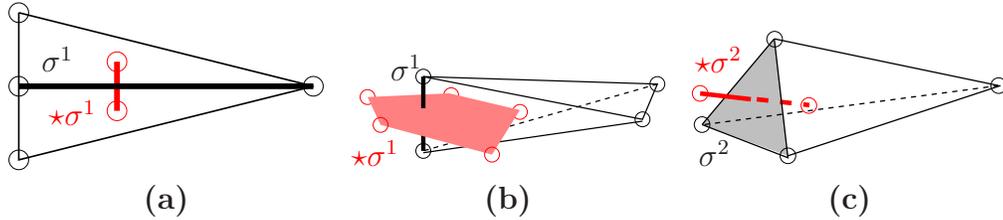
Figure 4.4: Examples illustrating how the measure of a primal simplex σ^k (black) and its dual $\star\sigma^k$ (red) need not be the same order of magnitude. **(a)** In this 2D example, the ratio $|\star\sigma^1|/|\sigma^1|$ can be made arbitrarily small by increasing the length of σ^1. **(b)** The ratio $|\star\sigma^1|/|\sigma^1|$ can be made arbitrarily large by decreasing the length of σ^1. **(c)** The ratio $|\star\sigma^2|/|\sigma^2|$ can be made arbitrarily large by decreasing the area of σ^2. Thus, a discrete Hodge star involving terms of the form $|\star\sigma^k|/|\sigma^k|$ may have a bad condition number unless primal *and* dual mesh quality is controlled.

For $\mathbb{M}_k^{Whit}$, on the other hand, the size of the matrix entries are con-

<center>123</center>
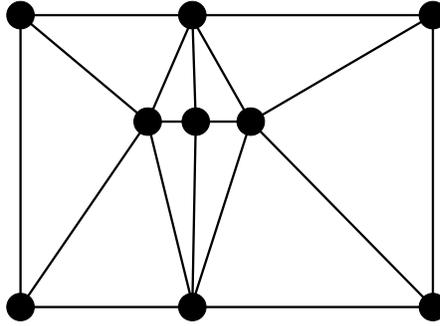
Figure 4.5: Graded meshes also present a problem for discrete Hodge stars involving primal-dual size ratios. The primal mesh shown here induces a wide variation in values of $|\star\sigma^k|/|\sigma^k|$ for $k = 0, 1, 2$. This can cause ill-conditioned $\mathbb{M}_k$ matrices, resulting in numerical instability.

trolled by the size of the inner products of Whitney basis forms. The integrals in (4.4) are on the order of the size of $|\sigma_k|$, meaning again that a large grada-tion in primal mesh element size could produce large condition numbers and hence numerical instability. Since it does not involve the size of dual mesh elements, however, $\mathbb{M}_k^{Whit}$ is more numerically stable against shape irregulari-ties of dual mesh elements. Analogously, $(\mathbb{M}_k^{Dual})^{-1}$ is more numerically stable against shape irregularities of primal mesh elements.

To provide concrete evidence for our intuitive numerical stability claims, we present a simple example in 2D showing how $\mathbb{M}_1^{Diag}$ and $\mathbb{M}_1^{Whit}$ can have condition numbers an order of magnitude worse than $(\mathbb{M}_1^{Dual})^{-1}$ on the same mesh. This serves as a proof of concept that the DEC-based dual formula-tion of a problem can provide practical advantages in cases of difficult mesh geometry.

In the 2D mesh shown in Figure 4.6, the labeled vertices of the primal
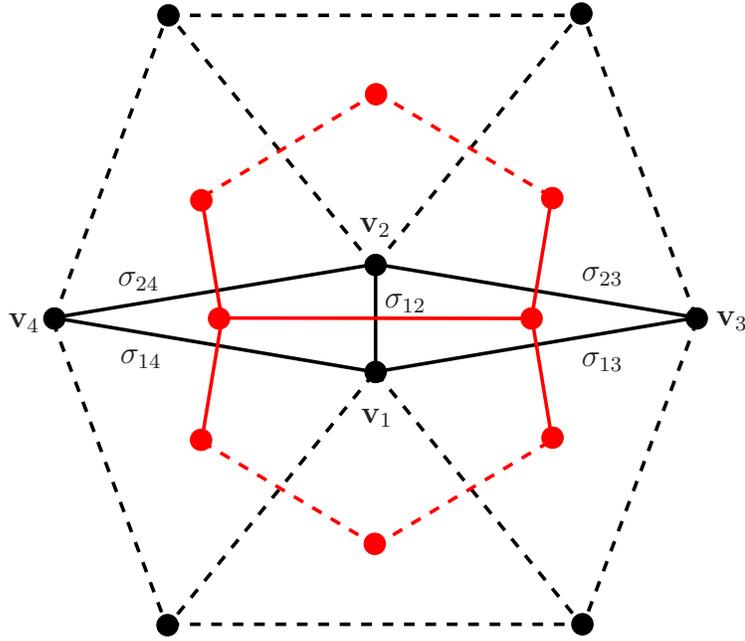
Figure 4.6: Mesh used for sample calculation of $\mathbb{M}_1$ matrices. The vertices have coordinates $\mathbf{v}_1 = (0,0)$, $\mathbf{v}_2 = (0,1)$, $\mathbf{v}_3 = (P, \frac{1}{2})$, $\mathbf{v}_4 = (-P, \frac{1}{2})$.

mesh have coordinates $\mathbf{v}_1 = (0,0)$, $\mathbf{v}_2 = (0,1)$, $\mathbf{v}_3 = (P, \frac{1}{2})$, and $\mathbf{v}_4 = (-P, \frac{1}{2})$, where P is a free parameter we can adjust to modify the geometry. The remaining vertices are chosen so that they form equilateral triangles with edges σ_{13}, σ_{23}, σ_{14}, and σ_{24}, as shown. The orthogonal, circumcenter-based dual mesh is shown in red.

Without loss of generality, fix any ordering on the mesh edges, beginning with

$$\{\sigma_{12}, \sigma_{13}, \sigma_{14}, \sigma_{23}, \sigma_{24}, \ldots\}. \tag{4.6}$$

We first calculate the upper left 5×5 block of each matrix, yielding the matrix values assigned to all possible interactions between pairs of these first five

edges. Using the circumcentric dual mesh and definition (2.9), we compute

$$\mathbb{M}_1^{Diag} = \begin{pmatrix} \dfrac{4P^2-1}{4P} & 0 & 0 & 0 & 0 & \cdots \\ 0 & \varrho & 0 & 0 & 0 & \cdots \\ 0 & 0 & \varrho & 0 & 0 & \cdots \\ 0 & 0 & 0 & \varrho & 0 & \cdots \\ 0 & 0 & 0 & 0 & \varrho & \cdots \\ \vdots & \vdots & \vdots & \vdots & \vdots & \ddots \end{pmatrix} \tag{4.7}$$

where $\varrho = \frac{1}{4P^4} + \frac{P}{\sqrt{3+12P^2}}$. Since $\mathbb{M}_1^{Diag}$ is diagonal, its condition number is the ratio of its largest diagonal entry to its smallest. The uncomputed diagonal entries will be very close to ϱ meaning the condition number can be approximated as

$$\mathrm{cond}\left(\mathbb{M}_1^{Diag}\right) \approx \frac{4P^2-1}{4P}/\varrho \in O(P).$$

Using the definition of $\mathbb{M}_1^{Whit}$ given in (2.11), we can also compute

$$\mathbb{M}_1^{Whit} = \begin{pmatrix} \alpha & \beta & \beta & \beta & \beta & \cdots \\ \beta & \gamma & 0 & \delta & 0 & \cdots \\ \beta & 0 & \gamma & 0 & \delta & \cdots \\ \beta & \delta & 0 & \gamma & 0 & \cdots \\ \beta & 0 & \delta & 0 & \gamma & \cdots \\ \vdots & \vdots & \vdots & \vdots & \vdots & \ddots \end{pmatrix} \tag{4.8}$$

where $\alpha = \frac{12P^2+1}{24P}$, $\beta = \frac{4P^2-1}{48P}$, $\gamma = \frac{12P^2+20\sqrt{3}P+21}{144P}$, and $\delta = \frac{4P^2-5}{48P}$. We note that some of the structure of $\mathbb{M}_1^{Whit}$ suggested by (4.8) is an artifice of our ordering

126

of the edges as stated in (4.6). However, the remaining diagonal entries of $\mathbb{M}_1^{Whit}$ are all close to γ, the entire matrix is symmetric, and the remaining non-zero off-diagonal terms are roughly the same size. Thus, the eigenvalues of the 5×5 matrix shown in (4.8) allow us to approximate the condition number of $\mathbb{M}_1^{Whit}$. Using Mathematica, we find analytical expressions for the max and min eigenvalues of the 5×5 matrix and take their ratio to approximate

$$\text{cond}\left(\mathbb{M}_1^{Whit}\right) \approx \frac{24P^2 + 5\sqrt{3}P + \sqrt{288P^4 - 120\sqrt{3}P^3 + 3P^2 + 9} + 3}{10\sqrt{3}P + 18} \in O(P)$$

Finally, we compute $(\mathbb{M}_1^{Dual})^{-1}$ using the Sibson functions (Definition 2.59) over the barycentric dual mesh, according to definition (4.3). This yields

$$\left(\mathbb{M}_1^{Dual}\right)^{-1} = \begin{pmatrix} \vartheta & \zeta & \zeta & \zeta & \zeta & \cdots \\ \zeta & \theta & \kappa & \xi & 0 & \cdots \\ \zeta & \kappa & \theta & 0 & \xi & \cdots \\ \zeta & \xi & 0 & \theta & \kappa & \cdots \\ \zeta & 0 & \xi & \kappa & \theta & \cdots \\ \vdots & \vdots & \vdots & \vdots & \vdots & \ddots \end{pmatrix} \tag{4.9}$$

where $\vartheta = \left(\eta_{\star\sigma_{12}^1}, \eta_{\star\sigma_{12}^1}\right)$, $\zeta = \left(\eta_{\star\sigma_{12}^1}, \eta_{\star\sigma_{13}^1}\right)$, $\theta = \left(\eta_{\star\sigma_{13}^1}, \eta_{\star\sigma_{13}^1}\right)$, $\kappa = \left(\eta_{\star\sigma_{13}^1}, \eta_{\star\sigma_{14}^1}\right)$ and $\xi = \left(\eta_{\star\sigma_{13}^1}, \eta_{\star\sigma_{23}^1}\right)$. Note that analytical expressions of these inner products are not feasible due to the need to compute areas of intersection of irregular polygons in the definition of the $\overline{\lambda}$ functions. Instead, using Matlab, we create a simple grid-based quadrature method to estimate the entries of $\left(\mathbb{M}_1^{Dual}\right)^{-1}$ for various values of P. As with $\mathbb{M}_1^{Whit}$, we then estimate the condition number

127

of the entire matrix by the ratio of the max and min eigenvalues of the 5×5 matrix given in (4.9).

We tested the cases $P = 2$, 5, and 10. The integral required to compute ξ has support outside of the portion of the dual mesh shown in Figure 4.6. We thus set ξ to be the same as ζ, since both are inner products associated to adjacent edges in the dual mesh. The computed values of κ were very small, as expected; we found that setting κ to zero did not affect the condition number estimate. Our results are summarized in Table 4.1.

P	cond $\left(\mathbb{M}_1^{Diag} \right)$	cond $\left(\mathbb{M}_1^{Whit} \right)$	cond $\left(\left(\mathbb{M}_1^{Dual} \right)^{-1} \right)$
2	6.3	3.2	1.5
5	17.2	9.9	1.3
10	34.6	21.6	1.4

Table 4.1: Comparison of condition numbers of different discrete Hodge stars for various values of P.

Our numerical experiments thus provide evidence for the claim

$$\text{cond} \left((\mathbb{M}_1^{Dual})^{-1} \right) \in O(1).$$

The above example confirms that while our dual discrete Hodge star has an analogous definition to the primal discrete Hodge star, its condition number is indeed controlled by the geometric properties of the dual mesh elements, not those of the primal mesh elements. This fact is especially useful for problems on tetrahedral meshes where slivers (narrow, nearly planar tetrahedra) frequently occur and are difficult to remove.

We conclude with a more general conjecture. The example just presented provides evidence for the case $n = 2$, $k = 1$.

Conjecture 4.14. *The condition number of $\left(\mathbb{M}_{n-k}^{Dual}\right)^{-1}$ is governed by different mesh geometry properties than the condition number of $\mathbb{M}_k^{Diag}$ and $\mathbb{M}_k^{Whit}$.*

Chapter 5

Conclusions and Future Work

This thesis can be viewed as a set of initial results toward a much broader theory of dual discretization methods. We have shown that discretization stability can be achieved using dual meshes as part of certain types of mixed methods (Sections 3.1-3.4) as well as in single variable, node-based methods in 2D (Section 3.6). Moreover, we have shown that Whitney-like functions with the proper conformity can be constructed in a natural way over 2D or 3D dual meshes (Section 4.1) and that using a discrete Hodge star associated with such functions may offer improved numerical stability results (Section 4.3). We now discuss a few possible directions that can be pursued from these beginnings.

Higher order $\overline{\mathcal{I}}_k$ functions. The interpolation functions we defined are 'lowest order' in the sense that are linear in $\overline{\lambda}_i$. A natural question to consider is how these might be extended toward higher order basis functions which maintain $H\Lambda^k$ conformity but obtain faster convergence estimates for the same data regularity assumptions. For primal discretization methods, this question has been studied in many papers relating to FEEC, for instance [3, 6, 49]. From a DEC standpoint, however, these approaches are less attractive

since the higher order $\mathcal{I}_k$ functions have many degrees of freedom associated with simplices of dimension greater than k.

To address this problem, Rapetti and Bossavit [78, 79] have given an alternate construction of higher order Whitney forms which keeps the degrees of freedom for a k-form associated with k-simplices. Their approach is based on ideas from Hiptmair [57] and others, but ultimately produces spanning sets larger of dimension larger than the requisite basis. As a result, certain functions must be discarded and the method relies on heuristics. Nevertheless, the large body of work on the topic of higher order interpolation points toward the possibility of higher order $\overline{\mathcal{I}}_k$ functions being developed.

Spectral analysis of $\mathbb{M}_k^{Whit}$ and $\left(\mathbb{M}_k^{Dual}\right)^{-1}$ As Conjecture 4.14 suggests, our dual discrete Hodge star may result in better conditioned linear systems in certain circumstances. We have shown in Lemma 4.13 that $\overline{\mathcal{I}}_k$ is bounded in an analogous sense to the $\mathcal{I}_k$ operator. Note that if we consider the dual cochain $\overline{A}$ with all entries 1 in this case, the result is close to an upper bound on the matrix 2-norm of $\left(\mathbb{M}_k^{Dual}\right)^{-1}$. The tools of spectral analysis may aid in proving specific results along these lines.

Surface finite elements. All the methods presented in this thesis are for 'flat' domains, i.e. n-manifolds with boundary embedded in $\mathbb{R}^n$. However, many important PDE problems are formulated and approximated using boundary domains, especially meshes of two-dimensional surfaces embedded in $\mathbb{R}^3$. Of relevance here is the work by Dziuk [36] for nodal finite elements on triangulated surfaces and its extension by Demlow [31] for higher order ap-

proximation. Holst and Stern [61] have recently developed a framework that generalizes those works by an extension of FEEC theory. Carrying out a similar type of analysis from a DEC perspective could allow for dual discretization methods on these sorts of boundary domains.

Alternate generalizations of barycentric coordinates. As mentioned in Section 2.10, the Sibson coordinates used in this paper are but one in a stable of many possible generalized barycentric coordinates. We have already analyzed the how the discretization stability estimates associated to a few of these types have distinct dependencies on geometric properties of 2D dual meshes [48]; a similar analysis for 3D dual meshes is underway.

Moreover, while many of these generalized coordinates have been implemented in computer graphics contexts, few have been incorporated into finite element codes as we have proposed here. The implementation of dual discretization methods with various coordinate definitions will help reveal which type in practice offers the best balance between accuracy of approximation and speed of computation.

Appendices

Appendix A

Continuous Hodge Star

The operator $*$ requires some work to be defined in a general sense as its definition has to be shown to be independent of the selected basis. We outline the standard approach to its definition here; more details can be found in many differential topology textbooks such as [1, 52].

Definition A.1. Let V be vector space of dimension n with a real inner product $< \cdot, \cdot >_V : V \times V \to \mathbb{R}$. The **inner product on** $\Lambda(V)$ denoted by $< \cdot, \cdot >$ is defined as follows. Let $\{v_1, \ldots, v_n\}$ be a basis of V. We say that elements of the form $v_{i_1} \wedge \ldots \wedge v_{i_k}$ have **grading** k. Define the inner product of elements with different gradings to be zero. Define

$$< v_{i_1} \wedge \ldots \wedge v_{i_k}, v_{j_1} \wedge \ldots \wedge v_{j_k} > := det \begin{pmatrix} < v_{i_1}, v_{j_1} >_V & \cdots & < v_{i_1}, v_{j_k} >_V \\ \vdots & \ddots & \vdots \\ < v_{i_k}, v_{j_1} >_V & \cdots & < v_{i_k}, v_{j_k} >_V \end{pmatrix}$$

For the inner product of arbitrary elements of $\Lambda(V)$, extend the above definitions bilinearly. ◇

We have a general result akin to Theorem 2.4.

Lemma A.2. *If* $\{e_1, \ldots, e_n\}$ *is an orthonormal basis of* V *then*

$$\{e_{i_1} \wedge \ldots \wedge e_{i_k} : 0 \leq i_1 < \cdots < i_k \leq n\}$$

is an orthonormal basis of $\Lambda(V)$.

The proof is lengthy but straightforward.

Lemma A.3. *Let V be a real vector space of dimension n with a real inner product $< \cdot, \cdot >_V : V \times V \to \mathbb{R}$. Let $\{e_1, \ldots, e_n\}$ be an orthonormal basis of V. Define g_{ij} by*

$$g_{ij} := < e_i, e_j >_V .$$

Given arbitrary $v := \sum v_i e_i$ and $w := \sum w_i e_i$ (with $v_i, w_i \in \mathbb{R}$), write

$$< v, w >_V = \sum_{i,j=1}^{n} v_i g_{ij} w_j.$$

Then (g_{ij}) forms a symmetric, positive definite, invertible n by n matrix.

Proof (Sketch): The symmetry follows from symmetry of the inner product. The positive definite claim comes from positive nature of inner product. Invertibility is a consequence of positive definiteness. $\square$

Definition A.4. Let V be vector space of dimension n with a real inner product $< \cdot, \cdot >_V : V \times V \to \mathbb{R}$. The **inner product on $\Lambda(V)$** denoted by $< \cdot, \cdot >$ is defined as follows. Let $\{e_1, \ldots, e_n\}$ be a basis of V. Let (g_{ij}) be the matrix defined in Lemma A.3 and (g^{ij}) its inverse. Let $\alpha, \beta \in \Lambda^k(V)$. Let I denote an increasing sequence of k indices $i_1 < \cdots < i_k$. Then α and β have unique expansions

$$\alpha = \sum_I \alpha_I e^I, \qquad \beta = \sum_I \beta_I e^I$$

where $\alpha_I, \beta_I \in \mathbb{R}$ and $e^I := e^{i_1} \wedge \ldots \wedge e^{i_k}$. Define

$$\beta^I := \sum_J g^{i_1 j_1} \cdots g^{i_k j_k} \beta_J$$

where J also ranges over increasing sequences of k indices $j_1 < \cdots < j_k$. Define

$$< \alpha, \beta >:= \sum_I \alpha_I \beta^I = \sum_I \left[\alpha_I \sum_J g^{i_1 j_1} \cdots g^{i_k j_k} \beta_J \right]$$

$\Diamond$

Definition A.5. Let $\{e_1, \ldots, e_n\}$ be an orthonormal basis for $\Lambda(V)$ with positive orientation. The **Hodge Star** operator denoted by $*$ is

$$* : \Lambda^k(V) \to \Lambda^{n-k}(V),$$

defined as follows. For $0 < k < n$, let $\sigma \in S_n$ satisfy $\sigma(1) < \cdots < \sigma(k)$ and $\sigma(k+1) < \cdots < \sigma(n)$. Then $*$ is defined by

$$* \left(e_{\sigma(1)} \wedge \ldots \wedge e_{\sigma(k)} \right) := \text{sign}(\sigma) \left(e_{\sigma(k+1)} \wedge \ldots \wedge e_{\sigma(n)} \right).$$

For $k = 0$ and $k = n$, $*$ is defined by

$$*(1) = \pm e_1 \wedge \cdots \wedge e_n \quad \text{and} \quad * (e_1 \wedge \cdots \wedge e_n) = \pm 1$$

where the sign is "+" if $e_1 \wedge \cdots \wedge e_n$ lies in the component of $\Lambda^n(V)$ determined by the orientation and "-" otherwise. $\Diamond$

Lemma A.6. *The Hodge Star is the unique operator satisfying the relationship*

$$\alpha \wedge *\beta =< \alpha, \beta > \mu \quad \forall \alpha, \beta \in \Lambda^k(V), \tag{A.1}$$

where μ is the volume element of $\Lambda(V)$. Therefore, $*$ is well-defined.

Proof. First we show that $*$ satisfies (A.1) and then show that it must be unique. Fix an orthonormal basis $\{e_1, \ldots, e_n\}$ of V such that $\mu = e_1 \wedge \ldots \wedge e_n$. Let $\alpha := e_{i_1} \wedge \ldots \wedge e_{i_k}$, $\beta := e_{\sigma(1)} \wedge \ldots \wedge e_{\sigma(k)}$ with $i_1 < \cdots < i_k$, $\sigma(1) < \cdots < \sigma(k)$, and $\sigma(k+1) < \cdots < \sigma(n)$, $\sigma \in S_n$. Let $I := \{1, \ldots, n\}$. Observe that $\sigma : I \to I$ is an isomorphism and $i_1, \ldots i_k$ are distinct elements of I. Therefore, either there exists L such that $i_L \in \{\sigma(l)\}$, $l = k + 1, \ldots, n$ or $\{i_j\} = \{\sigma(j)\}$, $j = 1, \ldots, k$. In the former case, e_{i_L} appears twice in $\alpha \wedge *\beta$ meaning $\alpha \wedge *\beta = 0$. In the latter case, both sequences are strictly increasing with respect to j meaning $i_j = \sigma(j)$ for $j = 1, \ldots, k$, and hence $\alpha = \beta$. Now observe that by definition

$$< \alpha, \beta > = \det(< e_{i_m}, e_{\sigma(n)} >_V)_{mn}.$$

The only non-zero entries of the matrix must lie on the diagonal since the e_i are an orthonormal basis. In the former case, $i_L \notin \{\sigma(1), \ldots, \sigma(k)\}$ so that the Lth row of the matrix is all zeros, yielding $< \alpha, \beta > = 0$ as desired. In the latter case, each diagonal entry is $< e_{\sigma(j)}, e_{\sigma(j)} >_V = 1$ so that $< \alpha, \beta > (=< \alpha, \alpha >) = 1$. Hence

$$
\begin{aligned}
\alpha \wedge *\alpha &= (e_{\sigma(1)} \wedge \ldots \wedge e_{\sigma(k)}) \wedge (\text{sign } \sigma) e_{\sigma(k+1)} \wedge \ldots \wedge e_{\sigma(n)} \\
&= (\text{sign } \sigma) e_{\sigma(1)} \wedge \ldots \wedge e_{\sigma(n)} \\
&= e_1 \wedge \ldots \wedge e_n \\
&= < \alpha, \alpha > \mu
\end{aligned}
$$

$\square$

We note that $*$ operates on forms in a natural way since $T_x(\Omega)^*$ is a vector space and a form is a smooth choice of bases for these spaces as x ranges over Ω.

Bibliography

[1] R. Abraham, J. E. Marsden, and T. Ratiu. *Manifolds, tensor analysis, and applications*, volume 75 of *Applied Mathematical Sciences*. Springer-Verlag, New York, second edition, 1988.

[2] R. A. Adams. *Sobolev Spaces*, volume 140 of *Pure and Applied Mathematics*. Academic Press, Oxford, second edition, 2003.

[3] M. Ainsworth and J. Coyle. Hierarchic finite element bases on unstructured tetrahedral meshes. *Int. J. Num. Methods in Engineering*, 58(14):2103–2130, 2003.

[4] M. A. Armstrong. *Basic topology.* Springer-Verlag, New York, 1983.

[5] D. Arnold, D. Boffi, and R. Falk. Approximation by quadrilateral finite elements. *Mathematics of Computation*, 71(239):909–922, 2002.

[6] D. Arnold, R. Falk, and R. Winther. Finite element exterior calculus, homological techniques, and applications. *Acta Numerica*, pages 1–155, 2006.

[7] D. Arnold, R. Falk, and R. Winther. Finite element exterior calculus: from Hodge theory to numerical stability. *Bulletin of the American Mathematical Society*, 47(2):281–354, 2010.

[8] B. Auchmann and S. Kurz. A geometrically defined discrete hodge operator on simplicial cells. *Magnetics, IEEE Transactions on*, 42(4):643–646, April 2006.

[9] D. Baldomir. Differential forms and electromagnetism in 3-dimensional Euclidean space $\mathbf{R}^3$. *Proc. IEE-A*, 133(3):139–143, 1986.

[10] M. L. Barton. *Tangentially continuous vector finite elements for nonlinear 3-D magnetic field problems*. PhD thesis, Carnegie-Mellon University, 1987.

[11] M. L. Barton and Z. J. Cendes. New vector finite elements for three-dimensional magnetic field computation. *Journal of Applied Physics*, 61(8):3919–3921, 1987.

[12] N. Bell and A. Hirani. PyDEC: Software and Algorithms for Discretization of Exterior Calculus. *arXiv:1103.3076*, 2011.

[13] W. N. Bell. *Algebraic Multigrid for Discrete Differential Forms*. PhD thesis, University of Illinois at Urbana-Champaign, 2008.

[14] P. Bochev and J. Hyman. Principles of mimetic discretizations of differential operators. In *Compatible Spatial Discretizations*, pages 89–119. Springer, 2006.

[15] A. Bossavit. Mixed finite elements and the complex of Whitney forms. In J. Whiteman, editor, *The mathematics of finite elements and applications VI*, pages 137–144. Academic Press, 1988.

[16] A. Bossavit. Whitney forms: a class of finite elements for three-dimensional computations in electromagnetism. *Proc. of the IEEE*, 135(8):493–500, 1988.

[17] A. Bossavit. *Computational Electromagnetism*. Academic Press Inc., San Diego, CA, 1998.

[18] A. Bossavit. Computational electromagnetism and geometry (3). *Journal of the Japan Society of Applied Electromagnetics*, 7(4):401–408, 1999.

[19] A. Bossavit. Computational electromagnetism and geometry (5). *Journal of the Japan Society of Applied Electromagnetics*, 8(2):203–209, 2000.

[20] A. Bossavit. Generalized finite differences in computational electromagnetics. *Progress In Electromagnetics Research*, 32:45–64, 2001.

[21] A. Bossavit. A uniform rationale for whitney forms on various supporting shapes. *Mathematics and Computers in Simulation*, 80(8):1567–1577, 2010.

[22] J. H. Bramble and S. R. Hilbert. Estimation of linear functionals on Sobolev spaces with application to Fourier transforms and spline interpolation. *SIAM Journal on Numerical Analysis*, 7(1):112–124, 1970.

[23] S. Brenner and L. Scott. *The Mathematical Theory of Finite Element Mehtods*. Springer-Verlag, New York, 2002.

[24] F. Brezzi and M. Fortin. *Mixed and hybrid finite element methods.* Springer, Berlin, 1991.

[25] P. Castillo, J. Koining, R. Rieben, M. Stowell, and D. White. Discrete differential forms: A novel methodology for robust computational electromagnetics. Technical report, Lawrence Livermore National Laboratory, Center for Applied Scientific Computing, 2003.

[26] S. H. Christiansen. A construction of spaces of compatible differential forms on cellular complexes. *Math. Models Methods Appl. Sci.*, 18(5):739–757, 2008.

[27] S. H. Christiansen and R. Winther. Smoothed projections in finite element exterior calculus. *Mathematics of Computation*, 77(262):813–829, 2008.

[28] E. Cueto, N. Sukumar, B. Calvo, M. A. Martínez, J. Cegoñino, and M. Doblaré. Overview and recent advances in natural neighbour Galerkin methods. *Arch. Comput. Methods Engrg.*, 10(4):307–384, 2003.

[29] S. Dekel and D. Leviatan. The Bramble-Hilbert lemma for convex domains. *SIAM Journal on Mathematical Analysis*, 35(5):1203–1212, 2004.

[30] L. Demkowicz, P. Monk, L. Vardapetyan, and W. Rachowicz. deRham diagram for hp finite element spaces. *Computers and Mathematics with Applications*, 39(7-8):29–38, 2000.

[31] A. Demlow. Higher-order finite element methods and pointwise error estimates for elliptic problems on surfaces. *SIAM J. Numer. Anal*, 47(2):805–827, 2009.

[32] M. Desbrun, A. N. Hirani, M. Leok, and J. E. Marsden. Discrete Exterior Calculus. *arXiv:math/0508341*, 2005.

[33] G. Deschamps. Electromagnetics and differential forms. *Proc. of the IEEE*, 69(6):676–696, 1981.

[34] A. DiCarlo, F. Milicchio, A. Paoluzzi, and V. Shapiro. Discrete physics using metrized chains. In *2009 SIAM/ACM Joint Conference on Geometric and Physical Modeling*, pages 135–145. ACM, 2009.

[35] J. Dodziuk. Finite-difference approach to the Hodge theory of harmonic forms. *Amer. J. Math.*, 98(1):79–104, 1976.

[36] G. Dziuk. Finite elements for the beltrami operator on arbitrary surfaces. *Partial differential equations and calculus of variations*, pages 142–155, 1988.

[37] H. G. Eggleston. *Convexity*, volume 47 of *Cambridge Tracts in Mathematics and Mathematical Physics*. Cambridge University Press, Cambridge, 1958.

[38] A. Ern and J.-L. Guermond. *Theory and practice of finite elements*, volume 159 of *Applied Mathematical Sciences*. Springer-Verlag, New York, 2004.

[39] T. Euler. *Consistent Discretization of Maxwell's Equations on Polyhedral Grids*. PhD thesis, TU Darmstadt, 2007.

[40] L. C. Evans. *Partial differential equations*, volume 19 of *Graduate Studies in Mathematics*. American Mathematical Society, second edition, 2010.

[41] G. Farin. Surfaces over Dirichlet tessellations. *Computer Aided Geometric Design*, 7(1-4):281–292, 1990.

[42] M. Floater. Mean value coordinates. *Computer Aided Geometric Design*, 20(1):19–27, 2003.

[43] M. Floater, K. Hormann, and G. Kós. A general construction of barycentric coordinates over convex polygons. *Advances in Computational Mathematics*, 24(1):311–331, 2006.

[44] M. Floater, G. Kós, and M. Reimers. Mean value coordinates in 3D. *Computer Aided Geometric Design*, 22(7):623–631, 2005.

[45] J. Frauendiener. Discrete differential forms in general relativity. *Classical and Quantum Gravity*, 23(16):S369–S385, 2006.

[46] A. Gillette and C. Bajaj. Dual formulations of mixed finite element methods. *Computer Aided Design*, Submitted, 2010.

[47] A. Gillette and C. Bajaj. A generalization for stable mixed finite elements. In *Proc. of the 14th ACM Symp. on Solid and Physical Modeling*, pages 41–50, 2010.

[48] A. Gillette, A. Rand, and C. Bajaj. Error estimates for generalized barycentric interpolation. *Advances in Computational Mathematics*, To appear, 2010.

[49] J. Gopalakrishnan, L. García-Castillo, and L. Demkowicz. Nédélec spaces in affine coordinates. *Computers and Mathematics with Applications*, 49(7-8):1285–1294, 2005.

[50] V. Gradinaru. *Whitney elements on sparse grids*. PhD thesis, Universität Tübingen, 2002.

[51] V. Gradinaru and R. Hiptmair. Whitney elements on pyramids. *Electronic Transactions on Numerical Analysis*, 8:154–168, 1999.

[52] V. Guillemin and A. Pollack. *Differential Topology*. Prentice-Hall Inc., Englewood Cliffs, New Jersey, 1974.

[53] A. Hatcher. *Algebraic topology*. Cambridge University Press, Cambridge, 2002.

[54] B. He. *Compatible Discretizations for Maxwell Equations*. PhD thesis, Ohio State University, 2006.

[55] R. Hiptmair. Canonical construction of finite elements. *Mathematics of Computation*, 68(228):1325–1346, 1999.

[56] R. Hiptmair. Discrete hodge-operators: an algebraic perspective. *Progress In Electromagnetics Research*, 32:247–269, 2001.

[57] R. Hiptmair. Higher order whitney forms. In F. Teixeira, editor, *Geometrical Methods in Computational Electromagnetics*, volume 32, pages 271–299. PIER, EMW Publishing, 2001.

[58] A. Hirani and K. Kalyanaraman. Numerical experiments for darcy flow on a surface using mixed exterior calculus methods. *arXiv:1103.4865*, 2011.

[59] A. N. Hirani. *Discrete Exterior Calculus.* PhD thesis, California Institute of Technology, 2003.

[60] A. N. Hirani, K. B. Nakshatrala, and J. H. Chaudhry. Numerical method for Darcy flow derived using Discrete Exterior Calculus. *arXiv:0810.3434*, 2008.

[61] M. Holst and A. Stern. Geometric variational crimes: Hilbert complexes, finite element exterior calculus, and problems on hypersurfaces. *arXiv:1005.4455*, 2010.

[62] K. Hormann and N. Sukumar. Maximum entropy coordinates for arbitrary polytopes. *Computer Graphics Forum*, 27(5):1513–1520, 2008.

[63] J. M. Hyman and M. Shashkov. Adjoint operators for the natural discretizations of the divergence gradient and curl on logically rectangular grids. *Appl. Numer. Math.*, 25(4):413–442, 1997.

[64] J. M. Hyman and M. Shashkov. Natural discretizations for the divergence, gradient, and curl on logically rectangular grids. *Computers and Mathematics with Applications*, 33(4):81 – 104, 1997.

[65] J. M. Hyman and M. Shashkov. The orthogonal decomposition theorems for mimetic finite difference methods. *SIAM Journal on Numerical Analysis*, 36(3):788–818, 1999.

[66] G. Leoni. *A First Course in Sobolev Spaces*, volume 105 of *Graduate Studies in Mathematics*. American Mathematical Society, Providence, RI, 2009.

[67] A. Logg and G. Wells. DOLFIN: Automated finite element computing. *ACM Transactions on Mathematical Software (TOMS)*, 37(2):1–28, 2010.

[68] W. McLean. *Strongly elliptic systems and boundary integral equations.* Cambridge University Press, Cambridge, 2000.

[69] M. Meyer, H. Lee, A. Barr, and M. Desbrun. Generalized barycentric coordinates on irregular polygons. *J. Graph. Tools*, 7(1):13–22, 2002.

[70] P. Milbradt and T. Pick. Polytope finite elements. *International Journal for Numerical Methods in Engineering*, 73(12):1811–1835, 2008.

[71] J. R. Munkres. *Elements of algebraic topology.* Addison-Wesley Publishing Company, Menlo Park, CA, 1984.

[72] J.-C. Nédélec. Mixed finite elements in $\mathbf{R}^3$. *Numer. Math.*, 35(3):315–341, 1980.

[73] J.-C. Nédélec. A new family of mixed finite elements in $\mathbf{R}^3$. *Numer. Math.*, 50(1):57–81, 1986.

[74] R. Nicolaides. Direct discretization of planar div-curl problems. *SIAM Journal on Numerical Analysis*, 29(1):32–56, 1992.

[75] A. Okabe and M. Aoyagi. Existence of equilibrium configurations of competitive firms on an infinite two-dimensional space. *Journal of Urban Economics*, 29(3):349 – 370, 1991.

[76] A. Okabe, B. Boots, K. Sugihara, and S. Chiu. *Spatial Tessellations: Concepts and Applications of Voronoi Diagrams*. Wiley, second edition, 2000.

[77] U. Pinkall and K. Polthier. Computing discrete minimal surfaces and their conjugates. *Exp. Math.*, 2(1):15–36, 1993.

[78] F. Rapetti. High order edge elements on simplicial meshes. *ESAIM:M2AN*, 41(6):1001–1020, 2007.

[79] F. Rapetti and A. Bossavit. Geometrical localisation of the degrees of freedom for whitney elements of higher order. *Science, Measurement and Technology, IET*, 1(1):63–66, January 2007.

[80] P.-A. Raviart and J. M. Thomas. A mixed finite element method for 2nd order elliptic problems. In *Mathematical aspects of finite element methods (Proc. Conf., Consiglio Naz. delle Ricerche (C.N.R.), Rome, 1975)*, pages 292–315. Lecture Notes in Math., Vol. 606. Springer, Berlin, 1977.

[81] J. Schöberl. A posteriori error estimates for Maxwell equations. *Math. Comp.*, 77(262):633–649, 2008.

[82] P. R. Scott and P. W. Awyong. Inequalities for convex sets. *Journal of Inequalities in Pure and Applied Mathematics*, 1(1):6, 2000.

[83] M. Shashkov and S. Steinberg. *Conservative finite-difference methods on general grids*. CRC, 1996.

[84] R. Sibson. A vector identity for the Dirichlet tessellation. *Math. Proc. Cambridge Philos. Soc.*, 87(1):151–155, 1980.

[85] N. Sukumar. Construction of polygonal interpolants: a maximum entropy approach. *International Journal for Numerical Methods in Engineering*, 61(12):2159–2181, 2004.

[86] N. Sukumar and E. A. Malsch. Recent advances in the construction of polygonal finite element interpolants. *Archives of Computational Methods in Engineering*, 13(1):129–163, 2006.

[87] N. Sukumar and A. Tabarraei. Conforming polygonal finite elements. *International Journal for Numerical Methods in Engineering*, 61(12):2045–2066, 2004.

[88] F. L. Teixeira and W. C. Chew. Lattice electromagnetic theory from a topological viewpoint. *Journal of Mathematical Physics*, 40(1):169–187, 1999.

[89] E. Tonti. Finite formulation of electromagnetic field. *IEEE Transactions on Magnetics*, 38(2):333–336, 2002.

[90] R. Verfürth. A note on polynomial approximation in Sobolev spaces. *Mathematical Modelling and Numerical Analysis*, 33(4):715–719, 1999.

[91] E. L. Wachspress. *A Rational Finite Element Basis*, volume 114 of *Mathematics in Science and Engineering*. Academic Press, 1975.

[92] M. Wardetzky. *Discrete Differential Operators on Polyhedral Surfaces - Convergence and Approximation*. PhD thesis, Freie Universitat Berlin, 2006.

[93] J. Warren. Barycentric coordinates for convex polytopes. *Advances in Computational Mathematics*, 6(1):97–108, 1996.

[94] J. Warren. On the uniqueness of barycentric coordinates. In *Topics in algebraic geometry and geometric modeling*, volume 334, page 93. American Mathematical Society, 2003.

[95] J. Warren, S. Schaefer, A. N. Hirani, and M. Desbrun. Barycentric coordinates for convex sets. *Advances in Computational Mathematics*, 27(3):319–338, 2007.

[96] H. Whitney. *Geometric Integration Theory*. Princeton University Press, 1957.

[97] S. O. Wilson. Cochain algebra on manifolds and convergence under refinement. *Topology Appl.*, 154(9):1898–1920, 2007.

[98] I. M. Yaglom and V. G. Boltyansky. *Convex Figures*. Holt, Rinehart and Winston, 1961.

[99] A. Yavari. On geometric discretization of elasticity. *Journal of Mathematical Physics*, 49(2):022901–1–36, 2008.

Index